Elsevier Editorial System(tm) for BBA - Molecular Cell Research
Manuscript Draft

Manuscript Number: BBAMCR-09-112R2

Title: Yeast prion [PSI+] lowers the levels of mitochondrial prohibitins

Article Type: Regular Paper

Keywords: differential proteomics; yeast mitochondria; yeast prions; prohibitins

Corresponding Author: Professor Magdalena Boguta,

Corresponding Author's Institution: Institute of Biochemistry and Biophysics

First Author: Jacek Sikora

Order of Authors: Jacek Sikora; Joanna Towpik; Damian Graczyk; Michał Kistowski; Tymon Rubel; Jarosław Poznanski; James Langridge; Chris Hughes; Michal Dadlez; Magdalena Boguta

Abstract: We report proteomic analyses that establish the effect of cytoplasmic prion [PSI+] on the protein complement of yeast mitochondria. A set of 44 yeast mitochondrial proteins whose levels were affected by [PSI+] was identified by two methods of gel-free and label-free differential proteomics. From this set we focused on prohibitins, Phb1 and Phb2, and the mitochondrially synthesized Cox2 subunit of cytochrome oxidase. By immunoblotting we confirmed the decreased level of Cox2 and reduced mitochondrial localization of the prohibitins in [PSI+] cells, which both became partially restored by [PSI+] curing. The presence of the [PSI+] prion also caused premature fragmentation of mitochondria, a phenomenon linked to prohibitin depletion in mammalian cells. By fractionation of cellular extracts we demonstrated a [PSI+]-dependent increased of the proportion of prohibitins in the high molecular weight fraction of aggregated proteins. We propose that the presence of the yeast prion causes newly synthesized prohibitins to aggregate in the cytosol, and therefore reduces their levels in mitochondria, which in turn reduces the stability of Cox2 and possibly of other proteins, not investigated here in detail.

Response to Reviewers:

REVIEWER 1:

I would only note that the last paragraph of the Discussion, in which the authors relate their findings to a putative increased "evolvability" weakens their paper considerably. This suggestion, made by True and Lindquist, has been discredited by several groups. A more direct explanation of the current results is that these results are suggestive of why [PSI+] is sufficiently detrimental to host cells that it is not found in the wild (by three groups).

Response

We agree that our results are not related to a putative evolutionary aspect of prion. The text has been changed to emphasize novelty of our hypothesis that [PSI+] may titrate host protein thereby affecting functioning of mitochondria.
We thank the referee for his careful analysis of our conclusions.

Warsaw, August 6, 2009

Dr. Nikolaus Pfanner
Executive Editor
BBA - Molecular Cell Research

Dear Dr. Pfanner,

I am really happy with your positive decision concerning publication of our article "Yeast prion [PSI+] lowers the levels of mitochondrial prohibitins" in BBA - Molecular Cell Research. I fully agree with the comment of the referee and modified a final paragraph of the discussion according to his suggestion.

Thank you for your assistance.

.

Sincerely yours,

Magdalena Boguta
Institute of Biochemistry and Biophysics
Polish Academy of Sciences

Response/rebuttal to the reviewers' comments

REVIEWER 1:

I would only note that the last paragraph of the Discussion, in which the authors relate their findings to a putative increased "evolvability" weakens their paper considerably. This suggestion, made by True and Lindquist, has been discredited by several groups. A more direct explanation of the current results is that these results are suggestive of why [PSI+] is sufficiently detrimental to host cells that it is not found in the wild (by three groups).

Response

We agree that our results are not related to a putative evolutionary aspect of prion. The text has been changed to emphasize novelty of our hypothesis that [PSI+] may titrate host protein thereby affecting functioning of mitochondria.
We thank the referee for his careful analysis of our conclusions.

Yeast prion [*PSI*$^{+}$] lowers the levels of mitochondrial prohibitins

Jacek Sikora[1], Joanna Towpik[1], Damian Graczyk[1], Michał Kistowski[1], Tymon Rubel[2], Jaroslaw Poznanski[1], James Langridge[3], Chris Hughes[3], Michał Dadlez[1,4], Magdalena Boguta[1,5*]

[1]Institute of Biochemistry and Biophysics, Polish Academy of Sciences, Pawinskiego 5a, 02 106 Warsaw, Poland; Institute of Radioelectronics, Warsaw University of Technology, Nowowiejska 15/19, 00 665 Warsaw, Poland; [3]Waters Corporation, Atlas Park, Simonsway, Manchester, M22 5PP, UK; [4]Institute of Genetics and Biotechnology, Faculty of Biology, University of Warsaw, Miecznikowa 1, 02-116 Warsaw, Poland; [5]Department of Chemistry, Warsaw University of Technology, Noakowskiego 3, 00 664 Warsaw, Poland

**Corresponding author*: Magdalena Boguta, Institute of Biochemistry and Biophysics, Polish Academy of Sciences, Pawińskiego 5a, 02-106 Warsaw, Poland; phone: (4822) 592 1312; fax: (4822) 658 4636; e-mail: magda@ibb.waw.pl

Running title:

Prion-dependent levels of mitochondrial prohibitins

Abstract

We report proteomic analyses that establish the effect of cytoplasmic prion [*PSI*$^{+}$] on the protein complement of yeast mitochondria. A set of 44 yeast mitochondrial proteins whose levels were affected by [*PSI*$^{+}$] was identified by two methods of gel-free and label-free differential proteomics. From this set we focused on prohibitins, Phb1 and Phb2, and the mitochondrially synthesized Cox2 subunit of cytochrome oxidase. By immunoblotting we confirmed the decreased level of Cox2 and reduced mitochondrial localization of the prohibitins in [*PSI*$^{+}$] cells, which both became partially restored by [*PSI*$^{+}$] curing. The presence of the [*PSI*$^{+}$] prion also caused premature fragmentation of mitochondria, a phenomenon linked to prohibitin depletion in mammalian cells. By fractionation of cellular extracts we demonstrated a [*PSI*$^{+}$]-dependent increased of the proportion of prohibitins in the high molecular weight fraction of aggregated proteins. We propose that the presence of the yeast prion causes newly synthesized prohibitins to aggregate in the cytosol, and therefore reduces their levels in mitochondria, which in turn reduces the stability of Cox2 and possibly of other proteins, not investigated here in detail.

1. Introduction

Prions are a unique class of infectious agents whose infectivity relies solely on protein. In mammals, they cause fatal neurodegenerative diseases such as Creutzfeldt-Jacob disease in man, ovine scrapie and bovine spongiform encephalopathy. All these diseases are related to the PrP protein whose conformationally altered form (PrP^{Sc}) is able to convert the normal host-encoded protein (PrP^{C}) into an altered prion form. While only one prion protein is known in mammals, the mammalian prions appear to represent just part of a much wider phenomenon, also being found in lower eukaryotes. In contrast to mammalian prions, those of lower eukaryotes cause non-chromosomal inheritance of phenotypic traits (reviewed in [1, 2]). From a structural point of view prion proteins, and also yeast prions, possess the ability for spontaneous assembly in an autocatalytic process into amyloid [3]. Amyloid-type protein aggregates are characterized by the so-called “cross-beta” alignment of monomeric units, and yeast prions are no exception [4-6]. Yeast prions may be used as a convenient model for elucidation of the factors interacting with human prions and other amyloids.

The yeast prion [*PSI*$^{+}$] is a self-perpetuating conformation of the translation termination factor Sup35 (eRF3) (for a review, see [7]). Sup35 forms a complex with Sup45/eRF1 that is involved in recognizing termination codons and releasing the translation product from the ribosome [8, 9]. The prion state of Sup35 can be propagated for many cellular generations in a stable way. This may be observed as the nonsense suppressor phenotype, [*PSI*$^{+}$], which reflects the reduced function of Sup35 due to aggregation of its prion form. It is noteworthy that [*PSI*$^{+}$] can also induce read-through of stop codons at the end of open reading frames of yeast wild type genes, which could be the reason for the variety of weak phenotypes manifested by [*PSI*$^{+}$] strains [10].

The study of the yeast prion [*PSI*$^{+}$] resulted in the first evidence connecting prions with a cellular stress defense system [11]. Various chaperones can either promote prion propagation and generation or eliminate it from the cell. [*PSI*$^{+}$] and other yeast prions, [*URE3*] and [*PIN*$^{+}$], are

maintained only in the presence of the chaperone Hsp104 (for a review see [1]). It has been shown that increasing or decreasing the level of Hsp104 results in the loss of [*PSI*$^+$]. The stress-inducible Ssa proteins generally help prions to propagate, while constitutively expressed proteins of the Ssb family are prion antagonists [12-14]. Hsp40 co-chaperones, Ydj1 and Sis1, as well as Sse1, a nucleotide exchange factor for Hsp70, exhibit various effects on yeast prions [15, 16]. Although numerous previous attempts have failed, most recent papers proved a physical interaction between Sup35 and Hsp104 in vitro and suggest its existence in vivo]. Sup35, preferentially in the [*PSI*$^+$] state interacts also directly with some other chaperones [17-19].

Our previous work indicated a connection between the yeast prion [*PSI*$^+$] and mitochondria. Although the [*PSI*$^+$] wild type strain exhibited no difference in respiration competence compared to the corresponding [*psi*$^-$], in combination with a mutant Nam9-1 protein of the mitochondrial ribosome [*PSI*$^+$] caused a lack of respiration [20]. This effect of [*PSI*$^+$] in the *nam9-1* mutant correlated with decreased levels of the mitochondrially encoded Cox2 and other subunits of cytochrome oxidase, a hetero-oligomeric protein complex located in the inner mitochondrial membrane. The respiratory deficiency in the *nam9-1* mutant was cured by overproduction or inactivation of Hsp104, exactly the same conditions that eliminate [*PSI*$^+$]. Another prion, [*PIN*$^+$], which often coexists with [*PSI*$^+$], was not known during the time of this study and [*PIN*] status of the *nam9-1* mutant was not determined. However [*PIN*$^+$] is not cured by overproduced Hsp104, therefore [*PIN*$^+$] could be excluded as a potential reason of respiratory deficiency in *nam9-1*. We then considered how the presence of [*PSI*$^+$] aggregates interferes with mitochondrial function. Since it had been reported that proteins can become trapped in [*PSI*$^+$] aggregates [21], we expected that recruitment of proteins interacting with the mitochondrial translation machinery by [*PSI*$^+$] aggregates might account for the respiratory deficiency in the presence of Nam9-1. It was also conceivable that [*PSI*$^+$] aggregates might change the level of cytosolic chaperones required for the translocation of proteins to mitochondria, which in turn might alter the relative level of one or more components of the mitochondrial translation system. Finally, one could expect that [*PSI*$^+$]-induced

stop codon readthrough generates one or more novel mitochondrial proteins bearing an extra C-terminal domain and causing repiratory deficiency in combination with Nam9-1. In this context it was of interest to perform a quantitative comparison of mitochondrial proteins in isogenic [*PSI*$^{+}$] and [*psi*$^{-}$] strains.

The mitochondrial proteome, being a relatively small, but still complicated protein network, has already been studied in considerable detail. Several reports describing the set of mitochondrial proteins from yeast and mammals have been published [22-35]. In addition, different genomic approaches have been integrated to define a complete protein repertoire of the organelle using yeast mitochondria as a model [24]. Moreover, a comprehensive network of protein interactions in a mitochondrial system, as part of the yeast interactome, has been built. This map of the interrelationships among mitochondrial proteins greatly facilitates the interpretation of the results of global analyses of the yeast mitochondrial proteome upon perturbation [36].

Here, global proteomic analysis was applied to search for the differences in the levels of mitochondrial proteins in two isogenic yeast [*psi*$^{-}$] and [*PSI*$^{+}$] strains. This analysis identified 44 candidate proteins of which the levels were significantly changed. The list includes, for instance, Cox2 protein, which was found in a previous study to be downregulated in the presence of [*PSI*$^{+}$]. Two other proteins from the list, prohibitins Phb1 and Phb2, immediate neighbors of Cox2 in the yeast mitochondrial interactome net, were selected for further analysis. Their downregulation in the presence of the prion [*PSI*$^{+}$] and their regulation by Hsp104 level was confirmed by Western blot analysis. Furthermore, fractionation of yeast cell lysates demonstrated [*PSI*$^{+}$]-dependent enrichment of prohibitins in the aggregated protein fraction. Our results indicate that depletion of prohibitins can provide the rationale for the mitochondrial functional defects observed earlier in [*PSI*$^{+}$] yeast cells.

2. Materials and Methods

2.1. Yeast strains and growth conditions

Saccharomyces cerevisiae strain GT197 (*MATα ade1-14 trp1-Δ ura3-52 leu2-3,112 lys2 his3*), referred to as [*psi*-] and the isogenic [*PSI*$^+$] strain GT81-1D [37] were used throughout this study. In the experiment shown in Fig. 2B derivatives of MB43-*nam9-1* (*MATa ura3 his3, his4C nam9-1* [*PSI*$^+$]) [20] were used. In order to prevent glucose repression yeast cells were grown in YPE medium (1% yeast extract, 2% bactopeptone, 2% ethanol) or in low-glucose medium (1% yeast extract, 2% bactopeptone, 0.5% glucose). Cultures were harvested at an optical density of 600 nm (OD_{600}) of 1.5 to 1.7, which corresponded, in the case of the low-glucose medium, to a point of glucose exhaustion, as determined with Glucostix (Bayer).

To assess mitochondria by fluorescence, GT197 [*psi*-] and the isogenic [*PSI*$^+$] GT81-1D strains were transformed with pYX323-mtGFP plasmid (2 μ, *TRP1*) encoding green florescence protein (GFP) with a mitochondrial localization sequence [38] .Transformants were grown in minimal SC-trp medium (0.67% yeast nitrogen base, 2% glucose) supplemented with all amino acids except tryptophan. Cells were harvested at OD_{600} = 1.2. Neither [*psi*-] nor the [*PSI*$^+$] strain has a tendency to become *rho*$^-$.

2.2. Isolation of mitochondria

Isolation of mitochondria was accomplished by differential centrifugation according to [39]. Crude mitochondria (protein concentration of 5 mg/ml) were suspended in SEM buffer (250 mM sucrose, 1 mM EDTA, 10 mM MOPS, pH 7.2) ensuring proper osmotic pressure for maintenance of organelle integrity and prevention of its decomposition. The suspension of crude mitochondria was loaded onto a three-step sucrose gradient composed of 1.5 ml 60%, 4 ml 32%, 1.5 ml 23% and 1.5 ml 15% sucrose in EM-buffer (1 mM EDTA, 10 mM MOPS, pH 7.2) and centrifuged for 1 h at 134 000 x g, yielding highly pure mitochondria at the 60/32% sucrose interface. The sucrose gradient step was performed twice.

2.3. Differential proteomics experiments

Two methods were used for identification of proteins differentially populated in the two [*psi*$^-$] and

[*PSI*$^+$] strains analyzed. Their detailed description is given in the Supporting Material and Method Section. In brief, in the first method, further referred to as FTICR, the protein ratios were measured by comparing the amplitudes of their corresponding peptide signals in the MS spectra obtained from a mitochondrial proteome tryptic peptide mixture in LC-MS experiments using an LTQ FTICR (Thermo) mass spectrometer. In the second method, further referred to as WPES, a commercially available Waters Protein Expression System, designed to carry out differential proteomics experiments, was used to extract differentially populated proteins. The final selection of mitochondrial proteins sensitive to the presence of the cytoplasmic prion [*PSI*$^+$] was based on statistical validation of the results of replicate experiments.

2.4. Peptide isoelectrofocusing

Peptide isoelectrofocusing was carried out as described previously [40] with a minor change to the protocol, as follows: 100 μg of proteins in 100 μl of 100 mM ammonium bicarbonate pH 8.5 was denatured for 5 min at 98 °C and cooled on ice. Ten microliters of modified sequencing grade trypsin (Promega), 100 ng/μl, was added and the samples were incubated o/n at 37 °C. The protein digest was dried in a speed-vac and suspended in 340 μl of sample buffer (7 M urea, 2 M thiourea, 2% Chaps, 0.5% β-mercaptoethanol, 0.006% IPG buffer pH 3.5–5.0 (Amersham). To remove insoluble material centrifugation at 15000 x g was performed for 15 min and supernatant was used for overnight passive rehydration of an 18 cm strip of the gel (pH 3.5–4.5) in IPG buffer. IEF was performed on a Multiphor II electrophoresis system (Amersham) using a three-step gradient program as follows: step 1: 500 V, 2 mA, 2 W, 1 h; step 2: 1000 V, 2 mA, 2 W, 2 h; step 3: 3500 V, 2 mA, 4 W, 45 h.

Following IEF, the strip was cut into ten pieces and peptides were eluted three times with 100 μl 0.1% TFA, 2% acetonitrile. Pooled fractions were filtered through a 50 kDa cut-off cellulose membrane (Millipore) and concentrated on a speed-vac. Qualitative analysis (protein identification) was carried out using merged datasets obtained for each of the ten pieces of the IPG strip, as described in Supporting Material Section S1 for the LTQ-FTICR qualitative analysis step.

2.5. Fractionation of yeast cell lysates

For the experiment presented in Fig. 2C, total cellular protein was extracted by alkaline lysis as described previously [41]. For the fractionation of aggregates (experiment presented in Fig. 3), cells were lysed by vortexing with glass beads in buffer A (25 mM Tris-HCl, pH 7.5, 50 mM KCl, 10 mM $MgCl_2$, 1 mM EDTA, 2% glycerol) along with 1 mM PMSF, 2 µg/ml aprotinin, 1 µg/ml pepstatin A, 0.5 µg/ml leupeptin, 2.5 µg/ml anti-pain, 0.5 µg/ml TLCK, 0.5 µg/ml TPCK, 0.1 mM benzamidine and 0.1 mM sodium metabisulfite. Cell debris and mitochondria were removed by centrifugation at 15, 000 × g for 10 min. Obtained supernatants were treated with RNase A (400 µg/ml) to disrupt polyribosomes. Extracts were then subjected to centrifugation through a sucrose cushion (1 ml of 30% sucrose in buffer A) in an SW50 rotor at 45 000 r.p.m. for 30 min at 4 °C. The resulting supernatants, intermediate fractions and pellets were analyzed by Western blotting.

2.6. Western blotting

For immunoblotting, protein extracts were separated by SDS-PAGE gels and transferred electrophoretically onto a nitrocellulose membrane (Millipore). After immunodecoration with the desired primary antibody, membranes were incubated with anti-rabbit or anti-mouse horseradish peroxidase-conjugated secondary antibody. Reaction with Immobilon Western Chemiluminescent HRP Substrate (Millipore) was performed according to the manufacturer's instructions and light emitted was subsequently captured on X-ray film (Amersham). Films were quantified using ImageQuant (GE Healthcare Life Sciences) with local average background correction.

2.7. Confocal microscopy

Cells were washed with water, plated on microscope glass slides and subjected to confocal laser scanning microscopy. An Eclipse TE2000-E microscope (Nikon), equipped with a Plan Apo 60X oil objective was used. mtGFP was excited with an Argon-Ion laser at 488 nm, and emission was detected at 515/30 nm. Images were collected with the EZ-C1 Confocal v. 3.6 program (Nikon) and then processed with EZ-C1 Viewer v. 3.6 (Nikon) and Adobe Photoshop 8.0.

3. Results

3.1. Analysis of mitochondrial proteome

Mitochondria were isolated from *Saccharomyces cerevisiae* prion-free strain GT197 referred to as [*psi*-] and the isogenic strain GT81-1D containing [PSI^+] referred to as [PSI^+]. Both [*psi*-] and [PSI^+] strains are respiratory competent and mitochondria were isolated using a standard fractionation procedure. The identification of mitochondrial proteins derived from [PSI^+] and [psi^-] strains was carried out by several rounds of LC-MS-MS/MS (Liquid Chromatography coupled to Mass Spectrometry in data-dependent switch to fragmentation mode) experiments using an LTQ FTICR spectrometer, as described in the Supporting Material and Method Section. The obtained list of 1275 mitochondrial proteins was compared with the mitochondrial proteome characterized previously by other authors [22-28], (Supporting Material Table S1). In all, 972 (76%) proteins were indicated as mitochondrial in earlier either MS-based or "*in silico*" studies (Supporting Material Fig. S1). We identified 34 mitochondrial proteins that are present in the MREF mitochondrial database [42] although, to our knowledge, they have not been identified previously by MS-based studies on the *S. cerevisiae* mitochondrial proteome[22-27], Prokish-unpublished dataset, [28] (Supporting Material Table S2). Our list of proteins contains representatives of 45 out of the 46 major functional modules of the yeast mitochondrial interactome constructed by Perocchi and co-workers [36] (Supporting Material Fig. S2 and Table S3).

Similarly to other proteomic studies, the number of detected proteins was higher than the number of proteins in the accepted mitochondrial reference set. Two factors may explain this apparent inconsistency. First, it is possible that the mitochondrial reference set is not yet complete and that the detected proteins are new mitochondrial proteins, or second, our preparation procedure did not fully eliminate non-mitochondrial proteins. It has to be noted, however, that the main aim of our experiment was to identify differential proteins between [PSI^+] and [psi^-] strains. Therefore the possible presence of non-mitochondrial proteins does not compromise the validity of our results.

In conclusion, our identification of mitochondrial proteins in [PSI^+] and [psi^-] strains,

proved to be of comparable quality to previous protein identification efforts. Thus we can state that the set of mitochondrial proteins considered in the differential analysis is reasonably complete and representative.

3.2. Prohibitins and Cox2 among proteins identified by differential proteomics of the mitochondria of [*PSI*$^+$] and [*psi*$^-$] strains

To obtain a list of proteins of which the levels are affected by the presence of prion [*PSI*$^+$], two independent methods of differential proteomics, named FTICR and WPES, were used and each was repeated three times (see the Supporting Material and Method Section for details of the methods, the statistical analysis and hit acceptance criteria). Figure 1 shows the comparison of protein level as the [*PSI*$^+$]/[*psi*$^-$] ratios. Forty-one of these proteins showed the same direction of expression changes in both experiments (Supporting Material Table S4). This fairly large number of detected differential proteins indicates that the presence of prion [*PSI*$^+$] in the yeast cytoplasm induces a complex response in mitochondria.

[*PSI*$^+$]-dependent proteins identified in our experiment belong to several annotation categories. [*PSI*$^+$] mitochondria showed decreased levels of several subunits of respiratory complexes, such as Cox2, Atp1, Atp2, Atp3 and Sdh1. There were also decreased levels of some enzymes of isocitrate metabolism. In addition we observed marked changes in the levels of some chaperones and receptors involved in mitochondrial protein import, such as Tom40, Tim13 and Ssc1. The identification of these proteins as affected by [*PSI*$^+$] links the prion with the reorganization of the mitochondrial import apparatus. Interestingly, both prohibitins Phb1 and Phb2 were also downregulated in the [*PSI*$^+$] mitochondria. Phb1 and Phb2 prohibitins act as membrane-bound chaperones involved in the stabilization of mitochondrial translation products including Cox2 [43-45]. Because of this relation, Cox2 and prohibitins are immediate neighbors in the yeast mitochondrial interactome [46] (Supporting Material Fig. S3). Moreover, Cox2 is known to be involved in prion-dependent phenomena in yeast [20]. Encouraged by the known functional links between Cox2, Phb1 and Phb2, we focused our attention on these three proteins.

Two independent proteomic methods showed that Cox2 and the two prohibitins, Phb1 and Phb2, are less abundant in mitochondria in [*PSI*$^+$] cells. In the [*PSI*$^+$] strain the Cox2 level was decreased over 3.5 fold (p=0.0048). The [*PSI*$^+$]/[*psi*$^-$] ratio for Cox2 was estimated on the basis of eleven peptides in FTICR and eight in the WPES experiment, respectively. Phb1 was decreased 1.9 fold (p=0.058) as estimated on the basis of seven peptides in FTICR and ten in WPES. For Phb2 17 peptides in FTICR, and 11 in WPES were used for ratio calculation giving a 1.3 fold decrease in [*PSI*$^+$] cells (p=0.11). The signal amplitude values of Phb1, Phb2 and Cox2 peptides are presented in the Supporting Material, Fig. S4.

3.3. Reduced levels of Cox2 and prohibitins in [*PSI*$^+$] mitochondria detected by immunoblotting

To provide independent confirmation of the MS differential analyses, mitochondria isolated from [*psi*$^-$] and [*PSI*$^+$] cells were analyzed by Western blotting with specific antibodies. The results (Fig. 2A) reproducibly confirm that the presence of [*PSI*$^+$] reduces the levels of mitochondrial Cox2, Phb1 and Phb2. We next investigated whether the amount of mitochondrial prohibitins was affected by curing of cells from [*PSI*$^+$]. Yeast may be cured from the [*PSI*$^+$] prion by overexpression or deletion of the gene encoding the Hsp104 chaperone [1, 2, 11]. We took advantage of two observations: first, that [*PSI*$^+$] curing by Hsp104 stabilized Cox2 in the MB43-*nam9-1* strain [20] and second, that prohibitins are known to stabilize mitochondrially synthesized proteins, including Cox2 [43-45]. Thus we considered the possibility that [*PSI*$^+$] curing may increase the levels of prohibitins in mitochondria and that this effect is a prerequisite for Cox2 stabilization. Indeed, the Western blot analysis of the mitochondria (Fig. 2B) showed that deletion or overexpression of the *HSP104* gene in [*PSI*$^+$] MB43-*nam9-1* cells resulted in an increase in Phb1 and Phb2 levels. These results clearly indicate a link between curing of the [*PSI*$^+$] prion and the levels of prohibitins and Cox2 in mitochondria.

For quantification, the intensities of bands were measured using nuclear-encoded mitochondrial malate dehydrogenase Mdh1 as an internal control. The results of MS and Western analyses

comparing the effect of [*PSI*$^+$] were consistent, even in cells of different genetic background (Table 1). Cox2 is a mitochondrially synthesized protein, the stability of which is known to be prion-dependent [20], and our work confirmed this. In contrast, prohibitins are synthesized in the cytoplasm and then imported to mitochondria. The observed decrease in the amount of mitochondrial prohibitins might result from their lower synthesis in [*PSI*$^+$] cells. Interestingly, Western blot analysis of total yeast extracts shows a decreased amount of Cox2 in the [*PSI*$^+$] strain, but does not reveal differences between the levels of prohibitins in the [*psi*$^-$] and [*PSI*$^+$] strains (Fig. 2C). This suggests that the observed depletion of mitochondrial prohibitins was due to their inefficient import into the mitochondria in cells with the [*PSI*$^+$] prion.

3.4. [*PSI*$^+$] causes enrichment of prohibitins in the cellular aggregates fraction

[*PSI*$^+$] is the prion conformation of the Sup35 protein, a cytoplasmic translation termination factor. [*PSI*$^+$] affected the levels of mitochondrial prohibitins but not their total amount in the yeast cell (Fig. 2), suggesting a defect in intracellular distribution. This might be due to a physical interaction of prohibitins with Sup35 aggregates occurring in the cytoplasm and affecting their import to mitochondria.

It has previously been shown that Sup35 forms high-molecular-weight aggregates in [*PSI*$^+$] cells, co-sedimenting with the heavy polyribosomal fraction and even larger structures [47]. Thus distribution of prohibitins between the soluble and aggregated fractions could be influenced by the [*PSI*] status of the cells. To check this, extracts of isogenic [*psi*$^-$] and [*PSI*$^+$] strains were prepared using the clarifying spin to eliminate the remaining mitochondria (see Materials and Methods). Extracts were fractionated by centrifugation through a sucrose cushion, and the fractions were analyzed by immunoblotting using antibodies against Sup35, Phb1 and Phb2. In agreement with previous results [47], after centrifugation most of the Sup35 protein was found in the pellet fraction in the [*PSI*$^+$] strain, whereas in the [*psi*$^-$] strain Sup35 remained in the supernatant (Fig. 3, upper panel). Prohibitins were detected almost exclusively in the pellet fraction, although some remained in the sucrose cushion. The presence of prohibitins in the pellet cannot be attributed to the residual

presence of contaminating mitochondria, as their absence was carefully controlled by the absence of the other mitochondrial protein, aconitase (Aco1) in the pellet. Interestingly, both Phb1 and Phb2 were relatively more abundant in the pellet fraction from the [*PSI*$^+$] strain than in the respective fraction from the [*psi*$^-$] strain (Fig. 3, lower panel). This suggests that prohibitins are partially trapped by cytoplasmic [*PSI*$^+$] prion aggregates, which in turn should decrease their availability for import into the mitochondria.

3.5. [*PSI*$^+$] causes premature fragmentation of mitochondria

The yeast mutants with inactive prohibitin showed abnormal mitochondrial morphology and defects of mitochondria segregation, especially in old cells [48]. A recent study in mammals revealed that prohibitins determine cristae morphogenesis and formation of tubular mitochondrial ultrastructures, since 90% of PHB2-deficient mouse cells contained fragmented mitochondria [49]. We explored the possibility that [*PSI*$^+$] could indirectly affect fusion of mitochondria in yeast by reduction of the levels of mitochondrial prohibitins. To investigate mitochondrial ultrastructure, [*psi*$^-$] and [*PSI*$^+$] cells were transformed with pYX323-mtGFP plasmid (2 μ, *TRP1*) encoding green fluorescent protein (GFP) containing a mitochondrial localization signal. To prevent the loss of plasmid, cells were cultivated in minimal medium lacking tryptophan. The growth rate was controlled by OD measurements, indicating no difference between [*psi*$^-$] and [*PSI*$^+$] strains. Cells were harvested at the same point in the late logarithmic phase and examined by confocal microscopy. Strikingly, [*PSI*$^+$] cells contained 95% of fragmented mitochondria whereas the majority of [*psi*$^-$] cells in the same phase contained regular tubular mitochondrial ultrastructures (Fig. 4). This showed premature fragmentation of mitochondria in [*PSI*$^+$] cells, providing a link between the presence of cytoplasmic prion [*PSI*$^+$] and defects in mitochondrial fusion, which may be caused by reduced prohibitins (see Discussion).

4. Discussion

Several years ago it was reported that stability of the mitochondria-encoded respiratory chain subunit Cox2 in a mitochondrial ribosomal mutant *nam9-1* depends on the yeast prion [PSI^+] [20]. This observation is striking because the prion is located in the cytosol, whereas the synthesis and assembly of Cox2 takes place in mitochondria. In order to obtain a better insight into this unexpected relation, we used a proteomics approach to search for differences in the levels of mitochondrial proteins in prion-positive [PSI^+] and prion-negative [psi^-] cells. We obtained a list of 44 mitochondrial proteins showing altered abundance depending on the presence of [PSI^+]. Among those were Cox2 and several other subunits of cytochrome oxidase and mitochondrial ATPase. Importantly, the levels of the two prohibitins, Phb1 and Phb2, were also reduced in mitochondria of [PSI^+] cells.

Prohibitins are evolutionarily conserved eukaryotic proteins that assemble in a large ring complex bound to inner mitochondrial membrane [51-53].. Earlier findings in yeast identified prohibitins in assemblies with ATP-dependent protease m-AAA involved in chaperoning and turnover of mitochondrial inner membrane proteins [43, 44]. Yeast mutants lacking functional prohibitins show accelerated proteolysis by m-AAA protease suggesting a regulatory role of prohibitins in the quality control of proteins in inner membrane [45, 50]. Phb1/2 complex, reminiscent of Hsp60-like chaperones, is proposed to act as a novel type of membrane-associated chaperone/holdase involved in higher order organization of respiratory chain complexes [51-53].

Using molecular methods provide evidence that Phb1, Phb2 and Cox2 are less abundant in mitochondria in [PSI^+] cells, thus confirming proteomic results and suggesting lowered mitochondrial prohibitins as a potential reason of Cox2 destabilization.

Another function of prohibitins described recently in mammals is the processing of the dynamin-like GTPase OPA1, an essential component of the mitochondrial fusion machinery [49]. OPA1 is a homologue of yeast Mgm1 protein also involved in mitochondria fusion [54]. Both OPA1 and Mgm1 exist in forms of different lengths and their function is regulated by proteolytic cleavage [55, 56] Only a long form of OPA1 (L-OPA1) is fusion competent [55], and maintenance of this

form requires prohibitins [49]. Depletion of prohibitins induces L-OPA1-dependent fragmentation of mitochondria and apoptosis. The mechanism underlying the selective loss of L-OPA1 in the absence of prohibitins remains to be elucidated [57].

Here we detected [*PSI*$^+$]-dependent premature fragmentation of yeast mitochondria in post-exponential growth phase. It is currently unknown whether the low level of mitochondrial prohibitins in [*PSI*$^+$] cells can provide the rationale for the observed negative effect on mitochondrial fusion. One interesting hypothesis is that depletion of prohibitins could contribute to the defect in the function of Mgm1, the OPA1 homologue, in the fusion of yeast mitochondria. Although Mgm1 processing is not strictly required for mitochondrial fusion [58], the balanced formation or regulated inter-conversion of the two isoforms of Mgm1 appear crucial [59]. Characterization of the effect of prohibitins on Mgm1 requires further study. Among the other mitochondrial proteins found to be affected by [*PSI*$^+$] in this work, the presence of Hsp78 is remarkable, because this chaperone functions in restoration of the mitochondrial network following heat stress [60].

Although the overall level of expression of prohibitins is the same in the [*PSI*$^+$] and [*psi*$^-$] strains, the *PSI* status affects their distribution within the cell. We were interested in why the mitochondrial localization of prohibitins was reduced by the [*PSI*$^+$] prion state. Fractionation of mitochondria-free lysates for soluble and aggregate parts showed enrichment of prohibitins in the aggregate fraction in [*PSI*$^+$] cells. This result suggests some interaction of Phb1/Phb2 with [*PSI*$^+$] possibly leading to sequestration of prohibitins by prion aggregates. The effect of [*PSI*$^+$] on sequestering of another cytoplasmic protein, translation termination factor Sup45, has been studied in the past, but the results were controversial. Sup45 was reported to be present in [*PSI*$^+$] aggregates in some [21, 61] but not other studies [62] and a decisive model of Sup45 sequestering is lacking. Similarly, further experiments are required to demonstrate and characterize a specific interaction of prohibitins with [*PSI*$^+$] aggregates. Here we just propose that the newly synthesized prohibitins are titrated by [*PSI*$^+$] aggregates in the cytosol before they reach mitochondrial location and therefore their level in mitochondria is lowered, which in turn reduces the stability of Cox2. Moreover, we

believe that prohibitins are not the only component mediating the effect of the [*PSI*$^+$] prion on mitochondrial function and the roles of other mitochondrial proteins identified by our proteomic study is worth to study as well.

A different scenario may be proposed of how presence of [*PSI*$^+$] aggregates interferes with mitochondrial function. Inefficient termination in cells containing [*PSI*$^+$] potentially allows for readthrough of stop codons nuclear mRNAs. Leakiness of stop codons is considered to be the reason for a variety a weak phenotypes manifested by [*PSI*$^+$] strains [10]. Nuclear-encoded mitochondrial proteins might be expressed in a C-terminally extended version(s) when low levels of functional Sup35 allow readthrough of nonsense codons. However, in this and other published studies no experimental evidence of C-terminally extended proteins in [*PSI*$^+$] mitochondria has been found.

The overall data presented here support the model that in *S. cerevisiae* the prion [*PSI*$^+$] interacts with prohibitins and possibly other proteins in the cytosol and thereby alters their distribution to mitochondria. Thus the hidden phenotypic variation generated by [*PSI*$^+$] may result from subtle alteration in sorting of particular proteins between cellular compartments. It is possible that some of the [*PSI*$^+$] manifestations can be related to the ability of Sup35 prion aggregates to titrate host proteins with important functions though this suggestion has never been supported.

Acknowledgments

We are grateful to Michael Ter-Avanesyan and Agnieszka Chacińska for critical reading of the manuscript. Help of Hans Vissers in the training in WPES software, technical help of Anna Anielska in confocal microscopy and Marta Tkaczyk in peptide IEF is kindly acknowledged. We thank Yury Chernoff for the strains, Thomas Langer for the Phb1 and Phb2 antibodies, Michael Ter-Avanesyan for the Sup35 antibodies and Róża Kucharczyk for the pYX323-mtGFP plasmid. This work was supported by the Ministry of Science and Higher Education, Poland (grants N301 023 32/1117 and 4/0-PBZ-MinI-2/1/2005, R130103) and the MITONET network.

Figure Legends

Fig. 1 . **Proteins showing [*PSI*$^+$]-dependent abundance in yeast mitochondria.** The [*PSI*$^+$]/[*psi*$^-$] ratios of differential proteins (log scale) detected by the two independent differential proteomic methods: FTICR and WPES (see text). The ratio obtained for each protein with the FTICR method is shown as a red bar and with WPES as a black bar, and the corresponding protein name abbreviation is marked along the upper horizontal axis. For the majority of proteins (41 out of 44) both methods gave the same direction of change i.e. up- or downregulation, however, the degree of change was often substantially different. Note the Phb1, Phb2 and Cox2 proteins (marked in green) downregulated in [*PSI*$^+$], as described in detail in the text.

Fig. 2.

[*PSI*$^+$] decreases amounts of Phb1, Phb2 and Cox2 in mitochondria.

Western blot analysis of Cox2, Phb1 and Phb2 levels in mitochondrial (**A, B**) and total protein extracts (**C**) prepared by alkaline lysis. Proteins were isolated from isogenic [*psi*$^-$] and [*PSI*$^+$] strains GT197 and GT81-1D (**A, C**) or isogenic derivatives of MB43-*nam9-1* strain cured from [*PSI*$^+$] by deletion [*Δ*] or overexpression [↑] of the *HSP104* gene (**B**). The levels of Hsp104 were determined in the total extracts. Mitochondrial malate dehydrogenase (Mdh1) was used as a loading control.

.

Fig. 3. Abundance of prohibitins in cellular aggregates depends on the [*PSI*] state of the cell.

Lysates of [*psi*$^-$] and [*PSI*$^+$] strains (GT197 and GT81-1D) were prepared as described in the Materials and Methods and were fractionated by centrifugation through a sucrose cushion. The distribution of Phb1, Phb2 and Sup35 between the supernatant soluble fraction, sucrose layer and high molecular structures in the pellet was determined by immunoblotting. To confirm that other mitochondrial proteins are not present in the pellet, the blot was also decorated with an antibody specific for aconitase Aco1, the protein imported to mitochondria from the cytoplasm. The gel was loaded using 20 μg of protein per lane for the supernatant and sucrose fractions and 5 μg of protein per lane for the pellet fraction.

Fig. 4. Fragmentation of mitochondria in prohibitin-deficient [*PSI*$^+$] cells.

[*psi*$^-$] and [*PSI*$^+$] strains (GT197 and GT81-1D) were transformed with pYX323-mtGFP plasmid encoding green fluorescence protein (GFP) with a mitochondrial localization sequence and analyzed by confocal laser scanning microscopy. Reconstruction of the mitochondrial network was done from about ten confocal sections with intervals of 0.5 μm and 1024 x 1024 resolution. The images presented are representative for [*psi*$^-$] and [*PSI*$^+$] cells. More than 400 cells were scored per experiment. The percentage of cells with tubular mitochondria is indicated.

Table Legends

Table 1

Levels of Phb1, Phb2 and Cox2 in [*PSI*$^+$] versus [*psi*$^-$] mitochondria.

[*PSI*$^+$]/[*psi*$^-$] protein ratios were measured by densitometry of Western blots and by differential proteomics.

In order to determine the relative amount of proteins in [*PSI*$^+$] and [*psi*$^-$] strains by immunoblotting, the amount of each protein present in [*PSI*$^+$], corrected by the loading control, was set to 1. Column 1 represents the quantified results of immunoblotting analysis of Phb1, Phb2 and Cox2 in mitochondria from [*PSI*$^+$] and [*psi*$^-$] strains GT197 and GT81-1D (Fig. 2A). Columns 2 and 3 show the quantified results of the immunoblotting analysis of Phb1 and Phb2 in mitochondria from different pairs of isogenic [*PSI*$^+$] and [*psi*$^-$] strains in the genetic background of MB43-*nam9-1*:: [*PSI*$^+$] and its [*psi*$^-$] derivative derived by deletion (column 2) or overexpression (clolumn 3) of the gene encoding Hsp104 chaperone (Fig. 2C). The complex effect of Hsp104 on Cox2 levels in [*PSI*$^+$] cells was determined previously [20]

[*PSI*$^+$]/[*psi*$^-$] protein ratios for Phb1, Phb2 and Cox2 were determined independently by using two MS-based methods, FTICR and WPES, as described in the text and presented in the Supporting Material (Table S4, Fig. S4). Of note is the consistency between the numbers obtained by each method.

Protein name	**[*PSI*$^+$]/[*psi*$^-$] ratio**				
	Western blots			**Differential proteomics**	
	1	**2**	**3**	**WPES**	**FTICR**
Phb1	**0.68**	**0.52**	**0.65**	**0.60**	**0.53**
Phb2	**0.34**	**0.44**	**0.40**	**0.71**	**0.75**
Cox2	**0.41**	**Nd**	**nd**	**0.41**	**0.28**

Table 1.

References:

[1] R.B. Wickner, H.K. Edskes, E.D. Ross, M.M. Pierce, U. Baxa, A. Brachmann and F. Shewmaker, Prion genetics: new rules for a new kind of gene., Annu Rev Genet, 38 (2004) 681-707.

[2] J. Shorter and S. Lindquist, Prions as adaptive conduits of memory and inheritance., Nat Rev Genet, 6 (2005) 435-450.

[3] K.J. Barnham, R. Cappai, K. Beyreuther, C.L. Masters and A.F. Hill, Delineating common molecular mechanisms in Alzheimer's and prion diseases., Trends Biochem Sci, 31 (2006) 465-472.

[4] J.R. Glover, A.S. Kowal, E.C. Schirmer, M.M. Patino, J.J. Liu and S. Lindquist, Self-seeded fibers formed by Sup35, the protein determinant of [PSI+], a heritable prion-like factor of S. cerevisiae., Cell, 89 (1997) 811-819.

[5] F. Shewmaker, E. Ross, R. Tycko and R. Wickner, Amyloids of Shuffled Prion Domains That Form Prions Have a Parallel In-Register beta-Sheet Structure., Biochemistry, 47 (2008) 4000-4007.

[6] R.B. Wickner, F. Dyda and R. Tycko, Amyloid of Rnq1p, the basis of the [PIN+] prion, has a parallel in-register beta-sheet structure., Proc Natl Acad Sci U S A, 105 (2008) 2403-2408.

[7] V.V. Kushnirov and M.D. Ter-Avanesyan, Structure and replication of yeast prions., Cell, 94 (1998) 13-16.

[8] I. Stansfield, K.M. Jones, V.V. Kushnirov, A.R. Dagkesamanskaya, A.I. Poznyakovski, S.V. Paushkin, C.R. Nierras, B.S. Cox, M.D. Ter-Avanesyan and M.F. Tuite, The products of the SUP45 (eRF1) and SUP35 genes interact to mediate translation termination in Saccharomyces cerevisiae., EMBO J, 14 (1995) 4365-4373.

[9] G. Zhouravleva, L. Frolova, X. Le Goff, R. Le Guellec, S. Inge-Vechtomov, L. Kisselev and M. Philippe, Termination of translation in eukaryotes is governed by two interacting

polypeptide chain release factors, eRF1 and eRF3, EMBO J, 14 (1995) 4065-72.
[10] H.L. True, I. Berlin and S.L. Lindquist, Epigenetic regulation of translation reveals hidden genetic variation to produce complex traits., Nature, 431 (2004) 184-187.
[11] Y.O. Chernoff, S.L. Lindquist, B. Ono, S.G. Inge-Vechtomov and S.W. Liebman, Role of the chaperone protein Hsp104 in propagation of the yeast prion-like factor [psi+]. Science, 268 (1995) 880-884.
[12] V.V. Kushnirov, D.S. Kryndushkin, M. Boguta, V.N. Smirnov and M.D. Ter-Avanesyan, Chaperones that cure yeast artificial [PSI+] and their prion-specific effects., Curr Biol, 10 (2000) 1443-1446.
[13] A. Chacinska, B. Szczesniak, N.V. Kochneva-Pervukhova, V.V. Kushnirov, M.D. Ter-Avanesyan and M. Boguta, Ssb1 chaperone is a [PSI+] prion-curing factor., Curr Genet, 39 (2001) 62-67.
[14] Y. Tutar, Y. Song and D.C. Masison, Primate chaperones Hsc70 (constitutive) and Hsp70 (induced) differ functionally in supporting growth and prion propagation in Saccharomyces cerevisiae., Genetics, 172 (2006) 851-861.
[15] R. Aron, T. Higurashi, C. Sahi and E.A. Craig, J-protein co-chaperone Sis1 required for generation of [RNQ+] seeds necessary for prion propagation, EMBO J, 26 (2007) 3794-803.
[16] D. Kryndushkin and R.B. Wickner, Nucleotide exchange factors for Hsp70s are required for [URE3] prion propagation in Saccharomyces cerevisiae, Mol Biol Cell, 18 (2007) 2149-54.
[17] J. Shorter and S. Lindquist, Hsp104, Hsp70 and Hsp40 interplay regulates formation, growth and elimination of Sup35 prions., EMBO J, 27 (2008) 2712-2724.
[18] S.N. Bagriantsev, E.O. Gracheva, J.E. Richmond and S.W. Liebman, Variant-specific [PSI+] infection is transmitted by Sup35 polymers within [PSI+] aggregates with heterogeneous protein composition., Mol Biol Cell, 19 (2008) 2433-2443.
[19] K.D. Allen, R.D. Wegrzyn, T.A. Chernova, S. Muller, G.P. Newnam, P.A. Winslett, K.B. Wittich, K.D. Wilkinson and Y.O. Chernoff, Hsp70 chaperones as modulators of prion life cycle: novel effects of Ssa and Ssb on the Saccharomyces cerevisiae prion [PSI+], Genetics, 169 (2005) 1227-42.
[20] A. Chacinska, M. Boguta, J. Krzewska and S. Rospert, Prion-dependent switching between respiratory competence and deficiency in the yeast nam9-1 mutant., Mol Cell Biol, 20 (2000) 7220-7229.
[21] K. Czaplinski, M.J. Ruiz-Echevarria, S.V. Paushkin, X. Han, Y. Weng, H.A. Perlick, H.C. Dietz, M.D. Ter-Avanesyan and S.W. Peltz, The surveillance complex interacts with the translation release factors to enhance termination and degrade aberrant mRNAs., Genes Dev, 12 (1998) 1665-1677.
[22] D. Pflieger, J.-P.L. Caer, C. Lemaire, B.A. Bernard, G.v. Dujardin and J. Rossier, Systematic identification of mitochondrial proteins by LC-MS/MS., Anal Chem, 74 (2002) 2400-2406.
[23] S. Ohlmeier, A.J. Kastaniotis, J.K. Hiltunen and U. Bergmann, The yeast mitochondrial proteome, a study of fermentative and respiratory growth., J Biol Chem, 279 (2004) 3956-3979.
[24] H. Prokisch, C. Scharfe, D.G. Camp, W. Xiao, L. David, C. Andreoli, M.E. Monroe, R.J. Moore, M.A. Gritsenko, C. Kozany, K.K. Hixson, H.M. Mottaz, H. Zischka, M. Ueffing, Z.S. Herman, R.W. Davis, T. Meitinger, P.J. Oefner, R.D. Smith and L.M. Steinmetz, Integrative analysis of the mitochondrial proteome in yeast., PLoS Biol, 2 (2004) e160.
[25] A. Sickmann, J. Reinders, Y. Wagner, C. Joppich, R. Zahedi, H.E. Meyer, B. Schonfisch, I. Perschil, A. Chacinska, B. Guiard, P. Rehling, N. Pfanner and C. Meisinger, The proteome of Saccharomyces cerevisiae mitochondria, Proc Natl Acad Sci U S A, 100 (2003) 13207-12.
[26] R.P. Zahedi, A. Sickmann, A.M. Boehm, C. Winkler, N. Zufall, B. Schonfisch, B. Guiard, N. Pfanner and C. Meisinger, Proteomic analysis of the yeast mitochondrial outer membrane reveals accumulation of a subclass of preproteins, Mol Biol Cell, 17 (2006) 1436-50.
[27] J. Reinders, R.P. Zahedi, N. Pfanner, C. Meisinger and A. Sickmann, Toward the complete

yeast mitochondrial proteome: multidimensional separation techniques for mitochondrial proteomics, J Proteome Res, 5 (2006) 1543-54.
[28] J. Reinders, K. Wagner, R.P. Zahedi, D. Stojanovski, B. Eyrich, M. van der Laan, P. Rehling, A. Sickmann, N. Pfanner and C. Meisinger, Profiling phosphoproteins of yeast mitochondria reveals a role of phosphorylation in assembly of the ATP synthase, Mol Cell Proteomics, 6 (2007) 1896-906.
[29] S.P. Gaucher, S.W. Taylor, E. Fahy, B. Zhang, D.E. Warnock, S.S. Ghosh and B.W. Gibson, Expanded coverage of the human heart mitochondrial proteome using multidimensional liquid chromatography coupled with tandem mass spectrometry., J Proteome Res, 3 (2004) 495-505.
[30] S.W. Taylor, E. Fahy, B. Zhang, G.M. Glenn, D.E. Warnock, S. Wiley, A.N. Murphy, S.P. Gaucher, R.A. Capaldi, B.W. Gibson and S.S. Ghosh, Characterization of the human heart mitochondrial proteome., Nat Biotechnol, 21 (2003) 281-286.
[31] P. Lescuyer, J.M. Strub, S. Luche, H. Diemer, P. Martinez, A. Van Dorsselaer, J. Lunardi and T. Rabilloud, Progress in the definition of a reference human mitochondrial proteome, Proteomics, 3 (2003) 157-67.
[32] X. Xie, H.H. Wilkinson, A. Correa, Z.A. Lewis, D. Bell-Pedersen and D.J. Ebbole, Transcriptional response to glucose starvation and functional analysis of a glucose transporter of Neurospora crassa., Fungal Genet Biol, 41 (2004) 1104-1119.
[33] M. Fountoulakis and E.J. Schlaeger, The mitochondrial proteins of the neuroblastoma cell line IMR-32, Electrophoresis, 24 (2003) 260-75.
[34] V.K. Mootha, J. Bunkenborg, J.V. Olsen, M. Hjerrild, J.R. Wisniewski, E. Stahl, M.S. Bolouri, H.N. Ray, S. Sihag, M. Kamal, N. Patterson, E.S. Lander and M. Mann, Integrated analysis of protein composition, tissue diversity, and gene regulation in mouse mitochondria., Cell, 115 (2003) 629-640.
[35] S.D. Cruz, I. Xenarios, J. Langridge, F. Vilbois, P.A. Parone and J.-C. Martinou, Proteomic analysis of the mouse liver mitochondrial inner membrane., J Biol Chem, 278 (2003) 41566-41571.
[36] F. Perocchi, L.J. Jensen, J. Gagneur, U. Ahting, C. von Mering, P. Bork, H. Prokisch and L.M. Steinmetz, Assessing systems properties of yeast mitochondria through an interaction map of the organelle., PLoS Genet, 2 (2006) e170.
[37] Y.O. Chernoff, G.P. Newnam, J. Kumar, K. Allen and A.D. Zink, Evidence for a protein mutator in yeast: role of the Hsp70-related chaperone ssb in formation, stability, and toxicity of the [PSI] prion., Mol Cell Biol, 19 (1999) 8103-8112.
[38] B. Westermann and W. Neupert, Mitochondria-targeted green fluorescent proteins: convenient tools for the study of organelle biogenesis in Saccharomyces cerevisiae., Yeast, (2000).
[39] C. Meisinger, T. Sommer and N. Pfanner, Purification of Saccharomcyes cerevisiae mitochondria devoid of microsomal and cytosolic contaminations., Anal Biochem, (2000).
[40] B.J. Cargile, J.R. Sevinsky, A.S. Essader, J.L. Stephenson and J.L. Bundy, Immobilized pH gradient isoelectric focusing as a first-dimension separation in shotgun proteomics., J Biomol Tech, 16 (2005) 181-189.
[41] M.P. Yaffe and G. Schatz, Two nuclear mutations that block mitochondrial protein import in yeast., Proc Natl Acad Sci U S A, 81 (1984) 4819-4823.
[42] H. Prokisch, C. Andreoli, U. Ahting, K. Heiss, A. Ruepp, C. Scharfe and T. Meitinger, MitoP2: the mitochondrial proteome database-now including mouse data., Nucleic Acids Res, 34 (2006) D705-D711.
[43] T. Langer, M. Kaser, C. Klanner and K. Leonhard, AAA proteases of mitochondria: quality control of membrane proteins and regulatory functions during mitochondrial biogenesis, Biochem Soc Trans, 29 (2001) 431-6.
[44] L.G. Nijtmans, L. de Jong, M.A. Sanz, P.J. Coates, J.A. Berden, J.W. Back, A.O. Muijsers, H. van der Spek and L.A. Grivell, Prohibitins act as a membrane-bound chaperone for the

stabilization of mitochondrial proteins., EMBO J, 19 (2000) 2444-2451.
[45] L.G.J. Nijtmans, S.M. Artal, L.A. Grivell and P.J. Coates, The mitochondrial PHB complex: roles in mitochondrial respiratory complex assembly, ageing and degenerative disease., Cell Mol Life Sci, 59 (2002) 143-155.
[46] L. Kiemer, S. Costa, M. Ueffing and G. Cesareni, WI-PHI: a weighted yeast interactome enriched for direct physical interactions., Proteomics, 7 (2007) 932-943.
[47] S.V. Paushkin, V.V. Kushnirov, V.N. Smirnov and M.D. Ter-Avanesyan, Propagation of the yeast prion-like [psi+] determinant is mediated by oligomerization of the SUP35-encoded polypeptide chain release factor., EMBO J, 15 (1996) 3127-3134.
[48] P.W. Piper, G.W. Jones, D. Bringloe, N. Harris, M. MacLean and M. Mollapour, The shortened replicative life span of prohibitin mutants of yeast appears to be due to defective mitochondrial segregation in old mother cells., Aging Cell, 1 (2002) 149-157.
[49] C. Merkwirth, S. Dargazanli, T. Tatsuta, S. Geimer, B. Lower, F.T. Wunderlich, J.C. von Kleist-Retzow, A. Waisman, B. Westermann and T. Langer, Prohibitins control cell proliferation and apoptosis by regulating OPA1-dependent cristae morphogenesis in mitochondria, Genes Dev, 22 (2008) 476-88.
[50] G. Steglich, W. Neupert and T. Langer, Prohibitins regulate membrane protein degradation by the m-AAA protease in mitochondria., Mol Cell Biol, (1999).
[51] C. Osman, C. Wilmes, T. Tatsuta and T. Langer, Prohibitins interact genetically with Atp23, a novel processing peptidase and chaperone for the F1Fo-ATP synthase., Mol Biol Cell, 18 (2007) 627-635.
[52] J.W. Back, M.A. Sanz, L.D. Jong, L.J.D. Koning, L.G.J. Nijtmans, C.G.D. Koster, L.A. Grivell, H.V.D. Spek and A.O. Muijsers, A structure for the yeast prohibitin complex: Structure prediction and evidence from chemical crosslinking and mass spectrometry., Protein Sci, 11 (2002) 2471-2478.
[53] T. Tatsuta, K. Model and T. Langer, Formation of membrane-bound ring complexes by prohibitins in mitochondria., Mol Biol Cell, (2005).
[54] S. Meeusen, R. DeVay, J. Block, A. Cassidy-Stone, S. Wayson, J.M. McCaffery and J. Nunnari, Mitochondrial inner-membrane fusion and crista maintenance requires the dynamin-related GTPase Mgm1., Cell, 127 (2006) 383-395.
[55] N. Ishihara, Y. Fujita, T. Oka and K. Mihara, Regulation of mitochondrial morphology through proteolytic cleavage of OPA1., EMBO J, 25 (2006) 2966-2977.
[56] K.L. Cerveny, Y. Tamura, Z. Zhang, R.E. Jensen and H. Sesaki, Regulation of mitochondrial fusion and division., Trends Cell Biol, 17 (2007) 563-569.
[57] C. Merkwirth, S. Dargazanli, T. Tatsuta, S. Geimer, C. Merkwirth and T. Langer, Prohibitin function within mitochondria: Essential roles for cell proliferation and cristae morphogenesis., Biochim Biophys Acta, 1793 (2009) 27-32.
[58] H. Sesaki, S.M. Southard, A.E.A. Hobbs and R.E. Jensen, Cells lacking Pcp1p/Ugo2p, a rhomboid-like protease required for Mgm1p processing, lose mtDNA and mitochondrial structure in a Dnm1p-dependent manner, but remain competent for mitochondrial fusion., Biochem Biophys Res Commun, 308 (2003) 276-283.
[59] M. Herlan, F. Vogel, C. Bornhovd, W. Neupert and A.S. Reichert, Processing of Mgm1 by the rhomboid-type protease Pcp1 is required for maintenance of mitochondrial morphology and of mitochondrial DNA., J Biol Chem, (2003).
[60] A. Lewandowska, M. Gierszewska, J. Marszalek and K. Liberek, Hsp78 chaperone functions in restoration of mitochondrial network following heat stress, Biochim Biophys Acta, 1763 (2006) 141-51.
[61] S.V. Paushkin, V.V. Kushnirov, V.N. Smirnov and M.D. Ter-Avanesyan, Interaction between yeast Sup45p (eRF1) and Sup35p (eRF3) polypeptide chain release factors: implications for prion-dependent regulation., Mol Cell Biol, 17 (1997) 2798-2805.
[62] M.M. Patino, J.J. Liu, J.R. Glover and S. Lindquist, Support for the prion hypothesis for inheritance of a phenotypic trait in yeast, Science, 273 (1996) 622-6.

Yeast prion [*PSI*$^{+}$] lowers the levels of mitochondrial prohibitins

Jacek Sikora[1], Joanna Towpik[1], Damian Graczyk[1], Michał Kistowski[1], Tymon Rubel[2], Jaroslaw Poznanski[1], James Langridge[3], Chris Hughes[3], Michał Dadlez[1,4], Magdalena Boguta[1,5*]

[1]Institute of Biochemistry and Biophysics, Polish Academy of Sciences, Pawinskiego 5a, 02 106 Warsaw, Poland; Institute of Radioelectronics, Warsaw University of Technology, Nowowiejska 15/19, 00 665 Warsaw, Poland; [3]Waters Corporation, Atlas Park, Simonsway, Manchester, M22 5PP, UK; [4]Institute of Genetics and Biotechnology, Faculty of Biology, University of Warsaw, Miecznikowa 1, 02-116 Warsaw, Poland; [5]Department of Chemistry, Warsaw University of Technology, Noakowskiego 3, 00 664 Warsaw, Poland

**Corresponding author*: Magdalena Boguta, Institute of Biochemistry and Biophysics, Polish Academy of Sciences, Pawińskiego 5a, 02-106 Warsaw, Poland; phone: (4822) 592 1312; fax: (4822) 658 4636; e-mail: magda@ibb.waw.pl

Running title:

Prion-dependent levels of mitochondrial prohibitins

Abstract

We report proteomic analyses that establish the effect of cytoplasmic prion [*PSI*$^{+}$] on the protein complement of yeast mitochondria. A set of 44 yeast mitochondrial proteins whose levels were affected by [*PSI*$^{+}$] was identified by two methods of gel-free and label-free differential proteomics. From this set we focused on prohibitins, Phb1 and Phb2, and the mitochondrially synthesized Cox2 subunit of cytochrome oxidase. By immunoblotting we confirmed the decreased level of Cox2 and reduced mitochondrial localization of the prohibitins in [*PSI*$^{+}$] cells, which both became partially restored by [*PSI*$^{+}$] curing. The presence of the [*PSI*$^{+}$] prion also caused premature fragmentation of mitochondria, a phenomenon linked to prohibitin depletion in mammalian cells. By fractionation of cellular extracts we demonstrated a [*PSI*$^{+}$]-dependent increased of the proportion of prohibitins in the high molecular weight fraction of aggregated proteins. We propose that the presence of the yeast prion causes newly synthesized prohibitins to aggregate in the cytosol, and therefore reduces their levels in mitochondria, which in turn reduces the stability of Cox2 and possibly of other proteins, not investigated here in detail.

1. Introduction

Prions are a unique class of infectious agents whose infectivity relies solely on protein. In mammals, they cause fatal neurodegenerative diseases such as Creutzfeldt-Jacob disease in man, ovine scrapie and bovine spongiform encephalopathy. All these diseases are related to the PrP protein whose conformationally altered form (PrP^{Sc}) is able to convert the normal host-encoded protein (PrP^{C}) into an altered prion form. While only one prion protein is known in mammals, the mammalian prions appear to represent just part of a much wider phenomenon, also being found in lower eukaryotes. In contrast to mammalian prions, those of lower eukaryotes cause non-chromosomal inheritance of phenotypic traits (reviewed in [1, 2]). From a structural point of view prion proteins, and also yeast prions, possess the ability for spontaneous assembly in an autocatalytic process into amyloid [3]. Amyloid-type protein aggregates are characterized by the so-called “cross-beta” alignment of monomeric units, and yeast prions are no exception [4-6]. Yeast prions may be used as a convenient model for elucidation of the factors interacting with human prions and other amyloids.

The yeast prion [*PSI*$^{+}$] is a self-perpetuating conformation of the translation termination factor Sup35 (eRF3) (for a review, see [7]). Sup35 forms a complex with Sup45/eRF1 that is involved in recognizing termination codons and releasing the translation product from the ribosome [8, 9]. The prion state of Sup35 can be propagated for many cellular generations in a stable way. This may be observed as the nonsense suppressor phenotype, [*PSI*$^{+}$], which reflects the reduced function of Sup35 due to aggregation of its prion form. It is noteworthy that [*PSI*$^{+}$] can also induce read-through of stop codons at the end of open reading frames of yeast wild type genes, which could be the reason for the variety of weak phenotypes manifested by [*PSI*$^{+}$] strains [10].

The study of the yeast prion [*PSI*$^{+}$] resulted in the first evidence connecting prions with a cellular stress defense system [11]. Various chaperones can either promote prion propagation and generation or eliminate it from the cell. [*PSI*$^{+}$] and other yeast prions, [*URE3*] and [*PIN*$^{+}$], are

maintained only in the presence of the chaperone Hsp104 (for a review see [1]). It has been shown that increasing or decreasing the level of Hsp104 results in the loss of [*PSI*$^+$]. The stress-inducible Ssa proteins generally help prions to propagate, while constitutively expressed proteins of the Ssb family are prion antagonists [12-14]. Hsp40 co-chaperones, Ydj1 and Sis1, as well as Sse1, a nucleotide exchange factor for Hsp70, exhibit various effects on yeast prions [15, 16]. Although numerous previous attempts have failed, most recent papers proved a physical interaction between Sup35 and Hsp104 in vitro and suggest its existence in vivo]. Sup35, preferentially in the [*PSI*$^+$] state interacts also directly with some other chaperones [17-19].

Our previous work indicated a connection between the yeast prion [*PSI*$^+$] and mitochondria. Although the [*PSI*$^+$] wild type strain exhibited no difference in respiration competence compared to the corresponding [*psi*$^-$], in combination with a mutant Nam9-1 protein of the mitochondrial ribosome [*PSI*$^+$] caused a lack of respiration [20]. This effect of [*PSI*$^+$] in the *nam9-1* mutant correlated with decreased levels of the mitochondrially encoded Cox2 and other subunits of cytochrome oxidase, a hetero-oligomeric protein complex located in the inner mitochondrial membrane. The respiratory deficiency in the *nam9-1* mutant was cured by overproduction or inactivation of Hsp104, exactly the same conditions that eliminate [*PSI*$^+$]. Another prion, [*PIN*$^+$], which often coexists with [*PSI*$^+$], was not known during the time of this study and [*PIN*] status of the *nam9-1* mutant was not determined. However [*PIN*$^+$] is not cured by overproduced Hsp104, therefore [*PIN*$^+$] could be excluded as a potential reason of respiratory deficiency in *nam9-1*. We then considered how the presence of [*PSI*$^+$] aggregates interferes with mitochondrial function. Since it had been reported that proteins can become trapped in [*PSI*$^+$] aggregates [21], we expected that recruitment of proteins interacting with the mitochondrial translation machinery by [*PSI*$^+$] aggregates might account for the respiratory deficiency in the presence of Nam9-1. It was also conceivable that [*PSI*$^+$] aggregates might change the level of cytosolic chaperones required for the translocation of proteins to mitochondria, which in turn might alter the relative level of one or more components of the mitochondrial translation system. Finally, one could expect that [*PSI*$^+$]-induced

stop codon readthrough generates one or more novel mitochondrial proteins bearing an extra C-terminal domain and causing repiratory deficiency in combination with Nam9-1. In this context it was of interest to perform a quantitative comparison of mitochondrial proteins in isogenic [*PSI*$^{+}$] and [*psi*$^{-}$] strains.

The mitochondrial proteome, being a relatively small, but still complicated protein network, has already been studied in considerable detail. Several reports describing the set of mitochondrial proteins from yeast and mammals have been published [22-35]. In addition, different genomic approaches have been integrated to define a complete protein repertoire of the organelle using yeast mitochondria as a model [24]. Moreover, a comprehensive network of protein interactions in a mitochondrial system, as part of the yeast interactome, has been built. This map of the interrelationships among mitochondrial proteins greatly facilitates the interpretation of the results of global analyses of the yeast mitochondrial proteome upon perturbation [36].

Here, global proteomic analysis was applied to search for the differences in the levels of mitochondrial proteins in two isogenic yeast [*psi*$^{-}$] and [*PSI*$^{+}$] strains. This analysis identified 44 candidate proteins of which the levels were significantly changed. The list includes, for instance, Cox2 protein, which was found in a previous study to be downregulated in the presence of [*PSI*$^{+}$]. Two other proteins from the list, prohibitins Phb1 and Phb2, immediate neighbors of Cox2 in the yeast mitochondrial interactome net, were selected for further analysis. Their downregulation in the presence of the prion [*PSI*$^{+}$] and their regulation by Hsp104 level was confirmed by Western blot analysis. Furthermore, fractionation of yeast cell lysates demonstrated [*PSI*$^{+}$]-dependent enrichment of prohibitins in the aggregated protein fraction. Our results indicate that depletion of prohibitins can provide the rationale for the mitochondrial functional defects observed earlier in [*PSI*$^{+}$] yeast cells.

2. Materials and Methods

2.1. Yeast strains and growth conditions

Saccharomyces cerevisiae strain GT197 (*MATα ade1-14 trp1-Δ ura3-52 leu2-3,112 lys2 his3*), referred to as [*psi*-] and the isogenic [*PSI*$^+$] strain GT81-1D [37] were used throughout this study. In the experiment shown in Fig. 2B derivatives of MB43-*nam9-1* (*MATa ura3 his3, his4C nam9-1* [*PSI*$^+$]) [20] were used. In order to prevent glucose repression yeast cells were grown in YPE medium (1% yeast extract, 2% bactopeptone, 2% ethanol) or in low-glucose medium (1% yeast extract, 2% bactopeptone, 0.5% glucose). Cultures were harvested at an optical density of 600 nm (OD_{600}) of 1.5 to 1.7, which corresponded, in the case of the low-glucose medium, to a point of glucose exhaustion, as determined with Glucostix (Bayer).

To assess mitochondria by fluorescence, GT197 [*psi*-] and the isogenic [*PSI*$^+$] GT81-1D strains were transformed with pYX323-mtGFP plasmid (2 μ, *TRP1*) encoding green florescence protein (GFP) with a mitochondrial localization sequence [38] .Transformants were grown in minimal SC-trp medium (0.67% yeast nitrogen base, 2% glucose) supplemented with all amino acids except tryptophan. Cells were harvested at OD_{600} = 1.2. Neither [*psi*-] nor the [*PSI*$^+$] strain has a tendency to become *rho*$^-$.

2.2. Isolation of mitochondria

Isolation of mitochondria was accomplished by differential centrifugation according to [39]. Crude mitochondria (protein concentration of 5 mg/ml) were suspended in SEM buffer (250 mM sucrose, 1 mM EDTA, 10 mM MOPS, pH 7.2) ensuring proper osmotic pressure for maintenance of organelle integrity and prevention of its decomposition. The suspension of crude mitochondria was loaded onto a three-step sucrose gradient composed of 1.5 ml 60%, 4 ml 32%, 1.5 ml 23% and 1.5 ml 15% sucrose in EM-buffer (1 mM EDTA, 10 mM MOPS, pH 7.2) and centrifuged for 1 h at 134 000 x g, yielding highly pure mitochondria at the 60/32% sucrose interface. The sucrose gradient step was performed twice.

2.3. Differential proteomics experiments

Two methods were used for identification of proteins differentially populated in the two [*psi*$^-$] and

[*PSI*$^+$] strains analyzed. Their detailed description is given in the Supporting Material and Method Section. In brief, in the first method, further referred to as FTICR, the protein ratios were measured by comparing the amplitudes of their corresponding peptide signals in the MS spectra obtained from a mitochondrial proteome tryptic peptide mixture in LC-MS experiments using an LTQ FTICR (Thermo) mass spectrometer. In the second method, further referred to as WPES, a commercially available Waters Protein Expression System, designed to carry out differential proteomics experiments, was used to extract differentially populated proteins. The final selection of mitochondrial proteins sensitive to the presence of the cytoplasmic prion [*PSI*$^+$] was based on statistical validation of the results of replicate experiments.

2.4. Peptide isoelectrofocusing

Peptide isoelectrofocusing was carried out as described previously [40] with a minor change to the protocol, as follows: 100 μg of proteins in 100 μl of 100 mM ammonium bicarbonate pH 8.5 was denatured for 5 min at 98 °C and cooled on ice. Ten microliters of modified sequencing grade trypsin (Promega), 100 ng/μl, was added and the samples were incubated o/n at 37 °C. The protein digest was dried in a speed-vac and suspended in 340 μl of sample buffer (7 M urea, 2 M thiourea, 2% Chaps, 0.5% β-mercaptoethanol, 0.006% IPG buffer pH 3.5–5.0 (Amersham). To remove insoluble material centrifugation at 15000 x g was performed for 15 min and supernatant was used for overnight passive rehydration of an 18 cm strip of the gel (pH 3.5–4.5) in IPG buffer. IEF was performed on a Multiphor II electrophoresis system (Amersham) using a three-step gradient program as follows: step 1: 500 V, 2 mA, 2 W, 1 h; step 2: 1000 V, 2 mA, 2 W, 2 h; step 3: 3500 V, 2 mA, 4 W, 45 h.

Following IEF, the strip was cut into ten pieces and peptides were eluted three times with 100 μl 0.1% TFA, 2% acetonitrile. Pooled fractions were filtered through a 50 kDa cut-off cellulose membrane (Millipore) and concentrated on a speed-vac. Qualitative analysis (protein identification) was carried out using merged datasets obtained for each of the ten pieces of the IPG strip, as described in Supporting Material Section S1 for the LTQ-FTICR qualitative analysis step.

2.5. Fractionation of yeast cell lysates

For the experiment presented in Fig. 2C, total cellular protein was extracted by alkaline lysis as described previously [41]. For the fractionation of aggregates (experiment presented in Fig. 3), cells were lysed by vortexing with glass beads in buffer A (25 mM Tris-HCl, pH 7.5, 50 mM KCl, 10 mM $MgCl_2$, 1 mM EDTA, 2% glycerol) along with 1 mM PMSF, 2 µg/ml aprotinin, 1 µg/ml pepstatin A, 0.5 µg/ml leupeptin, 2.5 µg/ml anti-pain, 0.5 µg/ml TLCK, 0.5 µg/ml TPCK, 0.1 mM benzamidine and 0.1 mM sodium metabisulfite. Cell debris and mitochondria were removed by centrifugation at 15, 000 × g for 10 min. Obtained supernatants were treated with RNase A (400 µg/ml) to disrupt polyribosomes. Extracts were then subjected to centrifugation through a sucrose cushion (1 ml of 30% sucrose in buffer A) in an SW50 rotor at 45 000 r.p.m. for 30 min at 4 °C. The resulting supernatants, intermediate fractions and pellets were analyzed by Western blotting.

2.6. Western blotting

For immunoblotting, protein extracts were separated by SDS-PAGE gels and transferred electrophoretically onto a nitrocellulose membrane (Millipore). After immunodecoration with the desired primary antibody, membranes were incubated with anti-rabbit or anti-mouse horseradish peroxidase-conjugated secondary antibody. Reaction with Immobilon Western Chemiluminescent HRP Substrate (Millipore) was performed according to the manufacturer's instructions and light emitted was subsequently captured on X-ray film (Amersham). Films were quantified using ImageQuant (GE Healthcare Life Sciences) with local average background correction.

2.7. Confocal microscopy

Cells were washed with water, plated on microscope glass slides and subjected to confocal laser scanning microscopy. An Eclipse TE2000-E microscope (Nikon), equipped with a Plan Apo 60X oil objective was used. mtGFP was excited with an Argon-Ion laser at 488 nm, and emission was detected at 515/30 nm. Images were collected with the EZ-C1 Confocal v. 3.6 program (Nikon) and then processed with EZ-C1 Viewer v. 3.6 (Nikon) and Adobe Photoshop 8.0.

3. Results

3.1. Analysis of mitochondrial proteome

Mitochondria were isolated from *Saccharomyces cerevisiae* prion-free strain GT197 referred to as [*psi*-] and the isogenic strain GT81-1D containing [PSI^+] referred to as [PSI^+]. Both [*psi*-] and [PSI^+] strains are respiratory competent and mitochondria were isolated using a standard fractionation procedure. The identification of mitochondrial proteins derived from [PSI^+] and [psi^-] strains was carried out by several rounds of LC-MS-MS/MS (Liquid Chromatography coupled to Mass Spectrometry in data-dependent switch to fragmentation mode) experiments using an LTQ FTICR spectrometer, as described in the Supporting Material and Method Section. The obtained list of 1275 mitochondrial proteins was compared with the mitochondrial proteome characterized previously by other authors [22-28], (Supporting Material Table S1). In all, 972 (76%) proteins were indicated as mitochondrial in earlier either MS-based or "*in silico*" studies (Supporting Material Fig. S1). We identified 34 mitochondrial proteins that are present in the MREF mitochondrial database [42] although, to our knowledge, they have not been identified previously by MS-based studies on the *S. cerevisiae* mitochondrial proteome[22-27], Prokish-unpublished dataset, [28] (Supporting Material Table S2). Our list of proteins contains representatives of 45 out of the 46 major functional modules of the yeast mitochondrial interactome constructed by Perocchi and co-workers [36] (Supporting Material Fig. S2 and Table S3).

Similarly to other proteomic studies, the number of detected proteins was higher than the number of proteins in the accepted mitochondrial reference set. Two factors may explain this apparent inconsistency. First, it is possible that the mitochondrial reference set is not yet complete and that the detected proteins are new mitochondrial proteins, or second, our preparation procedure did not fully eliminate non-mitochondrial proteins. It has to be noted, however, that the main aim of our experiment was to identify differential proteins between [PSI^+] and [psi^-] strains. Therefore the possible presence of non-mitochondrial proteins does not compromise the validity of our results.

In conclusion, our identification of mitochondrial proteins in [PSI^+] and [psi^-] strains,

proved to be of comparable quality to previous protein identification efforts. Thus we can state that the set of mitochondrial proteins considered in the differential analysis is reasonably complete and representative.

3.2. Prohibitins and Cox2 among proteins identified by differential proteomics of the mitochondria of [*PSI*$^+$] and [*psi*$^-$] strains

To obtain a list of proteins of which the levels are affected by the presence of prion [*PSI*$^+$], two independent methods of differential proteomics, named FTICR and WPES, were used and each was repeated three times (see the Supporting Material and Method Section for details of the methods, the statistical analysis and hit acceptance criteria). Figure 1 shows the comparison of protein level as the [*PSI*$^+$]/[*psi*$^-$] ratios. Forty-one of these proteins showed the same direction of expression changes in both experiments (Supporting Material Table S4). This fairly large number of detected differential proteins indicates that the presence of prion [*PSI*$^+$] in the yeast cytoplasm induces a complex response in mitochondria.

[*PSI*$^+$]-dependent proteins identified in our experiment belong to several annotation categories. [*PSI*$^+$] mitochondria showed decreased levels of several subunits of respiratory complexes, such as Cox2, Atp1, Atp2, Atp3 and Sdh1. There were also decreased levels of some enzymes of isocitrate metabolism. In addition we observed marked changes in the levels of some chaperones and receptors involved in mitochondrial protein import, such as Tom40, Tim13 and Ssc1. The identification of these proteins as affected by [*PSI*$^+$] links the prion with the reorganization of the mitochondrial import apparatus. Interestingly, both prohibitins Phb1 and Phb2 were also downregulated in the [*PSI*$^+$] mitochondria. Phb1 and Phb2 prohibitins act as membrane-bound chaperones involved in the stabilization of mitochondrial translation products including Cox2 [43-45]. Because of this relation, Cox2 and prohibitins are immediate neighbors in the yeast mitochondrial interactome [46] (Supporting Material Fig. S3). Moreover, Cox2 is known to be involved in prion-dependent phenomena in yeast [20]. Encouraged by the known functional links between Cox2, Phb1 and Phb2, we focused our attention on these three proteins.

Two independent proteomic methods showed that Cox2 and the two prohibitins, Phb1 and Phb2, are less abundant in mitochondria in [*PSI*$^+$] cells. In the [*PSI*$^+$] strain the Cox2 level was decreased over 3.5 fold (p=0.0048). The [*PSI*$^+$]/[*psi*$^-$] ratio for Cox2 was estimated on the basis of eleven peptides in FTICR and eight in the WPES experiment, respectively. Phb1 was decreased 1.9 fold (p=0.058) as estimated on the basis of seven peptides in FTICR and ten in WPES. For Phb2 17 peptides in FTICR, and 11 in WPES were used for ratio calculation giving a 1.3 fold decrease in [*PSI*$^+$] cells (p=0.11). The signal amplitude values of Phb1, Phb2 and Cox2 peptides are presented in the Supporting Material, Fig. S4.

3.3. Reduced levels of Cox2 and prohibitins in [*PSI*$^+$] mitochondria detected by immunoblotting

To provide independent confirmation of the MS differential analyses, mitochondria isolated from [*psi*$^-$] and [*PSI*$^+$] cells were analyzed by Western blotting with specific antibodies. The results (Fig. 2A) reproducibly confirm that the presence of [*PSI*$^+$] reduces the levels of mitochondrial Cox2, Phb1 and Phb2. We next investigated whether the amount of mitochondrial prohibitins was affected by curing of cells from [*PSI*$^+$]. Yeast may be cured from the [*PSI*$^+$] prion by overexpression or deletion of the gene encoding the Hsp104 chaperone [1, 2, 11]. We took advantage of two observations: first, that [*PSI*$^+$] curing by Hsp104 stabilized Cox2 in the MB43-*nam9-1* strain [20] and second, that prohibitins are known to stabilize mitochondrially synthesized proteins, including Cox2 [43-45]. Thus we considered the possibility that [*PSI*$^+$] curing may increase the levels of prohibitins in mitochondria and that this effect is a prerequisite for Cox2 stabilization. Indeed, the Western blot analysis of the mitochondria (Fig. 2B) showed that deletion or overexpression of the *HSP104* gene in [*PSI*$^+$] MB43-*nam9-1* cells resulted in an increase in Phb1 and Phb2 levels. These results clearly indicate a link between curing of the [*PSI*$^+$] prion and the levels of prohibitins and Cox2 in mitochondria.

For quantification, the intensities of bands were measured using nuclear-encoded mitochondrial malate dehydrogenase Mdh1 as an internal control. The results of MS and Western analyses

comparing the effect of [*PSI*$^+$] were consistent, even in cells of different genetic background (Table 1). Cox2 is a mitochondrially synthesized protein, the stability of which is known to be prion-dependent [20], and our work confirmed this. In contrast, prohibitins are synthesized in the cytoplasm and then imported to mitochondria. The observed decrease in the amount of mitochondrial prohibitins might result from their lower synthesis in [*PSI*$^+$] cells. Interestingly, Western blot analysis of total yeast extracts shows a decreased amount of Cox2 in the [*PSI*$^+$] strain, but does not reveal differences between the levels of prohibitins in the [*psi*$^-$] and [*PSI*$^+$] strains (Fig. 2C). This suggests that the observed depletion of mitochondrial prohibitins was due to their inefficient import into the mitochondria in cells with the [*PSI*$^+$] prion.

3.4. [*PSI*$^+$] causes enrichment of prohibitins in the cellular aggregates fraction

[*PSI*$^+$] is the prion conformation of the Sup35 protein, a cytoplasmic translation termination factor. [*PSI*$^+$] affected the levels of mitochondrial prohibitins but not their total amount in the yeast cell (Fig. 2), suggesting a defect in intracellular distribution. This might be due to a physical interaction of prohibitins with Sup35 aggregates occurring in the cytoplasm and affecting their import to mitochondria.

It has previously been shown that Sup35 forms high-molecular-weight aggregates in [*PSI*$^+$] cells, co-sedimenting with the heavy polyribosomal fraction and even larger structures [47]. Thus distribution of prohibitins between the soluble and aggregated fractions could be influenced by the [*PSI*] status of the cells. To check this, extracts of isogenic [*psi*$^-$] and [*PSI*$^+$] strains were prepared using the clarifying spin to eliminate the remaining mitochondria (see Materials and Methods). Extracts were fractionated by centrifugation through a sucrose cushion, and the fractions were analyzed by immunoblotting using antibodies against Sup35, Phb1 and Phb2. In agreement with previous results [47], after centrifugation most of the Sup35 protein was found in the pellet fraction in the [*PSI*$^+$] strain, whereas in the [*psi*$^-$] strain Sup35 remained in the supernatant (Fig. 3, upper panel). Prohibitins were detected almost exclusively in the pellet fraction, although some remained in the sucrose cushion. The presence of prohibitins in the pellet cannot be attributed to the residual

presence of contaminating mitochondria, as their absence was carefully controlled by the absence of the other mitochondrial protein, aconitase (Aco1) in the pellet. Interestingly, both Phb1 and Phb2 were relatively more abundant in the pellet fraction from the [*PSI*$^+$] strain than in the respective fraction from the [*psi*$^-$] strain (Fig. 3, lower panel). This suggests that prohibitins are partially trapped by cytoplasmic [*PSI*$^+$] prion aggregates, which in turn should decrease their availability for import into the mitochondria.

3.5. [*PSI*$^+$] causes premature fragmentation of mitochondria

The yeast mutants with inactive prohibitin showed abnormal mitochondrial morphology and defects of mitochondria segregation, especially in old cells [48]. A recent study in mammals revealed that prohibitins determine cristae morphogenesis and formation of tubular mitochondrial ultrastructures, since 90% of PHB2-deficient mouse cells contained fragmented mitochondria [49]. We explored the possibility that [*PSI*$^+$] could indirectly affect fusion of mitochondria in yeast by reduction of the levels of mitochondrial prohibitins. To investigate mitochondrial ultrastructure, [*psi*$^-$] and [*PSI*$^+$] cells were transformed with pYX323-mtGFP plasmid (2 μ, *TRP1*) encoding green fluorescent protein (GFP) containing a mitochondrial localization signal. To prevent the loss of plasmid, cells were cultivated in minimal medium lacking tryptophan. The growth rate was controlled by OD measurements, indicating no difference between [*psi*$^-$] and [*PSI*$^+$] strains. Cells were harvested at the same point in the late logarithmic phase and examined by confocal microscopy. Strikingly, [*PSI*$^+$] cells contained 95% of fragmented mitochondria whereas the majority of [*psi*$^-$] cells in the same phase contained regular tubular mitochondrial ultrastructures (Fig. 4). This showed premature fragmentation of mitochondria in [*PSI*$^+$] cells, providing a link between the presence of cytoplasmic prion [*PSI*$^+$] and defects in mitochondrial fusion, which may be caused by reduced prohibitins (see Discussion).

4. Discussion

Several years ago it was reported that stability of the mitochondria-encoded respiratory chain subunit Cox2 in a mitochondrial ribosomal mutant *nam9-1* depends on the yeast prion [PSI^+] [20]. This observation is striking because the prion is located in the cytosol, whereas the synthesis and assembly of Cox2 takes place in mitochondria. In order to obtain a better insight into this unexpected relation, we used a proteomics approach to search for differences in the levels of mitochondrial proteins in prion-positive [PSI^+] and prion-negative [psi^-] cells. We obtained a list of 44 mitochondrial proteins showing altered abundance depending on the presence of [PSI^+]. Among those were Cox2 and several other subunits of cytochrome oxidase and mitochondrial ATPase. Importantly, the levels of the two prohibitins, Phb1 and Phb2, were also reduced in mitochondria of [PSI^+] cells.

Prohibitins are evolutionarily conserved eukaryotic proteins that assemble in a large ring complex bound to inner mitochondrial membrane [51-53].. Earlier findings in yeast identified prohibitins in assemblies with ATP-dependent protease m-AAA involved in chaperoning and turnover of mitochondrial inner membrane proteins [43, 44]. Yeast mutants lacking functional prohibitins show accelerated proteolysis by m-AAA protease suggesting a regulatory role of prohibitins in the quality control of proteins in inner membrane [45, 50]. Phb1/2 complex, reminiscent of Hsp60-like chaperones, is proposed to act as a novel type of membrane-associated chaperone/holdase involved in higher order organization of respiratory chain complexes [51-53].

Using molecular methods provide evidence that Phb1, Phb2 and Cox2 are less abundant in mitochondria in [PSI^+] cells, thus confirming proteomic results and suggesting lowered mitochondrial prohibitins as a potential reason of Cox2 destabilization.

Another function of prohibitins described recently in mammals is the processing of the dynamin-like GTPase OPA1, an essential component of the mitochondrial fusion machinery [49]. OPA1 is a homologue of yeast Mgm1 protein also involved in mitochondria fusion [54]. Both OPA1 and Mgm1 exist in forms of different lengths and their function is regulated by proteolytic cleavage [55, 56] Only a long form of OPA1 (L-OPA1) is fusion competent [55], and maintenance of this

form requires prohibitins [49]. Depletion of prohibitins induces L-OPA1-dependent fragmentation of mitochondria and apoptosis. The mechanism underlying the selective loss of L-OPA1 in the absence of prohibitins remains to be elucidated [57].

Here we detected [*PSI*$^+$]-dependent premature fragmentation of yeast mitochondria in post-exponential growth phase. It is currently unknown whether the low level of mitochondrial prohibitins in [*PSI*$^+$] cells can provide the rationale for the observed negative effect on mitochondrial fusion. One interesting hypothesis is that depletion of prohibitins could contribute to the defect in the function of Mgm1, the OPA1 homologue, in the fusion of yeast mitochondria. Although Mgm1 processing is not strictly required for mitochondrial fusion [58], the balanced formation or regulated inter-conversion of the two isoforms of Mgm1 appear crucial [59]. Characterization of the effect of prohibitins on Mgm1 requires further study. Among the other mitochondrial proteins found to be affected by [*PSI*$^+$] in this work, the presence of Hsp78 is remarkable, because this chaperone functions in restoration of the mitochondrial network following heat stress [60].

Although the overall level of expression of prohibitins is the same in the [*PSI*$^+$] and [*psi*$^-$] strains, the *PSI* status affects their distribution within the cell. We were interested in why the mitochondrial localization of prohibitins was reduced by the [*PSI*$^+$] prion state. Fractionation of mitochondria-free lysates for soluble and aggregate parts showed enrichment of prohibitins in the aggregate fraction in [*PSI*$^+$] cells. This result suggests some interaction of Phb1/Phb2 with [*PSI*$^+$] possibly leading to sequestration of prohibitins by prion aggregates. The effect of [*PSI*$^+$] on sequestering of another cytoplasmic protein, translation termination factor Sup45, has been studied in the past, but the results were controversial. Sup45 was reported to be present in [*PSI*$^+$] aggregates in some [21, 61] but not other studies [62] and a decisive model of Sup45 sequestering is lacking. Similarly, further experiments are required to demonstrate and characterize a specific interaction of prohibitins with [*PSI*$^+$] aggregates. Here we just propose that the newly synthesized prohibitins are titrated by [*PSI*$^+$] aggregates in the cytosol before they reach mitochondrial location and therefore their level in mitochondria is lowered, which in turn reduces the stability of Cox2. Moreover, we

believe that prohibitins are not the only component mediating the effect of the [*PSI*$^+$] prion on mitochondrial function and the roles of other mitochondrial proteins identified by our proteomic study is worth to study as well.

A different scenario may be proposed of how presence of [*PSI*$^+$] aggregates interferes with mitochondrial function. Inefficient termination in cells containing [*PSI*$^+$] potentially allows for readthrough of stop codons nuclear mRNAs. Leakiness of stop codons is considered to be the reason for a variety a weak phenotypes manifested by [*PSI*$^+$] strains [10]. Nuclear-encoded mitochondrial proteins might be expressed in a C-terminally extended version(s) when low levels of functional Sup35 allow readthrough of nonsense codons. However, in this and other published studies no experimental evidence of C-terminally extended proteins in [*PSI*$^+$] mitochondria has been found.

The overall data presented here support the model that in *S. cerevisiae* the prion [*PSI*$^+$] interacts with prohibitins and possibly other proteins in the cytosol and thereby alters their distribution to mitochondria. Thus the hidden phenotypic variation generated by [*PSI*$^+$] may result from subtle alteration in sorting of particular proteins between cellular compartments. It is possible that some of the [*PSI*$^+$] manifestations can be related to the ability of Sup35 prion aggregates to titrate host proteins with important functions though this suggestion has never been supported.

Acknowledgments

We are grateful to Michael Ter-Avanesyan and Agnieszka Chacińska for critical reading of the manuscript. Help of Hans Vissers in the training in WPES software, technical help of Anna Anielska in confocal microscopy and Marta Tkaczyk in peptide IEF is kindly acknowledged. We thank Yury Chernoff for the strains, Thomas Langer for the Phb1 and Phb2 antibodies, Michael Ter-Avanesyan for the Sup35 antibodies and Róża Kucharczyk for the pYX323-mtGFP plasmid. This work was supported by the Ministry of Science and Higher Education, Poland (grants N301 023 32/1117 and 4/0-PBZ-MinI-2/1/2005, R130103) and the MITONET network.

Figure Legends

Fig. 1 . **Proteins showing [*PSI*$^+$]-dependent abundance in yeast mitochondria.** The [*PSI*$^+$]/[*psi*$^-$] ratios of differential proteins (log scale) detected by the two independent differential proteomic methods: FTICR and WPES (see text). The ratio obtained for each protein with the FTICR method is shown as a red bar and with WPES as a black bar, and the corresponding protein name abbreviation is marked along the upper horizontal axis. For the majority of proteins (41 out of 44) both methods gave the same direction of change i.e. up- or downregulation, however, the degree of change was often substantially different. Note the Phb1, Phb2 and Cox2 proteins (marked in green) downregulated in [*PSI*$^+$], as described in detail in the text.

Fig. 2.

[*PSI*$^+$] decreases amounts of Phb1, Phb2 and Cox2 in mitochondria.

Western blot analysis of Cox2, Phb1 and Phb2 levels in mitochondrial (**A, B**) and total protein extracts (**C**) prepared by alkaline lysis. Proteins were isolated from isogenic [*psi*$^-$] and [*PSI*$^+$] strains GT197 and GT81-1D (**A, C**) or isogenic derivatives of MB43-*nam9-1* strain cured from [*PSI*$^+$] by deletion [*Δ*] or overexpression [↑] of the *HSP104* gene (**B**). The levels of Hsp104 were determined in the total extracts. Mitochondrial malate dehydrogenase (Mdh1) was used as a loading control.

.

Fig. 3. Abundance of prohibitins in cellular aggregates depends on the [*PSI*] state of the cell.

Lysates of [*psi*$^-$] and [*PSI*$^+$] strains (GT197 and GT81-1D) were prepared as described in the Materials and Methods and were fractionated by centrifugation through a sucrose cushion. The distribution of Phb1, Phb2 and Sup35 between the supernatant soluble fraction, sucrose layer and high molecular structures in the pellet was determined by immunoblotting. To confirm that other mitochondrial proteins are not present in the pellet, the blot was also decorated with an antibody specific for aconitase Aco1, the protein imported to mitochondria from the cytoplasm. The gel was loaded using 20 μg of protein per lane for the supernatant and sucrose fractions and 5 μg of protein per lane for the pellet fraction.

Fig. 4. Fragmentation of mitochondria in prohibitin-deficient [*PSI*$^+$] cells.

[*psi*$^-$] and [*PSI*$^+$] strains (GT197 and GT81-1D) were transformed with pYX323-mtGFP plasmid encoding green fluorescence protein (GFP) with a mitochondrial localization sequence and analyzed by confocal laser scanning microscopy. Reconstruction of the mitochondrial network was done from about ten confocal sections with intervals of 0.5 μm and 1024 x 1024 resolution. The images presented are representative for [*psi*$^-$] and [*PSI*$^+$] cells. More than 400 cells were scored per experiment. The percentage of cells with tubular mitochondria is indicated.

Table Legends

Table 1

Levels of Phb1, Phb2 and Cox2 in [*PSI*$^+$] versus [*psi*$^-$] mitochondria.

[*PSI*$^+$]/[*psi*$^-$] protein ratios were measured by densitometry of Western blots and by differential proteomics.

In order to determine the relative amount of proteins in [*PSI*$^+$] and [*psi*$^-$] strains by immunoblotting, the amount of each protein present in [*PSI*$^+$], corrected by the loading control, was set to 1. Column 1 represents the quantified results of immunoblotting analysis of Phb1, Phb2 and Cox2 in mitochondria from [*PSI*$^+$] and [*psi*$^-$] strains GT197 and GT81-1D (Fig. 2A). Columns 2 and 3 show the quantified results of the immunoblotting analysis of Phb1 and Phb2 in mitochondria from different pairs of isogenic [*PSI*$^+$] and [*psi*$^-$] strains in the genetic background of MB43-*nam9-1*:: [*PSI*$^+$] and its [*psi*$^-$] derivative derived by deletion (column 2) or overexpression (clolumn 3) of the gene encoding Hsp104 chaperone (Fig. 2C). The complex effect of Hsp104 on Cox2 levels in [*PSI*$^+$] cells was determined previously [20]

[*PSI*$^+$]/[*psi*$^-$] protein ratios for Phb1, Phb2 and Cox2 were determined independently by using two MS-based methods, FTICR and WPES, as described in the text and presented in the Supporting Material (Table S4, Fig. S4). Of note is the consistency between the numbers obtained by each method.

Protein name	**[*PSI*$^+$]/[*psi*$^-$] ratio**				
	Western blots			**Differential proteomics**	
	1	**2**	**3**	**WPES**	**FTICR**
Phb1	**0.68**	**0.52**	**0.65**	**0.60**	**0.53**
Phb2	**0.34**	**0.44**	**0.40**	**0.71**	**0.75**
Cox2	**0.41**	**Nd**	**nd**	**0.41**	**0.28**

Table 1.

References:

[1] R.B. Wickner, H.K. Edskes, E.D. Ross, M.M. Pierce, U. Baxa, A. Brachmann and F. Shewmaker, Prion genetics: new rules for a new kind of gene., Annu Rev Genet, 38 (2004) 681-707.

[2] J. Shorter and S. Lindquist, Prions as adaptive conduits of memory and inheritance., Nat Rev Genet, 6 (2005) 435-450.

[3] K.J. Barnham, R. Cappai, K. Beyreuther, C.L. Masters and A.F. Hill, Delineating common molecular mechanisms in Alzheimer's and prion diseases., Trends Biochem Sci, 31 (2006) 465-472.

[4] J.R. Glover, A.S. Kowal, E.C. Schirmer, M.M. Patino, J.J. Liu and S. Lindquist, Self-seeded fibers formed by Sup35, the protein determinant of [PSI+], a heritable prion-like factor of S. cerevisiae., Cell, 89 (1997) 811-819.

[5] F. Shewmaker, E. Ross, R. Tycko and R. Wickner, Amyloids of Shuffled Prion Domains That Form Prions Have a Parallel In-Register beta-Sheet Structure., Biochemistry, 47 (2008) 4000-4007.

[6] R.B. Wickner, F. Dyda and R. Tycko, Amyloid of Rnq1p, the basis of the [PIN+] prion, has a parallel in-register beta-sheet structure., Proc Natl Acad Sci U S A, 105 (2008) 2403-2408.

[7] V.V. Kushnirov and M.D. Ter-Avanesyan, Structure and replication of yeast prions., Cell, 94 (1998) 13-16.

[8] I. Stansfield, K.M. Jones, V.V. Kushnirov, A.R. Dagkesamanskaya, A.I. Poznyakovski, S.V. Paushkin, C.R. Nierras, B.S. Cox, M.D. Ter-Avanesyan and M.F. Tuite, The products of the SUP45 (eRF1) and SUP35 genes interact to mediate translation termination in Saccharomyces cerevisiae., EMBO J, 14 (1995) 4365-4373.

[9] G. Zhouravleva, L. Frolova, X. Le Goff, R. Le Guellec, S. Inge-Vechtomov, L. Kisselev and M. Philippe, Termination of translation in eukaryotes is governed by two interacting

polypeptide chain release factors, eRF1 and eRF3, EMBO J, 14 (1995) 4065-72.
[10] H.L. True, I. Berlin and S.L. Lindquist, Epigenetic regulation of translation reveals hidden genetic variation to produce complex traits., Nature, 431 (2004) 184-187.
[11] Y.O. Chernoff, S.L. Lindquist, B. Ono, S.G. Inge-Vechtomov and S.W. Liebman, Role of the chaperone protein Hsp104 in propagation of the yeast prion-like factor [psi+]. Science, 268 (1995) 880-884.
[12] V.V. Kushnirov, D.S. Kryndushkin, M. Boguta, V.N. Smirnov and M.D. Ter-Avanesyan, Chaperones that cure yeast artificial [PSI+] and their prion-specific effects., Curr Biol, 10 (2000) 1443-1446.
[13] A. Chacinska, B. Szczesniak, N.V. Kochneva-Pervukhova, V.V. Kushnirov, M.D. Ter-Avanesyan and M. Boguta, Ssb1 chaperone is a [PSI+] prion-curing factor., Curr Genet, 39 (2001) 62-67.
[14] Y. Tutar, Y. Song and D.C. Masison, Primate chaperones Hsc70 (constitutive) and Hsp70 (induced) differ functionally in supporting growth and prion propagation in Saccharomyces cerevisiae., Genetics, 172 (2006) 851-861.
[15] R. Aron, T. Higurashi, C. Sahi and E.A. Craig, J-protein co-chaperone Sis1 required for generation of [RNQ+] seeds necessary for prion propagation, EMBO J, 26 (2007) 3794-803.
[16] D. Kryndushkin and R.B. Wickner, Nucleotide exchange factors for Hsp70s are required for [URE3] prion propagation in Saccharomyces cerevisiae, Mol Biol Cell, 18 (2007) 2149-54.
[17] J. Shorter and S. Lindquist, Hsp104, Hsp70 and Hsp40 interplay regulates formation, growth and elimination of Sup35 prions., EMBO J, 27 (2008) 2712-2724.
[18] S.N. Bagriantsev, E.O. Gracheva, J.E. Richmond and S.W. Liebman, Variant-specific [PSI+] infection is transmitted by Sup35 polymers within [PSI+] aggregates with heterogeneous protein composition., Mol Biol Cell, 19 (2008) 2433-2443.
[19] K.D. Allen, R.D. Wegrzyn, T.A. Chernova, S. Muller, G.P. Newnam, P.A. Winslett, K.B. Wittich, K.D. Wilkinson and Y.O. Chernoff, Hsp70 chaperones as modulators of prion life cycle: novel effects of Ssa and Ssb on the Saccharomyces cerevisiae prion [PSI+], Genetics, 169 (2005) 1227-42.
[20] A. Chacinska, M. Boguta, J. Krzewska and S. Rospert, Prion-dependent switching between respiratory competence and deficiency in the yeast nam9-1 mutant., Mol Cell Biol, 20 (2000) 7220-7229.
[21] K. Czaplinski, M.J. Ruiz-Echevarria, S.V. Paushkin, X. Han, Y. Weng, H.A. Perlick, H.C. Dietz, M.D. Ter-Avanesyan and S.W. Peltz, The surveillance complex interacts with the translation release factors to enhance termination and degrade aberrant mRNAs., Genes Dev, 12 (1998) 1665-1677.
[22] D. Pflieger, J.-P.L. Caer, C. Lemaire, B.A. Bernard, G.v. Dujardin and J. Rossier, Systematic identification of mitochondrial proteins by LC-MS/MS., Anal Chem, 74 (2002) 2400-2406.
[23] S. Ohlmeier, A.J. Kastaniotis, J.K. Hiltunen and U. Bergmann, The yeast mitochondrial proteome, a study of fermentative and respiratory growth., J Biol Chem, 279 (2004) 3956-3979.
[24] H. Prokisch, C. Scharfe, D.G. Camp, W. Xiao, L. David, C. Andreoli, M.E. Monroe, R.J. Moore, M.A. Gritsenko, C. Kozany, K.K. Hixson, H.M. Mottaz, H. Zischka, M. Ueffing, Z.S. Herman, R.W. Davis, T. Meitinger, P.J. Oefner, R.D. Smith and L.M. Steinmetz, Integrative analysis of the mitochondrial proteome in yeast., PLoS Biol, 2 (2004) e160.
[25] A. Sickmann, J. Reinders, Y. Wagner, C. Joppich, R. Zahedi, H.E. Meyer, B. Schonfisch, I. Perschil, A. Chacinska, B. Guiard, P. Rehling, N. Pfanner and C. Meisinger, The proteome of Saccharomyces cerevisiae mitochondria, Proc Natl Acad Sci U S A, 100 (2003) 13207-12.
[26] R.P. Zahedi, A. Sickmann, A.M. Boehm, C. Winkler, N. Zufall, B. Schonfisch, B. Guiard, N. Pfanner and C. Meisinger, Proteomic analysis of the yeast mitochondrial outer membrane reveals accumulation of a subclass of preproteins, Mol Biol Cell, 17 (2006) 1436-50.
[27] J. Reinders, R.P. Zahedi, N. Pfanner, C. Meisinger and A. Sickmann, Toward the complete

yeast mitochondrial proteome: multidimensional separation techniques for mitochondrial proteomics, J Proteome Res, 5 (2006) 1543-54.
[28] J. Reinders, K. Wagner, R.P. Zahedi, D. Stojanovski, B. Eyrich, M. van der Laan, P. Rehling, A. Sickmann, N. Pfanner and C. Meisinger, Profiling phosphoproteins of yeast mitochondria reveals a role of phosphorylation in assembly of the ATP synthase, Mol Cell Proteomics, 6 (2007) 1896-906.
[29] S.P. Gaucher, S.W. Taylor, E. Fahy, B. Zhang, D.E. Warnock, S.S. Ghosh and B.W. Gibson, Expanded coverage of the human heart mitochondrial proteome using multidimensional liquid chromatography coupled with tandem mass spectrometry., J Proteome Res, 3 (2004) 495-505.
[30] S.W. Taylor, E. Fahy, B. Zhang, G.M. Glenn, D.E. Warnock, S. Wiley, A.N. Murphy, S.P. Gaucher, R.A. Capaldi, B.W. Gibson and S.S. Ghosh, Characterization of the human heart mitochondrial proteome., Nat Biotechnol, 21 (2003) 281-286.
[31] P. Lescuyer, J.M. Strub, S. Luche, H. Diemer, P. Martinez, A. Van Dorsselaer, J. Lunardi and T. Rabilloud, Progress in the definition of a reference human mitochondrial proteome, Proteomics, 3 (2003) 157-67.
[32] X. Xie, H.H. Wilkinson, A. Correa, Z.A. Lewis, D. Bell-Pedersen and D.J. Ebbole, Transcriptional response to glucose starvation and functional analysis of a glucose transporter of Neurospora crassa., Fungal Genet Biol, 41 (2004) 1104-1119.
[33] M. Fountoulakis and E.J. Schlaeger, The mitochondrial proteins of the neuroblastoma cell line IMR-32, Electrophoresis, 24 (2003) 260-75.
[34] V.K. Mootha, J. Bunkenborg, J.V. Olsen, M. Hjerrild, J.R. Wisniewski, E. Stahl, M.S. Bolouri, H.N. Ray, S. Sihag, M. Kamal, N. Patterson, E.S. Lander and M. Mann, Integrated analysis of protein composition, tissue diversity, and gene regulation in mouse mitochondria., Cell, 115 (2003) 629-640.
[35] S.D. Cruz, I. Xenarios, J. Langridge, F. Vilbois, P.A. Parone and J.-C. Martinou, Proteomic analysis of the mouse liver mitochondrial inner membrane., J Biol Chem, 278 (2003) 41566-41571.
[36] F. Perocchi, L.J. Jensen, J. Gagneur, U. Ahting, C. von Mering, P. Bork, H. Prokisch and L.M. Steinmetz, Assessing systems properties of yeast mitochondria through an interaction map of the organelle., PLoS Genet, 2 (2006) e170.
[37] Y.O. Chernoff, G.P. Newnam, J. Kumar, K. Allen and A.D. Zink, Evidence for a protein mutator in yeast: role of the Hsp70-related chaperone ssb in formation, stability, and toxicity of the [PSI] prion., Mol Cell Biol, 19 (1999) 8103-8112.
[38] B. Westermann and W. Neupert, Mitochondria-targeted green fluorescent proteins: convenient tools for the study of organelle biogenesis in Saccharomyces cerevisiae., Yeast, (2000).
[39] C. Meisinger, T. Sommer and N. Pfanner, Purification of Saccharomcyes cerevisiae mitochondria devoid of microsomal and cytosolic contaminations., Anal Biochem, (2000).
[40] B.J. Cargile, J.R. Sevinsky, A.S. Essader, J.L. Stephenson and J.L. Bundy, Immobilized pH gradient isoelectric focusing as a first-dimension separation in shotgun proteomics., J Biomol Tech, 16 (2005) 181-189.
[41] M.P. Yaffe and G. Schatz, Two nuclear mutations that block mitochondrial protein import in yeast., Proc Natl Acad Sci U S A, 81 (1984) 4819-4823.
[42] H. Prokisch, C. Andreoli, U. Ahting, K. Heiss, A. Ruepp, C. Scharfe and T. Meitinger, MitoP2: the mitochondrial proteome database-now including mouse data., Nucleic Acids Res, 34 (2006) D705-D711.
[43] T. Langer, M. Kaser, C. Klanner and K. Leonhard, AAA proteases of mitochondria: quality control of membrane proteins and regulatory functions during mitochondrial biogenesis, Biochem Soc Trans, 29 (2001) 431-6.
[44] L.G. Nijtmans, L. de Jong, M.A. Sanz, P.J. Coates, J.A. Berden, J.W. Back, A.O. Muijsers, H. van der Spek and L.A. Grivell, Prohibitins act as a membrane-bound chaperone for the

stabilization of mitochondrial proteins., EMBO J, 19 (2000) 2444-2451.
[45] L.G.J. Nijtmans, S.M. Artal, L.A. Grivell and P.J. Coates, The mitochondrial PHB complex: roles in mitochondrial respiratory complex assembly, ageing and degenerative disease., Cell Mol Life Sci, 59 (2002) 143-155.
[46] L. Kiemer, S. Costa, M. Ueffing and G. Cesareni, WI-PHI: a weighted yeast interactome enriched for direct physical interactions., Proteomics, 7 (2007) 932-943.
[47] S.V. Paushkin, V.V. Kushnirov, V.N. Smirnov and M.D. Ter-Avanesyan, Propagation of the yeast prion-like [psi+] determinant is mediated by oligomerization of the SUP35-encoded polypeptide chain release factor., EMBO J, 15 (1996) 3127-3134.
[48] P.W. Piper, G.W. Jones, D. Bringloe, N. Harris, M. MacLean and M. Mollapour, The shortened replicative life span of prohibitin mutants of yeast appears to be due to defective mitochondrial segregation in old mother cells., Aging Cell, 1 (2002) 149-157.
[49] C. Merkwirth, S. Dargazanli, T. Tatsuta, S. Geimer, B. Lower, F.T. Wunderlich, J.C. von Kleist-Retzow, A. Waisman, B. Westermann and T. Langer, Prohibitins control cell proliferation and apoptosis by regulating OPA1-dependent cristae morphogenesis in mitochondria, Genes Dev, 22 (2008) 476-88.
[50] G. Steglich, W. Neupert and T. Langer, Prohibitins regulate membrane protein degradation by the m-AAA protease in mitochondria., Mol Cell Biol, (1999).
[51] C. Osman, C. Wilmes, T. Tatsuta and T. Langer, Prohibitins interact genetically with Atp23, a novel processing peptidase and chaperone for the F1Fo-ATP synthase., Mol Biol Cell, 18 (2007) 627-635.
[52] J.W. Back, M.A. Sanz, L.D. Jong, L.J.D. Koning, L.G.J. Nijtmans, C.G.D. Koster, L.A. Grivell, H.V.D. Spek and A.O. Muijsers, A structure for the yeast prohibitin complex: Structure prediction and evidence from chemical crosslinking and mass spectrometry., Protein Sci, 11 (2002) 2471-2478.
[53] T. Tatsuta, K. Model and T. Langer, Formation of membrane-bound ring complexes by prohibitins in mitochondria., Mol Biol Cell, (2005).
[54] S. Meeusen, R. DeVay, J. Block, A. Cassidy-Stone, S. Wayson, J.M. McCaffery and J. Nunnari, Mitochondrial inner-membrane fusion and crista maintenance requires the dynamin-related GTPase Mgm1., Cell, 127 (2006) 383-395.
[55] N. Ishihara, Y. Fujita, T. Oka and K. Mihara, Regulation of mitochondrial morphology through proteolytic cleavage of OPA1., EMBO J, 25 (2006) 2966-2977.
[56] K.L. Cerveny, Y. Tamura, Z. Zhang, R.E. Jensen and H. Sesaki, Regulation of mitochondrial fusion and division., Trends Cell Biol, 17 (2007) 563-569.
[57] C. Merkwirth, S. Dargazanli, T. Tatsuta, S. Geimer, C. Merkwirth and T. Langer, Prohibitin function within mitochondria: Essential roles for cell proliferation and cristae morphogenesis., Biochim Biophys Acta, 1793 (2009) 27-32.
[58] H. Sesaki, S.M. Southard, A.E.A. Hobbs and R.E. Jensen, Cells lacking Pcp1p/Ugo2p, a rhomboid-like protease required for Mgm1p processing, lose mtDNA and mitochondrial structure in a Dnm1p-dependent manner, but remain competent for mitochondrial fusion., Biochem Biophys Res Commun, 308 (2003) 276-283.
[59] M. Herlan, F. Vogel, C. Bornhovd, W. Neupert and A.S. Reichert, Processing of Mgm1 by the rhomboid-type protease Pcp1 is required for maintenance of mitochondrial morphology and of mitochondrial DNA., J Biol Chem, (2003).
[60] A. Lewandowska, M. Gierszewska, J. Marszalek and K. Liberek, Hsp78 chaperone functions in restoration of mitochondrial network following heat stress, Biochim Biophys Acta, 1763 (2006) 141-51.
[61] S.V. Paushkin, V.V. Kushnirov, V.N. Smirnov and M.D. Ter-Avanesyan, Interaction between yeast Sup45p (eRF1) and Sup35p (eRF3) polypeptide chain release factors: implications for prion-dependent regulation., Mol Cell Biol, 17 (1997) 2798-2805.
[62] M.M. Patino, J.J. Liu, J.R. Glover and S. Lindquist, Support for the prion hypothesis for inheritance of a phenotypic trait in yeast, Science, 273 (1996) 622-6.

Figure 1

Click here to download high resolution image

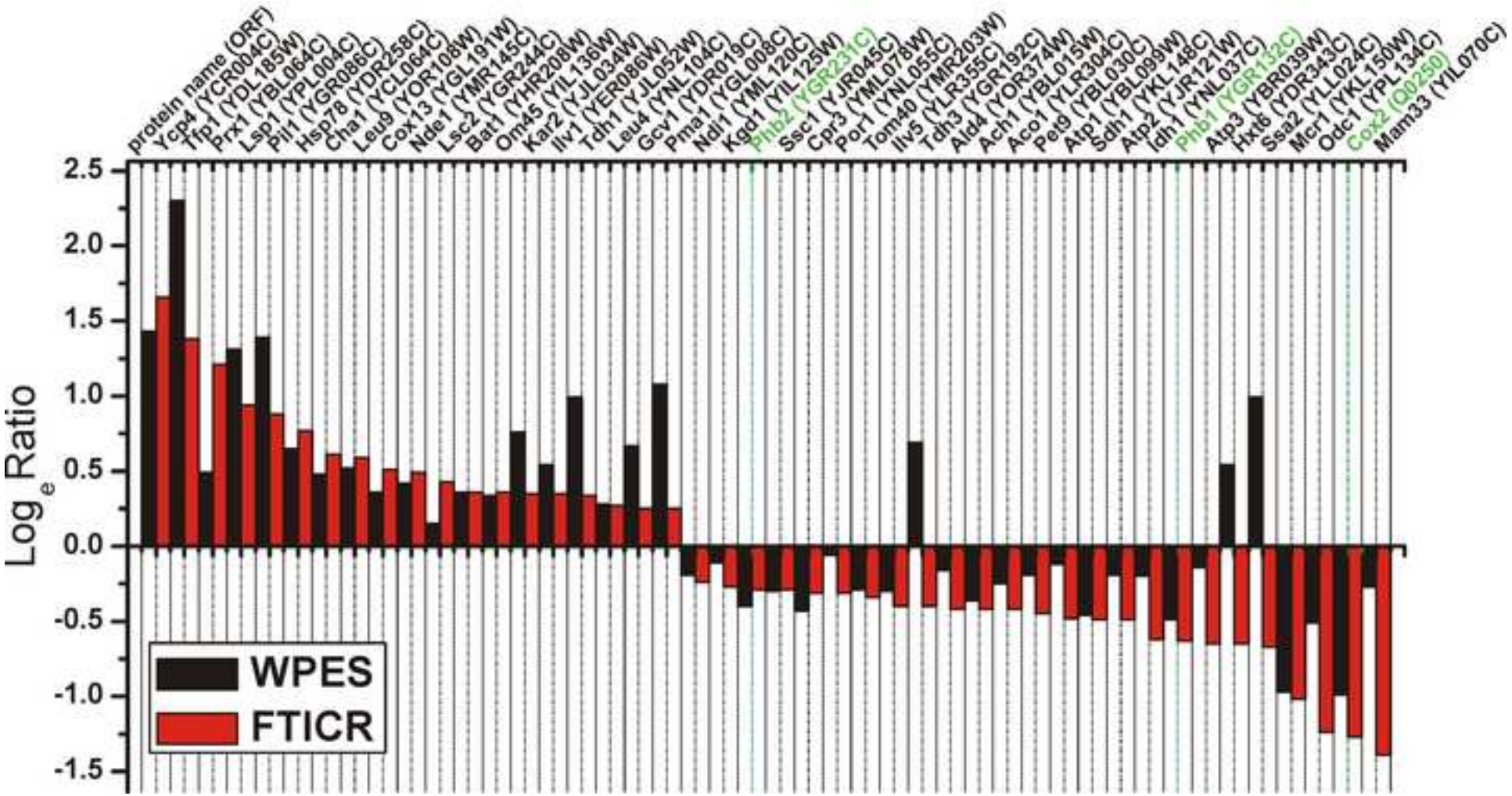

Figure 2

Click here to download high resolution image

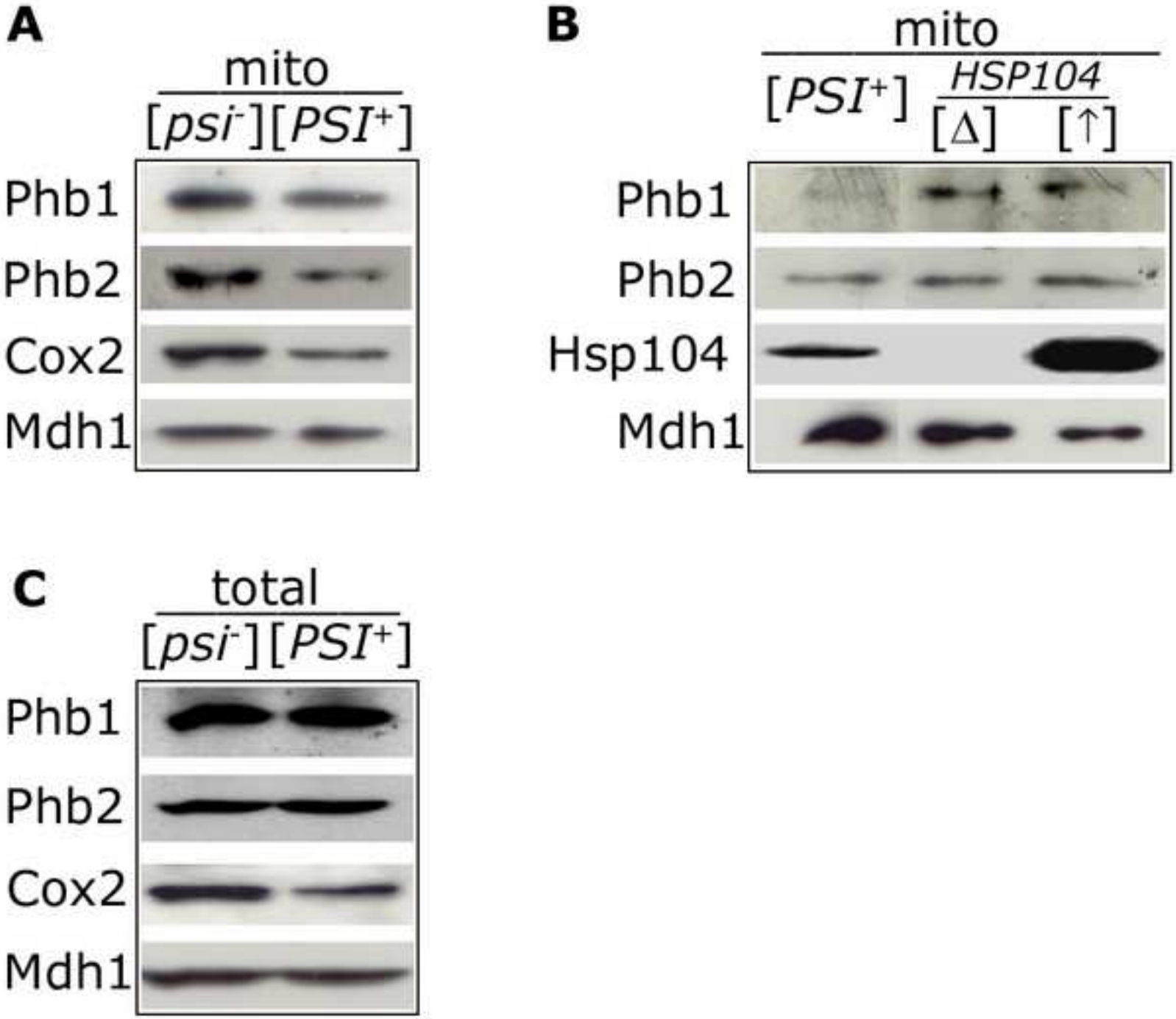

Figure 3

Click here to download high resolution image

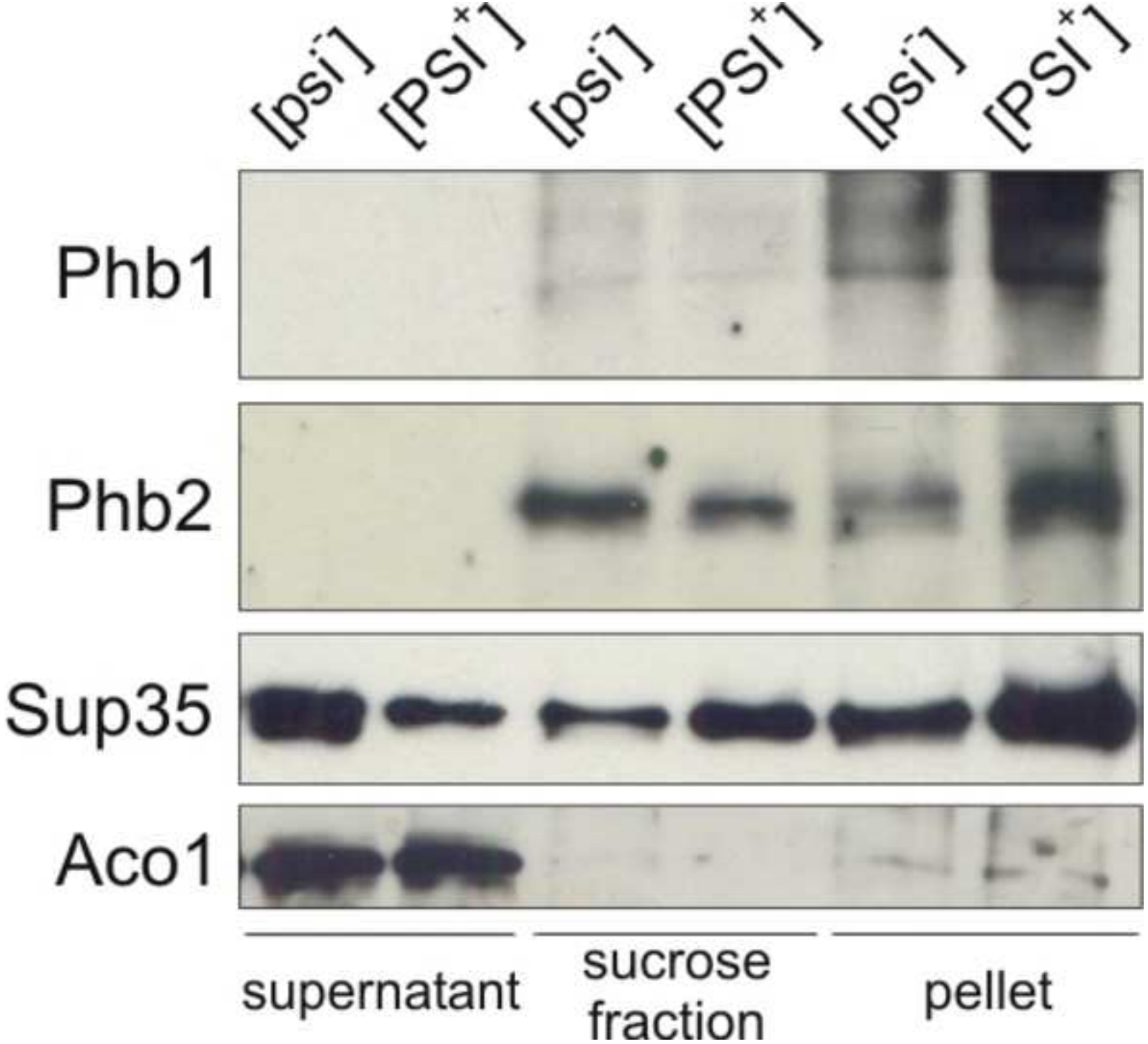

Figure 4

Click here to download high resolution image

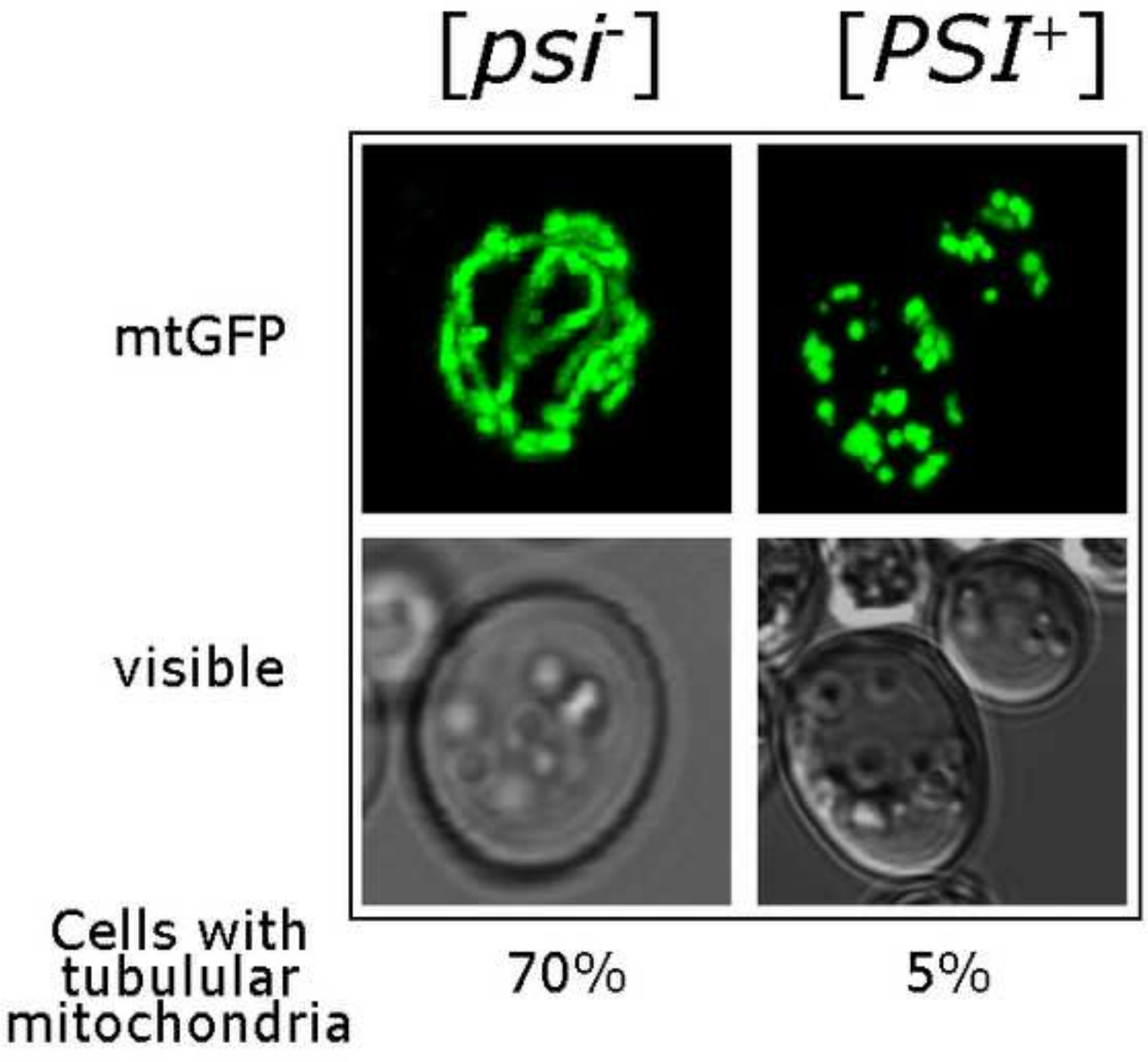

Supporting material

Supporting Material and Methods Section

Abbreviations

FC – Fold Change, equal to the ratio of protein levels for upregulated proteins (ratio>1) and to the reciprocal of the ratio for downregulated proteins (ratio<1).

FDR - False Discovery Rate

FTICR - Fourier Transform Ion Cyclotron Resonance

IEF - IsoElectric Focusing

IPG-immobilized pH gradient

LC-MS – Liquid Chromatography coupled to Mass Spectrometry in survey scan mode

LC-MS-MS/MS – Liquid Chromatography coupled to Mass Spectrometry in data-dependent switch to fragmentation mode

LTQ – Linear Trap Quadruple

MREF – Mitochondrial REference Dataset (according to [42])

MS – Mass Spectrometry

MS/MS – Mass Spectrometry in peptide fragmentation mode

OD – Optical Density

WPES – Waters Protein Expression System

Protein identification step

The identification of mitochondrial proteins derived from [PSI^{+}] and [psi^{-}] strains was carried out by several rounds of LC-MS-MS/MS experiments using an LTQ FTICR spectrometer.

The analysis was carried out in two stages. In the first stage, referred to as “LC-MS-MS/MS”, LC was the only fractionation step preceding the MS analysis of the tryptic digest of total mitochondrial proteins. Data obtained were then compared to a protein sequence database with the MASCOT [63] search engine. In stage two the sample was further fractionated by isoelectrofocusing and each fraction was subjected separately to LC-MS-MS/MS analysis (referred to as IEF-LC-MS-MS/MS). Additional MASCOT runs using the datasets from both stages were carried out against randomized databases, for calculation of the false discovery rate (FDR) values of our database’s search procedures. These additional runs showed that the FDR = 0.3%, i.e. accepting one false positive for each 300 true positive protein hits, corresponding to a MASCOT score of 40. Based on this result the protein hit was accepted if the list of assigned peptides contained at least one peptide with a score larger than 40.

In the first stage a list of 865 proteins was obtained. From this list, 160 protein identifications were based on two peptides and 358 on one peptide, so for 60% of protein hits the peptide coverage was insufficient. In the second stage (IEF-LC-MS-MS/MS), to obtain an increased coverage of mitochondrial proteins, the data collected from multiple LC-MS-MS/MS experiments were merged into one input data file, containing 56088 MS/MS fragmentation queries, and subjected to MASCOT database search and FDR analysis. This experiment resulted in an expanded list of 1064 proteins identified in stage two. This list was compared with the list of 865 proteins obtained in stage one. Stage two analysis confirmed the identification of 654 (76%) proteins from stage one. This means that a quarter of proteins from stage one were not confirmed in stage two. Interestingly, eight proteins identified with >=5 peptides in stage one did not appear in the list in stage two. This indicates the insufficiency of the narrow pH range (3.5–4.5) of the IEF gel used here, which might be the reason for loss of peptides originating from basic proteins and lack of detection of some proteins in the expanded experiment. On the other hand, in stage two we detected >400

proteins that were not detected in stage one. Twenty-nine proteins identified with five or more peptides in the second stage did not appear in the list in stage one. For example, the Hpd1 protein identified in the second stage by 47 peptides (Mascot Score = 3974) was not detected in the first stage. The complementarity of different proteomic approaches has frequently been noted (see e.g. [27]). Of the 358 proteins identified in the stage one analysis by a single peptide hit, 199 were confirmed. In the case of double-peptide identifications – 130 of 160 proteins were confirmed using the peptide IEF-LC-MS-MS/MS approach. In total 189 of these protein hits were not confirmed in the stage two analysis and were not included in the differential analysis. The final protein list assembled from both stages consisted of 1275 proteins (Table S1). The protein list obtained in this study was compared with the mitochondrial proteome characterized previously by other authors [22-28]. 753 proteins (59% of 1275) were found previously by MS-based mitochondrial proteome identification approaches [22-28]. Our dataset was also evaluated against "*in silico*" predictions of localization provided by the PSORT [64], Predator [65] and SubLoc [66] databases. Mitochondrial localization was predicted for 756 proteins (59% of 1275). In all, 972 (76%) of the 1275 proteins were indicated as mitochondrial in previous either MS-based or "*in silico*" studies. A Venn diagram comparing the results of our protein identification analysis with other methods characterizing the mitochondrial proteome is presented in Fig. S1. The level of agreement of our protein list with the MREF, the mitochondrial protein reference set in the Mitop2 database [42] that contains experimentally validated mitochondrial proteins, is also an important indicator of the quality of the present work. We detected 437 (80%) of the 546 proteins present in the MREF [42]. Thirty-four of these 437 proteins (listed in Table S2) were, to the best of our knowledge, identified in an MS-based study of yeast mitochondria for the first time. For comparison the fractional coverage of the MREF obtained in other studies [22, 25, 23, 27] was as follows: 145 (26%), 393 (72%), 158 (29%) and 435 (80%), respectively.

Our list contains representatives of 45 out of the 46 major functional modules of the yeast mitochondrial interactome constructed by Perocchi and co-workers [36]. Among the 164 predicted functional modules, 46 with five or more protein partners were considered as major. The coverage of protein identification obtained here within the individual 46 mitochondrial modules is presented in Fig. S2. For example all 13 proteins from the TCA cycle and 10 of 14 proteins from respiratory complex chain IV were detected. Within 34 of the 46 modules we were able to detect over 60% of partner proteins. Detailed information concerning identification of the components of the mitochondrial functional modules in this and other studies is presented in Table S3.

Differential proteomics

Following the protein identification step, two independent LC-MS differential methods (named FTICR and WPES) were used to obtain a list of proteins, the levels of which are affected by the presence of prion [*PSI*$^{+}$] (Table S4). Details of the methods, the statistical analysis and hit acceptance criteria are described below.

A. FTICR system

A.1. Sample preparation

Prior to MS analysis, crude mitochondria were resuspended in 50 mM ammonium bicarbonate/0.2% RapiGest^{TM} SF solution (Waters), which allows for complete lysis of mitochondria as indicated by the clarity of the resulting resuspension. Trypsin (sequencing grade; Promega, Madison, WI) was added at the concentration of 20 ng/µl and proteins were digested overnight at 37 °C. The enzyme to substrate ratio was 1:100 (w/w). The resulting peptide mixture was reduced with 10 mM DTT (Roth) and alkylated using 50 mM IAA. Samples were diluted with 0.1% TFA to the concentration of 0.1 µg/µl. 2 µg of tryptic

peptides in 20 µl were loaded on the column in each injection.

A.2. Liquid chromatography

Liquid chromatography (LC) – mass spectrometry (MS) analyses of the tryptic mixture of mitochondrial peptides were carried out using a nano-Acquity (Waters) LC system coupled to a LTQ FTICR (Thermo) mass spectrometer. Spectrometer parameters were as follows: capillary voltage: 2.5 kV, cone: 40 V, N_2 gas flow: 0, range 300–2000 (m/z). The spectrometer was calibrated on a weekly basis with Calmix (caffeine, MRFA, Ultramark 1621). The sample was first loaded from the autosampler tray cooled down to 10 ^{o}C to the pre-column (Symmetry C18, 180 µm × 20 mm, 5 µm (Waters, 186003514)), using a mobile phase of MilliQ H_2O acidified by 0.1% FA. The peptides were then transferred to the nano-UPLC column (BEH130 C18, 75 µm × 250 mm, 1.7 µm (Waters, 186003545)) by a gradient of 5–30% acetonitrile, 0.1% FA in 160 min and directly eluted to the ion-source of the mass spectrometer. [*psi*$^{-}$] LC runs were separated from [*PSI*$^{+}$] LC runs by a blank run, ensuring lack of carry-over of the material from the previous runs.

A.3. Mass spectrometry

The qualitative (LC-MS-MS/MS peptide identification runs) and quantitative (profile type peptide peak amplitude LC-MS runs) datasets were collected in separate experiments.

A.3.1. Qualitative runs. For peptide identification, a series of four LC-MS-MS/MS runs on [*psi*$^{-}$] and [*PSI*$^{+}$] samples were carried out with the spectrometer running in the data-dependent switch to peptide fragmentation mode (MS/MS). Up to ten fragmentation processes were allowed for each MS scan. Each run covered one of four sectors of m/z values: 300–600, 500–800, 700–1000, 900–2000. The sector overlap was introduced to avoid loss of instrument sensitivity at the high m/z value sector border. As a result, four sequencing runs were collected for each [*psi*$^{-}$] and [*PSI*$^{+}$] sample. This approach has been found to significantly improve the coverage of peptide identification.

The lists of parent masses and daughter fragment masses from both [*psi*$^-$] and [*PSI*$^+$] samples were prepared (merged into a single file) for the database search with MascotDistiller v2.1.1.0 software (MatrixScience) and searched against the *Saccharomyces cerevisiae* protein database from ftp://genomeftp.stanford.edu/pub/yeast/sequence/genomic_sequence/orf_protein/orf_trans_all.fasta.gz containing the amino acid sequences of all systematically named ORFs with the Mascot (Matrixscience) v2.3 search engine (8-processor site license). The protein database was enriched with trypsin and common contaminant keratin sequences. Mascot search parameters were as follows: fixed modification: Cys carbamidomethylation; variable modification: Met oxidation, Asn Gln deamidation; peptide mass tolerance: 40 ppm; fragment mass tolerance: 0.8 Da; enzyme: semi-trypsin. In total 42316 peptide fragmentation spectra were included in the search. The list of peptides from all eight [*psi*$^-$] and [*PSI*$^+$] runs matching the acceptance criteria (Mascot peptide score above 40) was merged into one peptide sequence list (Selected Peptides List – SPL) using an in-house MScan program (www.ire.pw.edu.pl/~trubel/soft/ms/mascotscan/). This list contains 6390 peptides, corresponding to 865 proteins along with the peptide m/z and LC retention time values. SPL was used further to overlay the results of qualitative and quantitative runs by tagging the corresponding MS peptide signals in quantitative, profile type data sets with peptide sequence tags, based on peptide m/z and retention time values, using in-house software (Poznański J. et al., unpublished) (see below).

In addition, to confirm the statistical validity of accepted protein hits the false-positive rate (FDR) values were calculated by performing Mascot searches on a decoy database, merged from an ordinary protein database and it's randomized version created using a Perl script supplied by Matrix Science (http://www.matrixscience.com/help/decoy_help.html). Computation was performed using a module of the in-house developed software MScan.

Briefly, the estimated FDR value is defined as double the number of queries assigned by Mascot to randomized sequences divided by the number of queries assigned to sequences originating from non-decoy yeast proteins. Both randomized and non-randomized hits must achieve a peptide score exceeding a given threshold, which can be manipulated depending on which FDR is adequate. For our experiment the accepted Mascot peptide score threshold of 40 corresponds to 0.29% of false positive identifications.

A.3.2. Quantitative runs. Profile (quantitative) runs were carried out in triplicate, as separate LC-MS runs for both [*psi*$^-$] and [*PSI*$^+$] using the same acetonitrile gradient. The spectrometer resolution was set at 50000. Raw datasets of collected mass spectra were converted to NMRPipe software: http://spin.niddk.nih.gov/NMRPipe/ data format by an in-house MS2Pipe data conversion tool. At this stage a series of MS spectra becomes a 2D array (2D peptide heat map) in which every feature represents the signal amplitude (quantity of ions) at a given m/z, eluted at a given time. The NMRPipe program was designed and thoroughly tested by many research groups for the analysis of nuclear magnetic resonance protein spectra. However, it can also be used for the analysis of multidimensional datasets of any kind, including LC-MS data, which have an inherent 2D character. NMRPipe along with Sparky NMR assignment software [67](converted to accept mass spectrometry data into an in-house "MSparky" tool (www.ire.pw.edu.pl/~trubel/soft/ms/msparky/)) allow for efficient multidimensional data processing and visualization. The data analysis steps may include noise reduction, smoothing, peak picking, conversion of a set of mass spectra to a list of mass peaks along with their amplitudes and coordinates on the m/z and retention time axis. Also when supported by an in-house procedure (TagProfile) it allows for identification of MS peaks corresponding to given peptides from the list, based on their m/z values and retention time coordinates providing an overlay of qualitative peptide sequence results on quantitative MS profile data.

A.3.3. Overlay of qualitative peptide sequence list on quantitative profile datasets. In the next step of analysis the peptides from SPL obtained from qualitative runs were overlaid on peptide heat maps using in-house TagProfile software (Poznański, J. unpublished) so that a monoisotopic peak on the profile map is assigned to each peptide from the list of identified peptides, if found. The program allows for efficient correction of the unavoidable differences in retention times between runs. The actual, measured retention time is recalculated as relative retention time domain to best overlay the qualitative run retention times of the peptides and the retention times of their corresponding peaks. The details of the program will be described elsewhere. As a result, selected monoisotopic peaks on the map become tagged with a peptide identity tag (Fig. S5). A peak integration tool is later used to carry out the integration of peaks (2, 3 or more) from tagged isotopic envelopes and the peptide list is expanded by fitted peak height and peak volume. On this list peptides that were not found or were found but did not meet the acceptance criteria are highlighted and can be verified or corrected manually in an interactive fashion using an in-house MSparky tool. Acceptance criteria include m/z value deviation, retention time deviation, Fit Root Mean Squared Error, Envelope Root Mean Squared Error (i.e. the deviation between the expected isotopic envelope peak heights and their experimental values) and charge state value. Peak volumes or amplitudes of corresponding peptides in two samples can be compared in the form of a scatter plot as described in Fig. S6.

A.3.4. Relative quantitation. The amplitude of the isotopic envelope corresponding to the various charge state signals of the peptide is used as a measure of relative peptide abundance. For the peptides of interest their corresponding monoisotopic peaks on the heat maps are localized using the ProfileTag tool, and their sequence tags are added to the heat map as shown in Fig. S5. Peaks from all tagged isotopic envelopes are then integrated by 2D fitting of a Gaussian curve to the peak by the least squares method. The peak amplitude is defined as

the height of the peak at its maximum calculated from the best fit of a Gaussian curve ("peak fit height" option in MSparky). Peptide relative abundance is calculated as the sum of peak amplitudes of two peaks from its isotopic envelope (monoisotopic peak and one peak corresponding to the presence of one ^{13}C atom). The list of peaks containing peptide sequences, charge, m/z, rt, and fit height was exported to file and analyzed using Perl scripts designed for statistical computing. A resampling procedure [68-70] with FDR [71, 72] control was used for estimation of significance. In the FTICR-based differential approach the estimated ratio was regarded as statistically significant if $p<0.1$, and 100 proteins with the lowest p values were selected for further analysis.

B. Waters Protein Expression System (WPES)

B.1. Sample preparation

Crude mitochondria were solubilized essentially in the same way as in the FTICR-based differential system except for the use of a 0.1% RapiGest™ SF solution. Proteins were reduced (10 mM DTT) and alkylated (10 mM IAA) prior to enzymatic digestion overnight with trypsin 1:50 (w/w) enzyme: protein ratio at 37 °C. RapiGest was removed by addition of 2 µl concentrated HCl, followed by centrifugation, and then the supernatant was collected. Samples were diluted with 0.1% formic acid to an appropriate final working concentration prior to analysis – corresponding to 0.3 µg protein digest loaded on the column.

B.2. LC conditions

Two experiments with different LC conditions were performed using WPES. Quantification experiments were conducted using a 180 min gradient at 250 nl/min (5 to 40% acetonitrile over 180 minutes) or 90 minutes (5 to 40% acetonitrile over 90 minutes) on a nanoACQUITY UPLC®System equipped with a Symmetry C18 pre-column (180 µm × 20 mm, 5 µm (Waters, 186003514)) and utilizing a 1.7 µm BEH C18 NanoEase™ 75 µm x 20 cm column. Each

sample was analyzed in triplicate in each LC condition.

B.3. MS conditions

The Q-Tof Premier^{TM} mass spectrometer was set to shift between normal (5 eV) and elevated (25–40 eV) collision energies on the gas cell, using a scan time of 1.5 s per function over 50–1990 m/z. All remaining settings were set according to the WPES manufacturer's recommendations.

B.4. Data processing and protein identification

Data alignment, protein identifications and quantitative analysis were conducted using dedicated algorithms (Waters Protein Expression Informatics-PLGS v2.3 build 020) and searching the *S. cerevisiae* protein database from www.yeastgenome.org enriched with trypsin and common keratin sequences as described for LTQ FTICR analysis. The principles of the applied data clustering and normalization have been explained in great detail in previous publications [73, 74]. In WPES the estimated ratio was regarded as statistically significant if the probability of regulation(p) ranged from 0 to 0.1, and 100 proteins with the lowest p values for the obtained [PSI^{+}]/[psi^{-}] ratios were accepted for further analysis

Forty-four proteins were indicated as differential by FTICR and WPES. In general, the qualitative agreement between the two methods was good. Out of 44 proteins identified by both methods as differentially expressed, 41 showed the same direction of expression changes in both experiments (Table S4). To assess the agreement on a quantitative level, the [PSI^{+}]/[psi^{-}] ratio values from both differential systems were compared for the 44 proteins common to both systems (Fig. 1). Only 57% of proteins had FC (fold change) values that did not differ by more than 30%. This observation indicates that the results of MS-based differential proteomic experiments have to be treated with caution especially with regards their quantitative aspects, and that an independent confirmatory test is still a must.

Supporting Material Section S2 - Legends for Supporting Tables and Figures

Supporting Material Table S1 List of all 1275 proteins identified in this study using the LC-MS-MS/MS method (both IEF and non-IEF approach). Columns from left to right contain: 1. Module number according to [36]; 2. Module name if provided [36]; 3. SGD protein name and ORF name in parentheses; [*PSI*$^{+}$] 4.-7. Mascot MudPit score and number of peptides identified from each protein in two steps of the analysis ("LC-MS-MS/MS only" and "peptide IEF-LC-MS-MS/MS"); 8.-14. Presence in previous MS-based studies [22-27, Prokish-unpublished dataset] marked by ”x”, 15.-17. ”*In silico*” prediction of mitochondrial localization according to PSORT [64], Predotar [65] (where ** stands for “mitochondrial”, and * for “possible mitochondrial”), SubLoc [66]; 18. Presence in the MREF (release 2007) [42].

Supporting Material Table S2. List of 34 proteins identified in mitochondrial preparations in this work that are present in the MREF database [42] and which, to our knowledge, have not been identified previously by MS-based studies on the *S. cerevisiae* mitochondrial proteome [22-28, Prokish-unpublished dataset].

Supporting Material Table S3. List of predicted mitochondrial functional modules [36] with number of proteins expected for each module (column 3) and number of proteins detected in this (column 4) and other work [22-27, Prokish-unpublished dataset] (columns 5-11).

Supporting Material Table S4 List of all proteins (156) for which the [*PSI*$^{+}$]/[*psi*-] ratios were measured with highest confidence. One hundred proteins from each differential system (FTICR or WPES) with the lowest estimated p values were accepted. In columns 1, 2, 3, the module number, module name (if present), as introduced in [36], and protein ORF name, are given, respectively. The protein [*PSI*+]/[*psi*-] ratio values and p-values are shown in columns 4 and 5 (FTICR method) and 6 and 7 (WPES method). Ratio values are the mean of three

independent experiments. Forty-one proteins for which the direction of change was the same in both methods are marked in green. Eight proteins which showed changes in opposite directions are marked in red. The mean FC value is given in the last column. *p* value 0.00 means $p<0.01$.

Figure S1. **Venn diagram illustrating the overlap of yeast mitochondrial protein lists obtained in this and earlier work.** Proteins attributed to yeast mitochondria (2537 proteins in total) are grouped in three datasets: proteins identified in this study (1275 proteins), proteins found previously in MS-based identification of mitochondrial proteins [22-28] (1148 proteins), and proteins implicated as mitochondrial by "*in silico*" predictions of mitochondrial localization (PSORT [64], Predator [65], SubLoc [66] – 1770 proteins). The total number of entries for each dataset along with the fraction (in %) of the total protein number is indicated outside each circle. The number inside each circle indicates the number of common entries between the datasets. Proportions of circles and overlapping regions reflect the fractional value of each category. A total of 537 proteins are common to all three groups, and 972 (537+216+219) proteins found in this study have already been attributed to mitochondria in previous work. A total of 753 proteins (537+216 – 59% of 1275) were found previously by MS-based mitochondrial proteome identification approaches. Mitochondrial localization was predicted for 756 proteins (537+219 – 59% of 1275). A total of 303 proteins were identified in yeast mitochondrial preparations for the first time.

Figure S2. Proteins subjected to differential proteomics cover major yeast mitochondrial functional modules. The GO terms-based module map of 46 functional modules consisting of five or more proteins is shown according to [36], with the indicated fraction of proteins identified in this work by two-step LC-MS-MS/MS analysis. Proteins identified at both stages of the analysis (LC-MS-MS/MS without or with peptide IEF prefractionation) are marked in

red. Proteins identified exclusively in the first stage – LC-MS-MS/MS – are marked in green. Proteins identified only in the second stage of the analysis – IEF-LC-MS-MS/MS – are marked in blue. Grey dots indicate proteins not detected in this study. Modules were named and assigned to cellular compartments based on GO terms. The localization of modules in three different compartments – nucleus, mitochondria, and cytoplasm – is indicated by sectors of different colors. When a module contains a mixture of proteins with different localizations it is annotated as shared between the different compartments. Modules that are shared between mitochondria and the nucleus or mitochondria and the cytoplasm belong to the green and yellow sectors, respectively. Cytoplasm refers to all contents of the cell excluding the mitochondria and nucleus but including the plasma membrane and other sub-cellular structures. For the majority of modules the coverage exceeds 50% and only in one module was no protein detected (Mismatch repair).

Figure S3. Prion-dependent changes detected in this work in yeast mitochondrial proteome overlaid onto the mitochondrial interactome. A simplified interactome [46] is shown that is limited to proteins present in the MREF [42] and their direct neighbors. Upregulated proteins are marked as red squares and downregulated proteins as blue squares with the color intensity depending on the log (fold change) values as described in the color scale shown. The enlarged part of the interactome shows a direct link between Cox2 and prohibitins.

Figure S4. MS analysis of Phb1, Phb2 and Cox2 peptide levels in [*psi*$^-$] and [*PSI*$^+$] strains. Comparison of MS signal intensities in [*psi*$^-$] (black bars) and [*PSI*$^+$] (red bars) obtained with the FTICR method (A), (C), (E), and WPES method (B), (D), (F) for individual peptides of Phb1 (A), (B), Phb2 (C), (D) and Cox2 (E), (F) proteins. The mean value of peptide signal amplitude (in arbitrary units) in three independent experiments is shown, with corresponding error bars. These results reveal a decrease in MS signals corresponding to

prohibitins and Cox2 protein in the mitochondria of [*PSI*$^{+}$] yeast.

Figure S5. 2D LC-MS map of tryptic peptides from the *S. cerevisiae* mitochondrial fraction of yeast. A heat map of peaks detected in a typical LC-MS analysis of digested mitochondrial fraction is presented in two panels of different magnification. Their retention times are shown on the vertical axis, m/z values on the horizontal axis, and the peak amplitudes are color-coded in a hypsometric rendering with their values increasing from red to blue. The map represents smoothed raw data with no further processing. Each peptide is represented by a characteristic group of peaks, an isotopic envelope, which originates from the presence of different isotopes, mainly ^{13}C instead of ^{12}C, in a fraction of the molecules. The upper panel shows a full range dataset with m/z values between 300 Th and 1500 Th and retention times between 40 and 180 min. Lower panel – a magnified section of 595–596 in the m/z and 96–108 min in the RT domain. The magnified panel shows that even peptides with close m/z and retention time values generate well-resolved isotopic envelopes. Monoisotopic peaks of isotopic envelopes assigned to peptides from the Selected Peptides List (refer to Supporting Material Section S1) are tagged by the protein name from the SGD, peptide sequence and charge. Crosses indicate two peaks of the isotopic envelope included in the quantification.

Figure S6. Scatter plots of MS signal intensities of 6390 peptides from mitochondrial proteins of [*psi*$^{-}$] and [*PSI*$^{+}$] strains compared by a typical differential experiment (FTICR method). (**A**) Comparison of signal amplitudes on a log scale of two replicates of [*psi*-] sample. (**B**) The amplitude of the peptide signal in the [*PSI*+] sample is shown on a log scale on the vertical axis and the signal of the same peptide in the [*psi*-] sample is shown on the horizontal axis.

References

(numbers are the same as in the text of the article)

[22] D. Pflieger, J.-P.L. Caer, C. Lemaire, B.A. Bernard, G. Dujardin, J. Rossier, Systematic identification of mitochondrial proteins by LC-MS/MS, Anal. Chem. 74 (2002) 2400–2406.

[23] S. Ohlmeier, A.J. Kastaniotis, J.K. Hiltunen, U.Bergmann, The yeast mitochondrial proteome, a study of fermentative and respiratory growth, J. Biol. Chem. 279 (2004) 3956–3979.

[24] H. Prokisch, C. Scharfe, D.G. Camp, W. Xiao, L. David, C. Andreoli, M.E. Monroe, R.J. Moore, M.A. Gritsenko, C. Kozany, K.K. Hixson, H.M. Mottaz, H. Zischka, M. Ueffing, Z.S. Herman, R.W. Davis, T. Meitinger, P.J. Oefner, R.D. Smith, L.M. Steinmetz, Integrative analysis of the mitochondrial proteome in yeast, PLoS Biol. 2 (2004) e160.

[25] A. Sickmann, J. Reinders, Y. Wagner, C. Joppich, R. Zahedi, H.E. Meyer, B. Schönfisch, I. Perschil, A. Chacinska, B. Guiard, P. Rehling, N. Pfanner, C. Meisinger, The proteome of Saccharomyces cerevisiae mitochondria, Proc. Natl. Acad. Sci. U. S. A. 100 (2003) 13207–13212.

[26] R.P. Zahedi, A. Sickmann, A.M. Boehm, C. Winkler, N. Zufall, B. Schönfisch, B. Guiard, N. Pfanner, C. Meisinger, Proteomic analysis of the yeast mitochondrial outer membrane reveals accumulation of a subclass of preproteins, Mol. Biol. Cell 17 (2006) 1436–1450.

[27] J. Reinders, R.P. Zahedi, N. Pfanner, C. Meisinger, A. Sickmann, Toward the complete yeast mitochondrial proteome: multidimensional separation techniques for mitochondrial proteomics, J. Proteome Res. 5 (2006) 1543–1554.

[28] J. Reinders, K. Wagner, R.P. Zahedi, D. Stojanovski, B. Eyrich, M. van der Laan, P. Rehling, A. Sickmann, N. Pfanner, C. Meisinger, Profiling phosphoproteins of yeast mitochondria reveals a role of phosphorylation in assembly of the ATP synthase, Mol. Cell. Proteomics 6 (2007) 1896–1906.

[36] F. Perocchi, L.J. Jensen, J. Gagneur, U. Ahting, C. von Mering, P. Bork, H. Prokisch, L.M. Steinmetz, Assessing systems properties of yeast mitochondria through an interaction map of the organelle, PloS Genet. 2 (2006) e170.

[42] H. Prokisch, C. Andreoli, U. Ahting, K. Heiss, A. Ruepp, C. Scharfe, T. Meitinger, Mitop2: the mitochondrial proteome database–now including mouse data, Nucleic Acids Res. 34 (Database issue) (2006) D705–D711.

[46] L. Kiemer, S. Costa, M. Ueffing, G. Cesareni, Wi-phi: a weighted yeast interactome enriched for direct physical interactions, Proteomics 7 (2007) 932–943.

[63] D.N. Perkins, D.J. Pappin, D.M. Creasy, J.S. Cottrell, Probability-based protein identification by searching sequence databases using mass spectrometry data, Electrophoresis 20 (1999) 3551–3567.

[64] K. Nakai, P. Horton, PSORT: a program for detecting sorting signals in proteins and predicting their subcellular localization, Trends Biochem. Sci. 24 (1999) 34–36.

[65] I. Small, N. Peeters, F. Legeai, C. Lurin, Predotar: A tool for rapidly screening proteomes for n-terminal targeting sequences, Proteomics. 4 (2004) 1581–1590.

[66] S. Hua, Z. Sun, Support vector machine approach for protein subcellular localization prediction, Bioinformatics. 17 (2001) 721–728.

[67] T.D. Goddard, D.G. Kneller, Sparky 3, Tech. rep, University of California, San Francisco.

[68] B. Efron, The jackknife, the bootstrap, and other resampling plans, Vol. 38, Society of

Industrial and Applied Mathematics CBMS-NSF Monographs, 1982.
[69] C.E. Lunneborg, Data Analysis by Resampling: Concepts and Applications, Duxbury Press, 1999.
[70] R.J.T. Bradley Efron, An Introduction to the Bootstrap (Monographs on Statistics and Applied Probability), Chapman & Hall/CRC, New York, 1994.
[71] H. Choi, A.I. Nesvizhskii, False discovery rates and related statistical concepts in mass spectrometry-based proteomics, J. Proteome. Res. 7 (2008) 47–50.
[72] D.B. Weatherly, J.A. Atwood, T.A. Minning, C. Cavola, R.L. Tarleton, R. Orlando, A heuristic method for assigning a false-discovery rate for protein identifications from mascot database search results, Mol. Cell. Proteomics. 4 (2005) 762–772.
[73] J. C. Silva, R. Denny, C.A. Dorschel, M. Gorenstein, I.J. Kass, G.-Z. Li, T. McKenna, M.J. Nold, K. Richardson, P. Young, S. Geromanos, Quantitative proteomic analysis by accurate mass retention time pairs, Anal. Chem. 77 (2005) 2187–2200.
[74] M.A. Hughes, J. C. Silva, S.J. Geromanos, C.A. Townsend, Quantitative proteomic analysis of drug-induced changes in mycobacteria, J. Proteome. Res. 5 (2006) 54–63.

Supporting Table S1

Click here to download Supplementary Material (for online publication): Supporting TableS1.xls

Modules according to Perocchi at al. [36]		protein name (ORF)	LC-MS-MS/MS only		peptide IEF-LC-MS-MS/MS		Other MS based proteomic studies							"in silico" prediction of mitochondrial localization			MREF [42] (release 2007)
No.	descrption		Mascot MudPIT score	Number of peptides	Mascot MudPIT score	Number of peptides	Pflieger et al. [22]	Ohlmeier et al. [23]	Prokisch et al. [24]	Sickmann at al. [25]	Zahedi et al. [26]	Reinders et al. [27]	Prokisch at al.N. crassa	PSORT II [64]	Predotar [65]	Subloc [66]	
1	Respiratory Chain Complex-IV	Cox9 (YDL067C)	110.7	3	87.4	2	X		X	X		X	X	*			X
		Cox4 (YGL187C)	2580.9	19	2199.9	14	X	X	X	X		X	X	*	**		X
		Cox12 (YLR038C)	314	5	459.6	3	X	X	X	X		X	X				X
		Cox6 (YHR051W)	1386.6	8	902.3	19	X	X	X	X		X	X	*	**		X
		Yhb1 (YGR234W)	58	1	120.3	3	X	X	X	X		X					X
		Cox13 (YGL191W)	101	2	75.5	6	X	X	X	X		X	X	*	**		X
		Cox8 (YLR395C)			41	1	X		X	X		X		*	*	*	X
		Cyc7 (YEL039C)	288.6	2					X	X		X				*	X
		Cox5a (YNL052W)	1402.7	9	978.1	12	X	X	X	X		X	X		**	*	X
		Cox2 (Q0250)	984.3	9	588.7	8	X		X	X		X	X				X
		Cox1 (Q0045)	795.8	1	397.3	3	X		X	X			X				X
2		Ykr016w (YKR016W)	2641.5	25	2502	25	X		X	X		X	X		**		
3		Coq9 (YLR201C)	166	1	356.3	2	X	X	X	X		X		*	**	*	X
		Atp23 (YNR020C)	121	1	42.5	1								*		*	X
4	Cell growth regulation	Top2 (YNL088W)			64	2				X		X				*	
		Lst8 (YNL006W)	88.5	1													
		Avo2 (YMR068W)			44	1											
5		Odc2 (YOR222W)	63	2					X	X		X	X			*	X
		Yjr085c (YJR085C)	70	1				X		X		X		*			
6	Mitochondrial organisation and morphology	Mmm1 (YLL006W)	46	1	43	1				X	X	X					X
		Phb2 (YGR231C)	851.5	12	773	8		X	X	X		X	X	*		*	X
		Phb1 (YGR132C)	459.8	11	1039	15	X	X	X	X		X	X				X
		Mdm32 (YOR147W)	91.8	3	162.3	3										*	X
		Mpm1 (YJL066C)	958.1	6	2408.6	20		X	X	X		X					X
		Mdm10 (YAL010C)	46	1	173.3	3					X						X
		Mdm34 (YGL219C)	97	1	180.5	2					X	X					X

7	Ubiquinone metabolism	Abc1 (YGL119W)			124.3	6		X	X	X		X		*	* *	*	X
		Coq3 (YOL096C)	145	3	228.8	3				X		X			* *		X
		Coq5 (YML110C)	628.8	2	1378.2	15		X	X	X		X		*	* *		X
		Ypl109c (YPL109C)			177.1	4				X		X					
		Coq6 (YGR255C)	94.7	2	308.6	6		X		X		X		*	* *	*	X
		Coq4 (YDR204W)	66	1					X					*	* *	*	X
		Cat5 (YOR125C)	124.6	2	85	1		X		X		X		*	*	*	X
		Coq1 (YBR003W)	79	3	251.9	14			X	X		X	X	*	* *		X
8	Branched chain amino acid biosynthesis	Bat1 (YHR208W)	1808.9	19	1285.8	19	X	X	X	X		X	X		* *	*	X
		Bat2 (YJR148W)	606.4	4					X				X			*	
		Ilv2 (YMR108W)	6884.7	38	4217.3	41	X	X	X	X	X	X	X		* *	*	X
		Ilv6 (YCL009C)	1554.2	26	858.8	11	X	X	X	X		X		*	* *	*	X
		Ilv5 (YLR355C)	4519.7	35	8530.9	52	X	X	X	X	X	X	X		* *	*	X
		Leu4 (YNL104C)	5142.5	34	2088.1	30	X	X	X	X		X					X
		Ecm31 (YBR176W)			101.4	4			X	X		X		*	*		
		Lys4 (YDR234W)	889.7	10	698.5	13		X	X	X		X		*	* *	*	X
		Ilv3 (YJR016C)	1079	15	1239.2	15	X	X	X	X		X	X	*	* *	*	X
9	Respiratory Chain Complex assembly 1	Atp11 (YNL315C)	307	3	480.3	5		X	X	X		X		*	* *	*	X
		Atp12 (YJL180C)	913.4	8	588.8	12						X		*	* *	*	X
		Fmc1 (YIL098C)			66	4			X	X		X			*	*	X
		Bcs1 (YDR375C)	113	2	172.5	4				X		X	X			*	X
		Mtm1 (YGR257C)	75	1										*			X
10	Mitochondrial protein targeting	Afg3 (YER017C)	371.6	8	609	15			X	X		X	X	*	* *	*	X
		Yta12 (YMR089C)	333.4	7	851.6	19			X	X		X	X	*	* *		X
		Msp1 (YGR028W)	139.7	2	572.3	5				X	X	X	X				X
		Hmg2 (YLR450W)	52	1	43.7	2									* *		
		Mba1 (YBR185C)	83	1	42	1		X		X		X	X	*	* *	*	X
11		Sry1 (YKL218C)			61.5	1											
		Emi5 (YOL071W)	227.4	2	608.8	4			X	X		X			*	*	X
12	Fatty acid biosynthesis	Hfa1 (YMR207C)			222	5				X		X				*	X
		Cem1 (YER061C)	101.5	1	73	3						X		*	*		X
13		Ggc1 (YDL198C)	344.6	5	594.5	12		X	X	X		X	X			*	X
		Mmf1 (YIL051C)	175.7	1	1397.6	14	X	X	X	X		X		*	* *	*	X
		Abf2 (YMR072W)	119.2	4	258.6	8	X	X	X	X		X			*	*	X
14		Taz1 (YPR140W)			188.3	4				X		X				*	X
		Yjr100c (YJR100C)			289.4	4		X				X		*	* *		
		Ylr253w (YLR253W)	93.5	1	82.3	2						X		*	* *	*	
15	Matrix protein import	Mcx1 (YBR227C)			303.2	8			X	X		X		*	* *		X
		Mge1 (YOR232W)	588.4	9	724.8	12	X	X	X	X		X	X	*	* *	*	X
		Ssc1 (YJR045C)	8246.6	74	9232.3	69	X	X	X	X	X	X		*	* *	*	X
		Hsp60 (YLR259C)	10136.1	49	10997.5	75	X	X	X	X	X	X	X		* *	*	X
		Hsp78 (YDR258C)	2702.5	22	2335.6	39	X	X	X	X		X			* *	*	X
		Hsp10 (YOR020C)	1478.6	14	1259.8	19	X	X	X	X	X	X				*	X
		Pim1 (YBL022C)	953.4	15	1631.4	29	X	X	X	X		X		*	* *		X

		Tam41 (YGR046W)			127.3	3							*	*	*	X
		Mdj1 (YFL016C)	1387.9	12	606.7	10		X	X	X		X		*	*	*	X
16	Tim23/Tim22 complex	Tim21 (YGR033C)	93	1	165.7	2				X		X			* *	*	X
		Pbp1 (YGR178C)			122.5	1				X		X					
		Tim8 (YJR135W-A)	324.2	5	69	1	X				X	X					X
		Mrs5 (YBR091C)	70	1						X		X		*			X
		Tim54 (YJL054W)	192.1	3	672.1	12			X	X		X	X				X
		Tim13 (YGR181W)	446	5	584.3	2				X		X		*			X
		Pam18 (YLR008C)	106	1	131	1			X	X		X				*	X
		Tim22 (YDL217C)	133.2	1	44	1				X		X		*		*	X
		Tim23 (YNR017W)	450.6	4	250.5	2		X	X	X		X	X			*	X
		Pam16 (YJL104W)	994.5	5	172.1	4		X		X		X			*		X
		Tim44 (YIL022W)	1754.2	19	2117.3	28		X	X	X	X	X	X		* *	*	X
		Tim50 (YPL063W)	663	11	649.2	19		X	X	X		X	X	*	* *		X
		Mrs11 (YHR005C-A)	775.6	7	245	3			X			X					X
		Tim17 (YJL143W)	98	2	81.8	2				X		X		*			X
		Tim9 (YEL020W-A)	829.5	6	523.9	3	X		X		X	X					X
		Tim18 (YOR297C)	58	2						X		X	X	*	*	*	X
17	Unknown module 2	Ppa2 (YMR267W)	108.8	2	291.8	9				X		X		*	*		X
		Ydr493w (YDR493W)	50.5	1	184.7	3				X		X			*		
18		Ecm19 (YLR390W)			106.4	5						X					
		Pet100 (YDR079W)			244.2	2				X		X			* *		X
		Acn9 (YDR511W)	323.9	4	391.1	8			X			X		*	* *	*	X
		Emi1 (YDR512C)	66	1	70.5	2											
19		Lys12 (YIL094C)	1185.4	13	783.5	11	X	X	X	X		X	X		* *	*	X
		Hem1 (YDR232W)	139.5	6	196.3	8			X	X		X		*	* *	*	X
		Grs1 (YBR121C)	148.7	2	321.4	7		X		X		X					X
20	Iron-sulfur cluster assembly	Isa2 (YPR067W)			147	1			X	X		X		*	* *	*	X
		Nfs1 (YCL017C)	797.5	10	1047.2	13		X	X	X		X		*	* *	*	X
		Cox15 (YER141W)	254.6	3	52.3	4	X		X	X		X			* *	*	X
		Yfh1 (YDL120W)	142	1	249.2	6			X	X		X			* *	*	X
		Grx5 (YPL059W)	380.5	4	648.2	9	X	X	X	X		X		*	*		X
		Ssq1 (YLR369W)	253.4	7	930.2	14		X	X	X		X		*	* *	*	X
		Isu2 (YOR226C)	80.5	2										*	* *		X
		Arh1 (YDR376W)	72	1	212.2	5		X	X	X		X		*	* *	*	X
		Jac1 (YGL018C)	179	2	274	3				X		X		*	* *	*	X
		Isu1 (YPL135W)	93.5	1	102	2						X		*	* *	*	X
		Nfu1 (YKL040C)	341.2	4	152.5	4		X	X	X		X		*	* *		X
21		Glo4 (YOR040W)			134.8	3	X		X	X		X		*	* *		X
		Tdh3 (YGR192C)	900.2	12	617.2	9	X	X	X			X		*			
22	Secretory pathway	Mrc1 (YCL061C)	75	1													
		Kar2 (YJL034W)	1247.2	16	845	16		X	X					*		*	
		Sss1 (YDR086C)	102.3	1	80.7	1								*		*	
		Sec63 (YOR254C)	104	2	358.3	6			X	X		X				*	

23		Ubp16 (YPL072W)	42	1	156.7	2					X						X
		Ymr098c (YMR098C)	41	1	282.9	5						X			*	*	
24	Glutamine family	Ctp1 (YBR291C)	98	1	93.3	2			X	X		X	X			*	X
25		Cbp3 (YPL215W)	306.6	4	586.3	9	X		X	X		X		*	* *	*	X
		Cbp4 (YGR174C)	77.7	2	290.3	6	X	X	X	X		X		*		*	X
26		Bna3 (YJL060W)			118.7	3			X			X		*	* *		
		Yil077c (YIL077C)	327.6	5	426.3	9						X				*	
		Agx1 (YFL030W)	272.9	3	443	11	X		X	X		X				*	
27	Unknown module 1	Cox16 (YJL003W)	70	1	96	2				X		X		*		*	X
		Ylr281c (YLR281C)			73	1									* *		
		Ylr290c (YLR290C)	53	1	73.3	2						X			*	*	
		Jid1 (YPR061C)			43.5	1										*	
28	Respiratory Chain Complex assembly 2	Atp10 (YLR393W)	88.7	2	175.3	3			X	X		X		*	*	*	X
		Ylr091w (YLR091W)			57	1				X		X				*	
		Mdm38 (YOL027C)	1209	8	1235.9	22	X		X	X		X			* *		X
		Sls1 (YLR139C)	102.3	3	97	6				X		X			* *	*	X
		Ymr166c (YMR166C)	50	1												*	X
29		Lsp1 (YPL004C)	1285.1	11	1076.4	16	X	X	X	X	X	X					
		Ape2 (YKL157W)	659.4	12	1682	21		X	X	X		X		*	* *		
30	Mitochondrial/cytoplasmic lipid metabolism	Yhm2 (YMR241W)	1501.7	6	587	7	X		X	X		X	X			*	X
		Oac1 (YKL120W)	116.2	3			X	X	X	X		X				*	X
		Psd1 (YNL169C)	387.1	5	402.7	5			X	X		X	X	*	* *		X
		Tsc13 (YDL015C)	66	1					X	X		X				*	
		Ayr1 (YIL124W)	128.5	1	205.3	2		X	X	X	X	X				*	
31	Glutamate biosynthesis	Mse1 (YOL033W)			191.4	3				X		X		*	* *	*	X
		Alt1 (YLR089C)	520.9	7	1179.7	16	X	X	X	X		X			* *	*	
		Put2 (YHR037W)	1030.4	13	974.3	17	X	X	X	X		X			* *		X
32		Oms1 (YDR316W)	415.1	4	357.8	8						X		*	* *	*	
		Oxa1 (YER154W)	303.3	3	322.6	2			X	X		X	X	*	* *	*	X
		Oma1 (YKR087C)	469.3	1										*	*		X
33		Tfc3 (YAL001C)	48	1					X	X		X				*	
		Itc1 (YGL133W)	43	1	111.7	3											
34		Sac1 (YKL212W)	134.2	3	122.6	4			X	X	X	X					
		Csf1 (YLR087C)			40	3				X		X		*			
35	Response to DNA damage	Mgm101 (YJR144W)	865.1	8	552.2	9			X	X		X		*	* *		X
		Rim1 (YCR028C-A)	896.8	10	1749.8	17	X	X	X	X		X			* *	*	X
		Vas1 (YGR094W)	119.8	3	403.9	15			X	X		X		*	* *		X
37	Pyruvate/α-ketoglutarate dehydrogenase	Pdb1 (YBR221C)	837.3	14	2202.2	23	X	X	X	X	X	X	X	*	* *	*	X
		Prx1 (YBL064C)	680.6	13	1213.3	18	X	X	X	X		X		*	* *		X
		Mae1 (YKL029C)	730.8	17	672	12	X	X	X	X		X		*	* *	*	X
		Tcm62 (YBR044C)	85	2	369.7	7		X		X		X	X	*	* *	*	X
		Pdx1 (YGR193C)	676.1	9	431.2	9		X	X	X		X	X		* *		X
		Cym1 (YDR430C)	156.4	5	1105	21		X	X	X		X			* *		
		Lpd1 (YFL018C)			3974.6	47	X	X	X	X		X	X	*	* *		X

		Pda1 (YER178W)	1350.1	16	1902.1	19	X	X	X	X	X	X	X			*	X
		Lat1 (YNL071W)	973.6	16	1662.4	14	X	X	X	X		X	X	*	**	*	X
		Kgd1 (YIL125W)	4400.8	50	4342.7	51	X	X	X	X	X	X	X		**		X
		Kgd2 (YDR148C)	2818.2	18	3270.3	27	X	X	X	X		X	X	*	**	*	X
38		Xdj1 (YLR090W)	169	3	56.3	2						X					
		Ygr021w (YGR021W)			139	3						X			**	*	
		Cox23 (YHR116W)	240	1	83	1											X
40		Ynl168c (YNL168C)	229.2	2	128.4	3			X	X		X		*	**		
		Nit3 (YLR351C)			195.4	4				X		X			*		
41	DNA replication	Adk1 (YDR226W)	67	2	140.2	3		X				X	X				X
		Mam33 (YIL070C)	964.3	12	1028.9	11		X	X	X		X			**		X
		Adk2 (YER170W)	303.4	4	172.6	5				X		X				*	X
42		Nam8 (YHR086W)	47	1													X
43		Cpr3 (YML078W)	1725.9	12	1633.2	16	X	X	X	X		X			**	*	X
		Ydl027c (YDL027C)	92	1								X			*	*	
		Etr1 (YBR026C)	814.7	12	440.5	12	X	X	X	X		X			*	*	X
45	Cytoplasmic lipid metabolism	Pil1 (YGR086C)	1642.8	12	1509.3	13	X	X	X	X	X	X		*			
		Scs2 (YER120W)	69	1	375	4			X								
		Num1 (YDR150W)			89	2				X		X					
46	Folate and glycine metabolism	Gcv1 (YDR019C)	1025.8	17	310.7	7			X	X		X		*	*	*	X
		Fol1 (YNL256W)			53	1				X		X		*	*		X
		Shm1 (YBR263W)	842.5	8	1288.1	18			X	X		X				*	X
		Mis1 (YBR084W)	386.3	9	1038.4	17		X	X	X		X		*	**	*	X
		Gcv2 (YMR189W)	1389.9	13	277.3	12	X	X	X	X		X	X	*	**	*	X
		Gcv3 (YAL044C)	1033.5	5	523.9	6	X	X	X	X		X		*	**		X
47		Ybr262c (YBR262C)	177.8	3	633.2	5			X	X		X			*		
		Ygl226w (YGL226W)			84.3	2							X		**	*	
48	Glycerol metabolism	Cds1 (YBR029C)			56	1											X
		Gpd1 (YDL022W)	83.5	2	152.8	3										*	
		Gut2 (YIL155C)	3866.8	38	3118.9	46	X	X	X	X	X	X	X		**	*	X
		Pgs1 (YCL004W)			81	2								*	**	*	X
		Gut1 (YHL032C)			157.3	2								*	**		
		Gpd2 (YOL059W)			87	1				X		X		*	**		
49	TOM complex	Tom70 (YNL121C)	1323.1	13	1610.5	29		X	X	X	X	X	X		**		X
		Tom22 (YNL131W)	1025	6	1405.8	16			X	X	X	X	X				X
		Tom5 (YPR133W-A)	119.3	2	341.5	5			X	X	X	X					X
		Tom40 (YMR203W)	1293.1	16	750.2	8	X	X	X	X	X	X	X				X
		Tom6 (YOR045W)	291.3	2	61.3	3				X		X					X
		Sam50 (YNL026W)	450	2	233	2		X	X	X	X	X	X			*	X
		Sam37 (YMR060C)	136.3	2	52	1	X				X	X					X
		Sam35 (YHR083W)	195.4	3	40	1	X			X	X	X					X
		Tom71 (YHR117W)	278.7	4	523.7	9			X	X	X	X	X		*		X
		Tom7 (YNL070W)			363.3	3			X	X	X	X					X
		Tom20 (YGR082W)	659.7	6	709.2	12		X	X	X	X	X	X				X

50		Mrh1 (YDR033W)	294.9	3	108	1			X	X		X					
		Pst2 (YDR032C)	104.5	1	314.6	4	X	X		X		X	X				
51	Arginine biosynthesis	Arg8 (YOL140W)	145.3	2	92	3		X	X	X		X		*	* *		X
		Ecm40 (YMR062C)	246.4	6	510.9	8		X	X	X		X	X		*	*	X
		Arg5	239.9	5	530.8	10		X	X	X		X		*	* *	*	X
52		Lap3 (YNL239W)	58.5	1	761.9	7			X	X		X		*	* *	*	
		Imp2' (YIL154C)			49	1											
53		Msk1 (YNL073W)	75.5	1	95	5		X		X		X			* *		X
		Zim17 (YNL310C)	152.8	2						X		X					X
54	Cell wall organisation and biogenesis	Gsc2 (YGR032W)			417.2	10			X								
		Fks1 (YLR342W)			533.3	11			X	X		X				*	
		Fen1 (YCR034W)	42	1	106	1											
		Gas1 (YMR307W)	545.5	6	153.3	5			X	X		X				*	
55		Yal046c (YAL046C)	57.5	1	119	1									* *		
		Pho88 (YBR106W)	146.7	3	271.8	5			X	X		X	X				
56		Cyc3 (YAL039C)	274.2	4	188.3	7				X		X					X
		Hem15 (YOR176W)	102.3	2	172.7	6	X		X	X		X	X	*	* *	*	X
		Hem14 (YER014W)	59	1	290.3	4		X	X	X		X		*	* *	*	X
57		Ftr1 (YER145C)	966.1	3	275.5	2											
58	Vacuolar acidification	Vph1 (YOR270C)	97	1	179.7	3											
		Tfp1 (YDL185W)	103.8	5	40	2		X	X								X
		Vma2 (YBR127C)	46	1				X									
59		Ygr012w (YGR012W)	313.9	5	190	4			X	X	X	X		*			
		Yor251c (YOR251C)	43	1	185	4		X	X								
60		Yml030w (YML030W)	207.3	3	395.2	10	X		X	X		X					
61	RNA splicing	Mss18 (YPR134W)			467.6	4				X		X					X
		Mrs1 (YIR021W)			246.8	3		X		X		X		*			X
		Mto1 (YGL236C)	170	3	410.3	8								*	* *		X
		Mrs4 (YKR052C)	90	2						X		X		*		*	X
		Nam2 (YLR382C)	175.7	5	875.5	14				X		X			* *		X
		Mtf2 (YDL044C)	83.5	1	574.2	8				X		X			* *		X
		Slm3 (YDL033C)	98	1	131	3							X	*	* *		X
		Mss116 (YDR194C)	392.1	6	1166.2	27		X	X	X		X			* *		X
62	Translation regulator activity	Pet112 (YBL080C)			386.1	6				X		X		*	* *		X
		Aep1 (YMR064W)			194	2									*		
		Aep2 (YMR282C)	107	1	221.5	4				X		X		*	* *	*	X
		Mss51 (YLR203C)	239.3	4	459.6	12	X	X		X		X	X	*	*	*	X
		Pet309 (YLR067C)			40	2				X		X			* *	*	X
		Cbp6 (YBR120C)			235.6	3			X	X		X				*	X
		Dss1 (YMR287C)	41	1	164.2	6				X		X			* *		X
		Pet494 (YNR045W)			80	2				X		X			*		X
		Sov1 (YMR066W)	133	1	98	1				X		X		*	* *		
		Pet111 (YMR257C)			67	1				X		X		*	* *		X
		Pet54 (YGR222W)	204.6	3	463.7	8	X			X		X			*	*	X

63		Cox20 (YDR231C)	470	3	490.6	5			X	X		X					X
		Odc1 (YPL134C)	286.2	6	515.9	9	X		X	X		X	X			*	X
		Ybr269c (YBR269C)	593.4	4	516.4	9			X	X		X		*	* *		
64	Fusion/fission	Mgm1 (YOR211C)	332.7	4	860.8	14			X	X	X	X	X		* *	*	X
		Fzo1 (YBR179C)			218	3			X	X	X	X	X			*	X
		Fis1 (YIL065C)	156	1	397	3	X	X	X	X	X	X	X				X
		Ugo1 (YDR470C)	100.5	2	221.4	5				X	X	X	X			*	X
		Mdv1 (YJL112W)	167.7	2	100.3	5					X	X					X
65		Pus4 (YNL292W)			79.5	2											X
		Ifm1 (YOL023W)	141.4	4	173.5	4				X		X		*	* *	*	X
66	Amino acid metabolism	Mst1 (YKL194C)	121.7	2	221.7	4				X		X			* *	*	X
		Dia4 (YHR011W)	218.5	1	302.5	5									* *	*	X
		Ilv1 (YER086W)	1874.8	14	1052.3	15		X	X	X		X			* *	*	X
		Cha1 (YCL064C)	404.1	5	122.7	2		X	X			X		*	* *	*	X
67		Mef1 (YLR069C)	1112.9	14	1296.7	17		X	X	X		X			* *		X
		Mef2 (YJL102W)	261.6	3	118.5	2				X		X			* *		
		Tuf1 (YOR187W)	2689.6	35	2934.4	23	X	X	X	X		X	X	*	* *	*	X
68		Qri7 (YDL104C)	341.7	4	120.3	3						X		*	* *		
		Ydl119c (YDL119C)	41	1								X		*		*	X
69	Respiratory Chain Complex-IV assembly	Sco2 (YBR024W)	162.7	3	191	3				X		X	X	*	* *		X
		Cox11 (YPL132W)	45	1	95	1			X	X		X		*	* *		X
		Sco1 (YBR037C)	88.7	2	229.3	4		X	X	X		X	X	*	* *	*	X
70		Tat1 (YBR069C)			104	2											
		Dug1 (YFR044C)			438.5	8		X	X			X					
		Mir1 (YJR077C)	3406.8	32	991.9	12	X	X	X	X	X	X	X	*		*	X
71		Cyc1 (YJR048W)	1179.7	8	843.3	8	X		X	X	X	X		*		*	X
		Osm1 (YJR051W)	46	1	217.3	4				X		X		*		*	X
		Ccp1 (YKR066C)	426.8	9	744.4	16	X	X	X	X		X	X	*	* *		X
72		Nuc1 (YJL208C)	157	3	155.6	3	X	X	X	X	X	X					X
73		Pkp1 (YIL042C)			95	1			X			X	X	*	* *	*	X
74		Nat2 (YGR147C)	149	1	190.3	3				X		X		*	* *	*	
75		Erg6 (YML008C)	1142.3	11	895.5	13		X	X	X	X	X					
		Faa1 (YOR317W)	489.9	5	460.3	7		X	X	X	X	X	X	*			
		Eht1 (YBR177C)	186	2	304.8	7			X	X	X	X					
76		Ygl059w (YGL059W)			193.5	3						X		*	*		
		Yjl161w (YJL161W)			40	1				X		X		*	* *	*	
77		Ynl100w (YNL100W)	42	1	332.2	7	X		X	X		X				*	
		Ydl157c (YDL157C)	50	1						X		X		*			
78		Mrf1 (YGL143C)			186.8	4				X		X			* *	*	X
		Sua5 (YGL169W)			86.5	1									*		
		Mrpl13 (YKR006C)	483.3	9	763.5	10				X		X		*	* *		X
		Mrpl32 (YCR003W)	90.5	1	70.5	4	X			X		X				*	X
		Mrpl49 (YJL096W)	347.4	3	253.8	3			X	X		X				*	X
		Mrpl50 (YNR022C)	43	1	80.5	2			X			X			*		X

79	Components of the large subunit of mitochondrial ribosomes-MRPL	Mrpl31 (YKL138C)	50	1	89.5	1							X		* *	*	X
		Bud3 (YCL014W)			40	3											
		Mnp1 (YGL068W)	810	8	881.9	11		X	X	X		X	X	*	* *	*	X
		Mrpl16 (YBL038W)			129.8	4				X		X		*	* *	*	X
		Img2 (YCR071C)			106.2	4				X		X		*	* *		X
		Mrp49 (YKL167C)			71.7	3		X		X		X			* *	*	X
		Mrp20 (YDR405W)	138	3	74.6	3	X			X		X	X		* *	*	X
		Mrpl24 (YMR193W)	263.8	3	497.1	6			X	X		X			* *	*	X
		Yml6 (YML025C)	267.7	7	488.7	11	X			X		X		*	*	*	X
		Mrh4 (YGL064C)			143	4				X		X	X	*		*	X
		Mrpl3 (YMR024W)	545.2	6	297.1	6	X	X	X	X		X		*	* *	*	X
		Mrpl19 (YNL185C)	259.4	2			X		X	X		X					X
		Mrpl17 (YNL252C)	309.1	5	815.4	13	X	X	X	X		X		*	* *	*	X
		Mrpl37 (YBR268W)	164.5	1	41	1				X		X		*	* *		X
		Mrpl36 (YBR122C)	177.4	2	848.4	8				X		X					X
		Mrpl25 (YGR076C)	115.7	2	81.7	3				X		X	X			*	X
		Mrpl10 (YNL284C)	98	2	209.3	5			X	X		X		*		*	X
		Mrpl27 (YBR282W)	203.8	2	110.4	2				X		X			*	*	X
		Mrpl8 (YJL063C)	199.1	4	413.7	6			X	X		X				*	X
		Mrpl15 (YLR312W-A)	196.3	2	273.1	2			X	X		X			*		X
		Mrpl28 (YDR462W)	76.5	2	87	1	X		X	X		X			* *	*	X
		Mrpl7 (YDR237W)	58	1	154.3	2			X	X		X			*	*	X
		Mhr1 (YDR296W)	113	1	234.6	3			X	X	X	X		*	*	*	X
		Mrpl4 (YLR439W)	110	1	486.5	6	X		X	X		X			* *		X
		Mrpl44 (YMR225C)	352.8	1	587.8	4				X		X		*	* *	*	X
		Mrpl51 (YPR100W)	329.5	4	218.1	5			X	X		X		*	* *		X
		Mrpl38 (YKL170W)	279.1	4			X					X				*	X
		Mrp7 (YNL005C)	650.2	6	412.3	8			X	X		X				*	X
		Mrpl35 (YDR322W)	478.6	5	461.2	9		X	X	X		X		*	* *	*	X
		Rml2 (YEL050C)	232.4	2	169.8	3							X	*	* *		X
		Mrpl33 (YMR286W)	211.4	4	65	1			X	X		X		*	* *	*	X
		Img1 (YCR046C)	106.7	3	258.6	5	X			X		X		*	* *	*	X
		Mrpl40 (YPL173W)	431.3	6	781.5	13	X	X	X	X		X					X
		Mrpl1 (YDR116C)	248.3	4	373.8	8			X	X		X			* *		X
		Mrpl6 (YHR147C)	276.6	3	114.3	5	X		X	X		X		*	* *	*	X
		Mrpl11 (YDL202W)	500.6	9	765.2	7			X	X		X			* *	*	X
		Mrpl23 (YOR150W)	113	2	41	1				X		X				*	X
		Mrpl22 (YNL177C)	461	3	367.9	6	X			X		X			*	*	X
		Mrpl20 (YKR085C)	202.8	3	261.7	4			X	X		X			* *	*	X
		Mrpl9 (YGR220C)	245.4	4	140.1	3			X	X		X	X		* *	*	X
80	tRNA aminoacylation	Msd1 (YPL104W)	59	2	378.3	10		X	X	X		X		*	* *		X
		Msy1 (YPL097W)	341	4	563.4	8			X	X		X		*	* *	*	X
		Msf1 (YPR047W)	264	4	76.4	6				X		X			*	*	X
		Aat1 (YKL106W)			111.3	2				X		X	X	*	* *	*	X

		Aat2 (YLR027C)	135	2	101	1							X			*	
81		Sod1 (YJR104C)	632.6	6	819.4	7		X	X	X		X					X
		Sod2 (YHR008C)			1792.3	11	X	X	X	X		X	X	*	* *	*	X
82		Hir2 (YOR038C)			74	2										*	
83		Yme2 (YMR302C)	580.4	11	801	15	X		X	X		X	X	*	* *	*	X
		Yme1 (YPR024W)	1881.3	17	943.1	20			X	X		X	X	*	*	*	X
		Rex2 (YLR059C)	57	1						X		X		*	* *		X
84		Msr1 (YHR091C)	50	1	161.2	7				X		X			* *	*	X
		Ism1 (YPL040C)	40	1	339.9	6				X		X		*	* *	*	X
85		Ecm33 (YBR078W)	1114.6	8	187.8	1				X		X	X	*	* *	*	
86		Ptc5 (YOR090C)	56	1	99	7				X		X			*		X
87		Yer078c (YER078C)	66.5	1	279.6	5		X				X		*	* *		
		Rim2 (YBR192W)			75.5	2			X			X				*	X
89		Mia40 (YKL195W)	1040.2	13	985.7	15		X	X	X	X	X			*		X
90		Yhl021c (YHL021C)	310.4	3	675	15	X	X	X	X		X			* *		X
91		Yor285w (YOR285W)	157.7	1	165.3	4		X		X	X	X					
		Dpm1 (YPR183W)	108.8	3	265.6	4			X	X	X	X					
92		Cdc9 (YDL164C)	43	1	206	4								*	* *		X
93		Por1 (YNL055C)	8606.7	58	4139.2	34	X	X	X	X	X	X	X	*		*	X
		Cyc2 (YOR037W)			48	2				X		X				*	X
		Por2 (YIL114C)	96.5	1	63	1		X		X	X	X	X				X
94		Sec4 (YFL005W)	85.5	1	163.2	4			X	X	X	X	X			*	
95	NAD metabolism/TCA cycle	Mdh1 (YKL085W)	4833.9	35	2964.2	36	X	X	X	X	X	X	X		* *		X
		Yor356w (YOR356W)	202.7	4	589.1	10	X	X	X	X		X			* *		X
		Cyb2 (YML054C)	1738.5	18	1735	25	X	X	X	X	X	X			* *		X
		Fum1 (YPL262W)	2081.4	25	1695.3	17	X		X	X		X	X	*	* *		X
		Ygr207c (YGR207C)	236.6	5	336.3	10			X	X	X	X		*		*	X
		Dld1 (YDL174C)	1701.7	24	1752.6	32	X	X	X	X		X	X	*	* *		X
		Cit2 (YCR005C)	450.8	6	784.7	7			X	X		X	X			*	
		Ndi1 (YML120C)	1911.7	24	2467.9	31	X		X	X	X	X	X		* *	*	X
		Nde2 (YDL085W)	685.5	11	628.4	10	X		X	X		X	X	*	* *	*	X
		Cit3 (YPR001W)	113.4	3	348.9	9			X	X		X		*	* *		X
		Ypr004c (YPR004C)	1200.6	8	585.8	7		X	X	X		X		*	* *		
		Cit1 (YNR001C)	3480.1	35	5102.5	46	X	X	X	X		X	X		* *	*	X
		Nde1 (YMR145C)	2221.8	27	1390.4	23	X	X	X	X	X	X	X		* *	*	X
96		Atm1 (YMR301C)			322.5	6			X	X		X		*	* *	*	X
		Mdl2 (YPL270W)	446.5	9	389.7	8			X	X		X					X
		Mdl1 (YLR188W)	194.8	4	599.9	9			X	X		X			* *	*	X
97		Pet127 (YOR017W)	71	1	261.5	5				X		X		*	* *		X
		Cbp2 (YHL038C)	48	1	161.8	2									*		X
98	tRNA/rRNA processing	Rpm2 (YML091C)	51	1	204	3			X	X		X			*	*	X
		Mrps28 (YDR337W)	360.3	6	800	12			X	X		X	X	*	* *	*	X
		Mrps17 (YMR188C)	194.7	4	434.7	6				X	X	X			*	*	X
		Mrp4 (YHL004W)	249.2	3	619	12		X	X	X		X		*	* *	*	X

99	Components of the small subunit of mitochondrial ribosomes-MRPS	Rsm18 (YER050C)	63.5	2	123	2			X	X		X			* *	*	X
		Rsm10 (YDR041W)	189.6	3	548.7	9			X	X		X		*	* *	*	X
		Mrp51 (YPL118W)	161.7	3	282.5	8			X	X		X				*	X
		Ymr31 (YFR049W)	819.2	5	184.2	3		X	X	X		X		*	* *	*	X
		Mrps18 (YNL306W)	292.3	3	477.1	8	X		X	X		X	X		* *	*	X
		Mrps16 (YPL013C)			59	2				X		X		*	* *	*	X
		Rsm25 (YIL093C)	269.9	5	749.1	10	X	X	X			X					X
		Mrps9 (YBR146W)			375.8	7			X	X		X			* *	*	X
		Ehd3 (YDR036C)	388.7	9	743.4	8			X	X		X		*	* *		
		Mrps8 (YMR158W)	397.1	3	97.4	3			X	X		X			*	*	X
		Pet123 (YOR158W)	462.2	4	760.5	14			X	X	X	X			* *	*	X
		Mrp17 (YKL003C)			386.6	6				X		X				*	X
		Mrps35 (YGR165W)	485.4	8	347.2	8			X			X		*	*	*	X
		Ynr036c (YNR036C)	363.7	2	225.2	3						X		*	* *		X
		Fyv4 (YHR059W)			94	1									*	*	
		Rsm26 (YJR101W)			460.5	5		X	X	X		X			* *		X
		Mrp1 (YDR347W)	737.4	7	965.1	7	X	X	X	X		X		*	* *	*	X
		Mrp10 (YDL045W-A)	80.5	1													X
		Rsm22 (YKL155C)	177.4	4	618.1	10						X		*	* *		X
		Rsm7 (YJR113C)	181.7	5	384.7	6			X	X		X			* *	*	X
		Rsm27 (YGR215W)	200.5	1	145.8	3			X	X		X					X
		Yor205c (YOR205C)	82.7	2	111.2	5				X		X		*	* *	*	
		Mrp21 (YBL090W)	123	2	423.4	5				X		X		*	* *		X
		Mrps5 (YBR251W)	163.6	4	348.8	12				X		X	X	*	*		X
		Rsm23 (YGL129C)	265.6	5	613.4	13			X	X		X				*	X
		Rsm24 (YDR175C)	269.1	6	742.9	10		X	X	X		X		*	*	*	X
		Nam9 (YNL137C)	285	4	593.1	12			X	X		X	X		*	*	X
		Ygr150c (YGR150C)	255.8	2	159.1	8						X		*	*	*	
		Mrp13 (YGR084C)	248.7	2	202.1	6			X	X		X		*		*	X
		Sws2 (YNL081C)	50	1											*	*	X
100		Yor286w (YOR286W)	49	1	272.2	5			X	X		X		*	* *		
101		Guf1 (YLR289W)	82.5	1	400.5	7									* *	*	X
102		Leu5 (YHR002W)			136	1						X				*	X
		Leu9 (YOR108W)	2682.5	18	399	13		X	X			X			*		X
103	Alcohol/aldehyde dehydrogenase	Acs1 (YAL054C)	43	1	115.5	3				X		X					
		Adh3 (YMR083W)	252.3	4	765.1	16	X	X	X	X		X	X	*	* *		X
		Ach1 (YBL015W)	3393.2	33	3499.1	48	X	X	X	X		X	X	*	*		X
		Adh4 (YGL256W)			116.5	2			X						*	*	
		Ald5 (YER073W)	1499.9	20	2307	28		X	X	X		X		*	* *		X
		Ald4 (YOR374W)	10956.2	74	15669.4	113	X	X	X	X	X	X		*	* *		X
		Acs2 (YLR153C)	44	1													
104		Sfc1 (YJR095W)	486	12	449.8	6	X		X	X		X				*	X
		Jen1 (YKL217W)	563.3	6	181.5	2			X	X		X					
106		Cox14 (YML129C)	380	3	162	2	X	X		X		X			*	*	X

106		Shy1 (YGR112W)	423.3	6	137.4	3			X	X		X	X		**	*	X
107		Mss2 (YDL107W)			131.8	3									*		X
		Pnt1 (YOR266W)	141.3	2	300.8	2						X		*	*	*	X
108		Acp1 (YKL192C)	363.6	4	251.3	2			X	X		X	X		**	*	X
		Hts1 (YPR033C)	128.3	2	247.5	7		X						*	**	*	X
109		Icl2 (YPR006C)	383.8	8	841.3	17	X	X	X	X		X		*		*	X
		Om45 (YIL136W)	5321.4	46	4383.5	45	X	X	X	X	X	X					X
		Pdh1 (YPR002W)	912.1	18	699.9	16	X	X	X	X	X	X			*	*	
110		Yor022c (YOR022C)	72	1								X		*	**		
111		Trr2 (YHR106W)	207	2	222.3	3						X		*	**	*	X
		Trx3 (YCR083W)	145	2	69	2	X			X		X		*	**		X
		Glr1 (YPL091W)			209.6	4			X	X		X		*	*		
113		Bio2 (YGR286C)	56	1	112.3	3			X					*	**	*	X
115	Transport	Ypr011c (YPR011C)	42	1	59	1						X					X
		Yfr045w (YFR045W)	59	1	85	1							X			*	X
		Sal1 (YNL083W)			59	1				X		X					X
		Agc1 (YPR021C)			172.8	5				X		X	X			*	X
		Crc1 (YOR100C)	138.7	2	117	1			X	X		X				*	X
116		Hmi1 (YOL095C)			95	1				X		X				*	X
		Ydr332w (YDR332W)			319.3	5								*	*	*	
117		Pet117 (YER058W)			82.8	3						X		*			X
118		Mtg2 (YHR168W)	178.3	1	72	1									*	*	X
119		Mmt1 (YMR177W)			134	2				X		X	X		**	*	X
		Mmt2 (YPL224C)	45	1						X		X	X	*	*	*	X
120		Stf1 (YDL130W-A)	1299.5	4	390.7	4			X	X		X		*	**	*	X
121		Fmp45 (YDL222C)			162	3			X	X		X				*	
		Ptc7 (YHR076W)	85	2	354.4	6		X		X		X		*	**	*	X
122		Yir024c (YIR024C)			71.3	5				X		X			**	*	
123		Cat2 (YML042W)	492.6	12	802.9	18	X	X	X	X		X				*	X
124		Ato3 (YDR384C)			77.3	4				X		X					
		Ato2 (YNR002C)			189	3				X		X		*		*	
126		Rmd9 (YGL107C)	401.9	3	966.2	13			X	X		X		*	**	*	X
127		Mct1 (YOR221C)	87	2	117.6	3			X			X			**		X
		Oar1 (YKL055C)			52	1									*		X
128		Gtt1 (YIR038C)	47	1	99	3	X	X		X	X	X					
		Grx2 (YDR513W)	280.9	3	91.3	2			X	X		X					X
129		Msw1 (YDR268W)	59	1	179.3	4		X		X		X		*	**	*	X
130		Pth2 (YBL057C)	225.6	3	215.8	2				X	X	X		*	*	*	
131		Mas2 (YHR024C)	576.3	11	1062.3	16		X	X	X		X			**		X
		Mas1 (YLR163C)	604.3	9	880.8	8		X	X	X		X	X	*	**	*	X
132	Cytoplasmic ribosome	Rps18a (YDR450W)	78	1	88	2			X	X		X		*		*	
		Rpl23b (YER117W)	79	1	129	1			X				X				
		Rps14a (YCR031C)	120.5	2	301.9	4	X		X				X			*	
		Rpl9a (YGL147C)	89	1					X							*	

132	Cytoplasmic Ribosome	Rps5 (YJR123W)	115	1	64	1									*	
		Rpl9b (YNL067W)	89	1					X						*	
		Rps14b (YJL191W)	120.5	2	301.9	4			X				X		*	
		Rpl2b (YIL018W)			48	1								*		
133		Sun4 (YNL066W)			40	1										X
134		Pet9 (YBL030C)	1139.3	25	2221.8	30	X	X	X	X		X	X	*		*	X
135		Hnt2 (YDR305C)			139.8	4						X		*		*	
136		Apn1 (YKL114C)			89	1									*		X
137		Som1 (YEL059C-A)			103.5	1											X
		Ylr218c (YLR218C)	71.5	1	123.5	2											
138		Lip2 (YLR239C)	72	2	140	2			X	X		X			**		X
		Lip5 (YOR196C)	573.9	5	289.7	5				X		X		*	**	*	X
140		Tcb3 (YML072C)	136	5	420.6	9			X	X		X	X				
		Pdr5 (YOR153W)	98.5	2	71	4			X	X		X					
141		Ybl059w (YBL059W)	85.3	2	47.5	2						X					
142		Scm4 (YGR049W)	48	1						X	X	X				*	
143		Ylr036c (YLR036C)			43	1											
		Pam17 (YKR065C)	123.3	1	270	3	X	X	X	X		X			**		X
144		Cyt2 (YKL087C)	118.5	2	83.3	3				X		X					X
146		Fmt1 (YBL013W)			119	2				X		X		*	**		X
		Msm1 (YGR171C)	114	1	70	4				X		X			*	*	X
147	Respiratory Chain Complex-II	Lsc2 (YGR244C)	2263.6	26	3609.9	35	X	X	X	X		X	X	*	**		X
		Yjl045w (YJL045W)			416.3	7			X	X		X	X	*	**	*	X
		Sdh3 (YKL141W)	72	1	284.1	2	X		X	X		X	X		**	*	X
		Sdh4 (YDR178W)	287	4	382.5	6	X	X	X	X		X	X	*	**	*	X
		Sdh2 (YLL041C)	1378.9	17	1225.9	13	X	X	X	X	X	X	X	*	**		X
		Lsc1 (YOR142W)	2677.3	29	1575.8	10	X	X	X	X		X	X	*	**		X
		Sdh1 (YKL148C)	3781.6	44	1844.7	28	X	X	X	X	X	X	X		**	*	X
148		Mcr1 (YKL150W)	623.6	9	1002	15	X	X	X	X	X	X	X	*	**		X
		Cbr1 (YIL043C)	94	2	41	2				X	X	X	X		*	*	
149	Isocitrate metabolism	Aco1 (YLR304C)	6915.1	68	6785.7	71	X	X	X	X		X	X		**		X
		Idp1 (YDL066W)	2761	25	4554.8	24	X	X	X	X		X	X		**	*	X
		Aco2 (YJL200C)	713.3	14	986.8	16		X	X	X		X			**	*	
		Idh1 (YNL037C)	3398.5	24	3662.9	33	X	X	X	X		X	X	*	**	*	X
		Idh2 (YOR136W)	4756	30	3440.4	16	X	X	X	X		X	X	*	**	*	X
150		Hsc82 (YMR186W)			171.3	2		X	X	X		X					
153		Sac6 (YDR129C)			76.5	1											
		Dld2 (YDL178W)	497.8	13	733.9	12		X	X	X		X	X		**	*	X
154		Caf17 (YJR122W)	54	1	371.5	3						X			**		
		Atp14 (YLR295C)	553.3	8	1023.6	11			X	X		X	X	*	**		X
		Atp6 (Q0085)	269.2	1	244	3			X	X		X	X				X
		Atp7 (YKL016C)	1115.1	11	1099.4	12	X	X	X	X		X	X				X
		Atp15 (YPL271W)	504.4	9	488.7	5	X		X	X	X	X			**		X
		Atp4 (YPL078C)	1400.7	17	1749.7	14	X	X	X	X		X	X		**	*	X

155	Respiratory Chain Complex-V	Tim11 (YDR322C-A)	975.4	7	543.9	7	X	X	X	X		X					X
		Atp19 (YOL077W-A)	45	1					X	X		X					X
		Atp1 (YBL099W)	7364.8	51	8990.7	59	X	X	X	X		X	X	*	* *	*	X
		Atp2 (YJR121W)	14609.9	71	11454.1	71	X	X	X	X	X	X	X	*	* *		X
		Atp16 (YDL004W)	835	11	691.1	8		X	X	X		X	X	*	* *		X
		Atp20 (YPR020W)	89.5	3	154.5	3	X		X	X		X	X		* *	*	X
		Atp5 (YDR298C)	1391.8	11	3080.3	20	X	X	X	X	X	X	X		* *		X
		Atp17 (YDR377W)	111.2	3	70	1	X		X	X		X	X	*	* *		X
		Inh1 (YDL181W)	636.8	7	997.3	7	X		X	X		X		*	* *	*	X
		Atp3 (YBR039W)	2922.7	32	3590.7	33	X	X	X	X	X	X	X	*	* *	*	X
		Atp18 (YML081C-A)			290.7	5	X	X	X			X	X			*	X
156	Respiratory Chain Complex-III	Qcr8 (YJL166W)	236.1	2	479.1	3			X	X		X	X			*	X
		Qcr2 (YPR191W)	5529.5	28	4012.1	45	X	X	X	X	X	X	X	*	* *		X
		Qcr6 (YFR033C)	263	5	121.8	4	X		X	X		X					X
		Qcr10 (YHR001W-A)	137.8	2	257.4	4		X	X	X		X	X	*	*	*	X
		Rip1 (YEL024W)	619.2	11	1847	25	X	X	X	X		X	X	*	* *	*	X
		Qcr9 (YGR183C)	158	1	140.3	2				X		X		*	*		X
		Cor1 (YBL045C)	5052.4	46	3200.5	31	X	X	X	X	X	X	X	*	* *	*	X
		Cyt1 (YOR065W)	3630.4	17	2548.7	18	X		X	X		X	X		* *	*	X
		Qcr7 (YDR529C)	1500.1	10	1283.3	16	X	X	X	X		X	X				X
157		Mtf1 (YMR228W)	58	1	242.8	4						X					X
		Rpo41 (YFL036W)	54	1	419.9	8				X		X		*	* *	*	X
158		Pma1 (YGL008C)	5012.5	34	4100.1	34			X	X		X	X				
		Pma2 (YPL036W)			3140.4	22			X	X		X	X				
160		Hxt7 (YDR342C)	401.8	8	420.1	6			X	X		X					
		Hxt6 (YDR343C)	601.3	10	402.3	5			X	X		X					
		Efb1 (YAL003W)			93	1											
		Tif3 (YPR163C)			44	1											X
		Pct1 (YGR202C)			43	1								*			
		Ypr115w (YPR115W)			43	1			X								
		Tes1 (YJR019C)			100	2	X			X		X				*	
		Wwm1 (YFL010C)	276.5	2						X		X					
		Acb1 (YGR037C)			42	1								*			
		Nop9 (YJL010C)			42	1										*	
		Pfk2 (YMR205C)			42	1							X			*	
		Asi3 (YNL008C)			40	1								*			
		Sir3 (YLR442C)			42	1				X		X				*	
		Shr3 (YDL212W)			42	1											
		Atg11 (YPR049C)			42	1											
		Ydr286c (YDR286C)			43	2								*	*	*	
		Hmx1 (YLR205C)	56	1	133	1											
		Ynl247w (YNL247W)			95	3									* *		
		Dpb4 (YDR121W)			85.5	2											
		Bud21 (YOR078W)			42	1								*			

		Rps13 (YDR064W)			42.5	1	X		X							*	
		Spo73 (YER046W)			50	1										*	
		Tdh1 (YJL052W)	787.5	11	586.6	7	X		X					*			
		Ant1 (YPR128C)	406.4	3	92	1									*	*	
		Rsc30 (YHR056C)	319	4	74	1											
		Ypr091c (YPR091C)	56	1	253.6	6											
		Nbp1 (YLR457C)			50.5	1											
		Rpl31b (YLR406C)			49	1										*	
		Yil055c (YIL055C)			45	1											
		Utp8 (YGR128C)			50	1									*		
		Ygl057c (YGL057C)			50	1						X		*	* *	*	
		Yhl018w (YHL018W)			50	3									*	*	
		Cdc19 (YAL038W)			54	1									*		
		Rpl21a (YBR191W)			52.7	2									*	*	
		Ioc2 (YLR095C)			55	1								*			
		Ubc6 (YER100W)			75.5	1											
		Cdc33 (YOL139C)			54	1								*			
		Idp2 (YLR174W)	560.8	6	396.5	3			X				X				
		Nup49 (YGL172W)			51.5	3									*		
		Ydr070c (YDR070C)			53.5	2			X	X		X		*	* *		X
		Rps27a (YKL156W)	62	1													
		Rsn1 (YMR266W)			179.3	3			X								
		Ykl063c (YKL063C)			45	1											
		Mss4 (YDR208W)			45	1											
		Ebp2 (YKL172W)			48	1										*	
		Tif4631 (YGR162W)			45.5	1				X		X					
		Dat1 (YML113W)			45.5	2											
		Htb1 (YDR224C)	115.8	2	93	3	X		X				X				
		Ydr282c (YDR282C)	50	1											* *	*	
		Sen34 (YAR008W)			65	2					X	X					
		Knh1 (YDL049C)			45	1											
		Sik1 (YLR197W)			41	2											
		Lpe10 (YPL060W)			48	1								*	* *	*	X
		Sil1 (YOL031C)			46	1								*			
		Erg26 (YGL001C)	177.2	2	199.4	4		X									
		Rvs167 (YDR388W)			49	2								*	*	*	
		Nhp10 (YDL002C)	89	1													
		Rpl13b (YMR142C)	116	2									X		*	*	
		Nas2 (YIL007C)			46	2											
		Yil156w-b (YIL156W-B)			86	1											
		Yll029w (YLL029W)			46.5	1											
		Gpb2 (YAL056W)			46	1										*	
		Erp1 (YAR002C-A)	273.5	1	149	1				X		X					
		Msc6 (YOR354C)	269.9	4	543.3	13			X	X		X		*	*		

		Ynl054w-b (YNL054W-B)	334.5	5										*			
		Taf12 (YDR145W)	288.1	4										*			
		Erg28 (YER044C)	74.3	2	65	1								*			
		Fbp1 (YLR377C)	86	2	67	1											
		Ist2 (YBR086C)	253.8	2	66	3								*			
		Pmt1 (YDL095W)	248.2	2	131	1			X					*			
		Gpi17 (YDR434W)			51.5	1											
		Pom152 (YMR129W)	269.2	4	195.3	3				X		X					
		Tra1 (YHR099W)	45	1	53	4											
		Rvb1 (YDR190C)	303.8	2	182.2	4		X								*	
		Pgk1 (YCR012W)	348.6	7	219.2	4		X	X			X					
		Vps5 (YOR069W)			40	1										*	
		Ycl057c-a (YCL057C-A)	361.4	6	309.7	4			X			X				*	
		Ylr077w (YLR077W)	354.1	5	174.9	5	X			X		X			* *	*	
		Emp24 (YGL200C)	322	2	48	1		X								*	
		Yer182w (YER182W)	210.3	4	62.5	2	X	X	X	X		X			* *	*	X
		Yel007w (YEL007W)	349	3													
		Cdc14 (YFR028C)	54	1	54	1											
		Rpp0 (YLR340W)	44	1	40	2		X									
		Taf10 (YDR167W)	350.6	3	68	2											
		Yor215c (YOR215C)	223	2	735.8	12	X	X	X	X		X			* *		
		Mdj2 (YNL328C)			113	1										*	X
		Eno1 (YGR254W)	247	5	176.2	3		X	X								
		Rpl11b (YGR085C)	241.6	1	63.5	3										*	
		Cam1 (YPL048W)			133	1									*		
		Rsc6 (YCR052W)	223.8	3	117.5	2											
		Hsp30 (YCR021C)	211.6	2													
		Sur4 (YLR372W)	211.3	3	176.3	1											
		Ykl207w (YKL207W)	64	1												*	
		Rsc2 (YLR357W)	217.3	1	152	3								*			
		Abf1 (YKL112W)	215.3	3	70.5	2											
		Tpo1 (YLL028W)	213	3										*			
		Yck2 (YNL154C)	241.2	3	50	1							X				
		Pcs60 (YBR222C)	156.4	6	203.5	1		X									
		Eno2 (YHR174W)	248	5	233	2		X									
		Nhp6b (YBR089C-A)	101.7	2	300	3								*		*	
		Rpl11a (YPR102C)	241.6	1	63.5	3										*	
		Aep3 (YPL005W)			75	1									*	*	X
		Hhf1 (YBR009C)	227.9	3			X		X				X				
		Hhf2 (YNL030W)	227.9	3					X				X				
		Cue4 (YML101C)	240	1	158.5	1											
		Net1 (YJL076W)	238	1													
		Pet10 (YKR046C)	235.6	3	137.5	3										*	
		Erv1 (YGR029W)	450.5	4	596.6	4	X			X		X					X

		Dic1 (YLR348C)			40	1			X	X		X				*	X
		Spg1 (YGR236C)			41	1				X		X				*	
		Srp101 (YDR292C)			69	1								*		*	
		Spa2 (YLL021W)			40	2			X								
		Yor084w (YOR084W)	883	6	93	1								*			
		Yer080w (YER080W)	882.9	14	1263.6	20	X	X	X	X		X		*	* *		
		Ynl208w (YNL208W)	882.9	7	329.9	3				X		X					
		Ras2 (YNL098C)	1133.2	9	62	1											
		Tef2 (YBR118W)	896.9	16	450.6	13			X				X	*			
		Abp1 (YCR088W)			61	1								*			
		Snf6 (YHL025W)			41	1											
		Ylr361c-a (YLR361C-A)			41	1											
		Ykl077w (YKL077W)			42	1											
		Gvp36 (YIL041W)			42	2		X									
		Snf2 (YOR290C)			41.3	3											
		Rgd2 (YFL047W)			40	1											
		Pnc1 (YGL037C)			97.5	1											
		Ynl146w (YNL146W)			40	1											
		Prp24 (YMR268C)			45	1											
		Arg81 (YML099C)			40.3	2											
		Stb4 (YMR019W)			42	1										*	
		Hta2 (YBL003C)	493.7	6	128.3	2			X				X	*			
		Slm5 (YCR024C)	464.1	6	321.8	6				X		X			* *		X
		Ai1 (Q0050)			120	3							X			*	X
		Gas5 (YOL030W)	757.6	6											* *	*	
		Ypt7 (YML001W)			523.7	6					X		X				
		Bdf1 (YLR399C)	809.1	2	150.5	3											
		Ymr157c (YMR157C)	391.9	2	416	5				X		X		*	* *		
		Nce102 (YPR149W)	390.8	3	49	1				X		X		*			
		Car2 (YLR438W)	81	1	173	2											
		Fox2 (YKR009C)	434.8	4	96.5	1		X								*	
		Gpa2 (YER020W)	434.7	2	117.5	1				X		X					
		Ctr1 (YPR124W)	417.4	5	159.6	4											
		Aro2 (YGL148W)			83	1											
		Yjr080c (YJR080C)	723.2	9	481.3	6			X	X		X	X		*	*	
		Taf14 (YPL129W)	143.8	1													
		Opi3 (YJR073C)			50	1				X		X					
		Pck1 (YKR097W)	772.6	7													
		Rsc8 (YFR037C)	610.1	5	268	2											
		Rpl26b (YGR034W)			80	1									*		
		Yfr011c (YFR011C)	269.2	6	741.7	11		X	X	X		X	X				
		Pdi1 (YCL043C)	685.8	13	512.1	7		X	X								
		Zeo1 (YOL109W)	669.9	7	122.5	6			X	X	X	X				*	
		Rpl19a (YBR084C-A)	98	2	233	2			X				X		* *	*	

		Pdr12 (YPL058C)			924.1	11			X								
		Ynr018w (YNR018W)	221.3	5	166.4	6			X	X		X				*	
		Jip4 (YDR475C)			112.3	2											
		Ies1 (YFL013C)			112.3	3											
		Rpl20b (YOR312C)	96.3	2	74	1							X		*	*	
		Ybl055c (YBL055C)			116	1								*	* *		
		Adr1 (YDR216W)			113	1											
		Htd2 (YHR067W)			110.5	1						X			*		X
		Gnd1 (YHR183W)			108.3	4				X		X					
		Vma22 (YHR060W)			121	1								*			
		Erg5 (YMR015C)			111.5	2								*			
		Gdi1 (YER136W)	42	1													
		Msc1 (YML128C)			110.7	2	X			X		X					
		Arn1 (YHL040C)			122.5	2											
		Yor164c (YOR164C)			107	1								*		*	
		Yjl147c (YJL147C)			149	3									* *	*	
		Did2 (YKR035W-A)			129.8	2											
		Ydl183c (YDL183C)	77.5	1										*	* *	*	
		Ymc2 (YBR104W)			126.5	1				X		X	X	*		*	X
		She10 (YGL228W)			135.3	4											
		Hnt1 (YDL125C)			118.6	4			X								
		Erv41 (YML067C)			117.5	1											
		Erg2 (YMR202W)			120.3	2							X	*			
		Caj1 (YER048C)			119	1										*	
		Ena1 (YDR040C)			296.2	3											
		Mip1 (YOR330C)			101	1				X		X					X
		Rot2 (YBR229C)			100.5	2		X		X		X		*			
		Ssp120 (YLR250W)			44	2								*			
		Pot1 (YIL160C)			102.5	1								*			
		Rpl22a (YLR061W)			102	1										*	
		Ypt32 (YGL210W)			101.3	2					X					*	
		Sps19 (YNL202W)	45	1													
		Nup157 (YER105C)			96	2										*	
		Sbp1 (YHL034C)			96	2											
		Ipp1 (YBR011C)			99	1		X								*	
		Cmd1 (YBR109C)			99	1											
		Ioc4 (YMR044W)			98	1											
		Ybr159w (YBR159W)	50	1	59	1								*			
		Npl6 (YMR091C)	69	1													
		Osh6 (YKR003W)			105	1											
		Ost2 (YOR103C)			107	1										*	
		Yck1 (YHR135C)	625.2	3	120.5	2						X	X				
		Yor131c (YOR131C)			106	1		X	X								
		Cyb5 (YNL111C)			103	2							X				

		Sgf29 (YCL010C)	66	1													
		Rpl12b (YDR418W)			102.7	3							X			*	
		Rps9a (YPL081W)	121	1	143	2									*		
		Rer1 (YCL001W)			104	1											
		Lys1 (YIR034C)			103	1		X							*		
		Sey1 (YOR165W)			203.2	4								*			
		App1 (YNL094W)			200.6	3											
		Rco1 (YMR075W)	43	1													
		Eug1 (YDR518W)			207.2	3		X								*	
		Rho3 (YIL118W)	56	1	64	1											
		Rpc19 (YNL113W)			204.3	3											
		Tcb2 (YNL087W)			183.6	3							X				
		Ecm37 (YIL146C)			181	1											
		Rps2 (YGL123W)			180.5	1							X			*	
		Yer093c-a (YER093C-A)			198	4											
		Pan5 (YHR063C)			196.7	3			X								
		Sec11 (YIR022W)			190	2								*			
		Ies6 (YEL044W)	73	1													
		Erv25 (YML012W)			257.8	6							X			*	
		Hbt1 (YDL223C)			254.4	4										*	
		Pho84 (YML123C)			354.8	7			X								
		Ena5 (YDR038C)			296.2	3											
		Ena2 (YDR039C)			296.2	3				X		X					
		Rpp2a (YOL039W)			232.8	3							X				
		Spf1 (YEL031W)	115.3	4	274.9	7			X	X		X					
		Fet3 (YMR058W)			225.2	2											
		Heh2 (YDR458C)	42	1													
		Trr1 (YDR353W)			243.3	2								*		*	
		Ybl107c (YBL107C)	49	1	88.5	2											
		Rps4b (YHR203C)			136	3			X					*	*	*	
		Rps4a (YJR145C)			136	3			X					*	*	*	
		Gpa1 (YHR005C)	48	1	91.5	2							X				
		Ydl121c (YDL121C)			147.5	1											
		Yor1 (YGR281W)			139.5	4			X								
		Src1 (YML034W)			137	2											
		Rps10b (YMR230W)	51.5	1													
		Fus3 (YBL016W)			131	1				X		X			*		
		Mne1 (YOR350C)			130.4	4									* *	*	
		Hbn1 (YCL026C-B)			134	2											
		Sis1 (YNL007C)	226.6	3	149.5	3										*	
		Asc1 (YMR116C)			133	3		X									
		Rps28a (YOR167C)	50	1	51	1								*	*	*	
		Sec23 (YPR181C)			169.2	5											X
		Yjl046w (YJL046W)			166	5											

		Rpl21b (YPL079W)			52.7	2								*	*	*	
		Ai2 (Q0055)			176	5							X	*		*	X
		Chd1 (YER164W)			175.5	2				X		X					
		Ssa3 (YBL075C)			152.3	2							X				
		Ylr118c (YLR118C)			150.5	1									*		
		Asi2 (YNL159C)			106	1											
		Rpl5 (YPL131W)			162	4			X				X	*			
		Tal1 (YLR354C)			45	1								*			
		Sed5 (YLR026C)			157	1											
		Vps21 (YOR089C)			95	2				X	X	X					
		Rps26a (YGL189C)			66	1											
		Trx2 (YGR209C)			66	1											
		Nat3 (YPR131C)			82	1											
		Yim1 (YMR152W)			67	2				X	X	X					X
		Yil083c (YIL083C)	75	1													
		Nup159 (YIL115C)			66.5	2											
		Tef1 (YPR080W)	896.9	16	450.6	13		X	X				X				
		Tef4 (YKL081W)			64	1				X		X					
		Loc1 (YFR001W)			64	1								*			
		Rtt102 (YGR275W)	378.7	3													
		Ptc6 (YCR079W)			66	2											
		Ncb2 (YDR397C)			45	1											
		Yol092w (YOL092W)			70	1											
		Sth1 (YIL126W)			70	2											
		Ygr043c (YGR043C)	138.4	4													
		Dsl1 (YNL258C)			72	1			X					*			
		Pho86 (YJL117W)			71	1										*	
		Yjr003c (YJR003C)			70.5	2		X				X					
		Lcb1 (YMR296C)	176.5	2	174.7	3			X								
		Ydr514c (YDR514C)			67	1								*		*	
		Tma19 (YKL056C)			67	1											
		Yjl062w-a (YJL062W-A)			68	1						X					
		Ygr110w (YGR110W)			68	1								*	* *	*	
		Ypl103c (YPL103C)			68	2				X		X		*	* *		
		Rpl4a (YBR031W)	96.7	2	138.6	2			X				X	*			
		Mnn5 (YJL186W)			57.5	1								*			
		Spc3 (YLR066W)			57	1								*	*		
		Fsh3 (YOR280C)			56	1										*	
		Vph2 (YKL119C)			58	1											
		Hir1 (YBL008W)			58	1											
		Rxt3 (YDL076C)			56	1								*			
		Ycl045c (YCL045C)			56	2											
		Ssa1 (YAL005C)	235.2	7				X					X				
		Sur7 (YML052W)			61.5	3				X		X					

		Sec66 (YBR171W)			57	2											
		Rlf2 (YPR018W)			57	2											
		Mdm35 (YKL053C-A)			62.5	2										*	
		Trx1 (YLR043C)			62.5	2											
		Nic96 (YFR002W)			62	1										*	
		Yhr097c (YHR097C)			63.7	4											
		Cdc42 (YLR229C)	57	2													
		Ynk1 (YKL067W)			63	2						X					
		Ygr266w (YGR266W)	110.3	2	186	1				X	X	X					
		Pdr16 (YNL231C)			60	1											
		Lys20 (YDL182W)			60	3				X		X					
		Tpo3 (YPR156C)	90.7	2	96	1											
		Asi1 (YMR119W)			57	1											
		Kin1 (YDR122W)			84	1											
		Taf4 (YMR005W)			61	1											
		Yol053w (YOL053W)			83.8	2			X							*		
		Om14 (YBR230C)	726.8	9			X	X	X	X		X					
		Q0297 (Q0297)			42	1											
		Yos1 (YER074W-A)			85	1											
		Clu1 (YMR012W)			85	1											
		Scp160 (YJL080C)			81.3	3											
		Rer2 (YBR002C)			81	1										*	
		Ssz1 (YHR064C)			51	1								*	*		
		Rot1 (YMR200W)			82	1									* *		
		Yhr003c (YHR003C)			276.2	3				X	X	X		*		*	
		Ypt31 (YER031C)			81.8	2					X					*	
		Mmr1 (YLR190W)			92	1				X	X	X					X
		Mtg1 (YMR097C)			92	1						X				*	X
		Iml2 (YJL082W)			92	2				X	X	X					
		Hop1 (YIL072W)			43	2											
		Yhr100c (YHR100C)			94.5	2						X					
		Nip1 (YMR309C)			94	1											
		Snf7 (YLR025W)	114.7	2													
		Csr2 (YPR030W)			88	2											
		Mob1 (YIL106W)	68	1										*			
		Sec22 (YLR268W)			91	2											
		Pbn1 (YCL052C)			90	1											
		Tgl4 (YKR089C)			89.5	1							X				
		Ykt6 (YKL196C)			75.5	2				X		X					
		Dip5 (YPL265W)			75.2	3			X								
		Gpx2 (YBR244W)			75	1											
		Kre6 (YPR159W)			76.5	2								*			X
		Rxt2 (YBR095C)			76	1											
		Nop58 (YOR310C)			55	1											

		Sna2 (YDR525W-A)			73	1											
		Dpp1 (YDR284C)			64.5	1								*			
		Yol114c (YOL114C)			72	1								*			
		Ylh47 (YPR125W)	234.5	2	402.7	11		X	X			X		*	* *	*	
		Rki1 (YOR095C)			74.3	2								*			
		Rpl40a (YIL148W)	70	1	144	1											
		Yer087w (YER087W)	183	2	559.9	8			X			X		*	* *		
		Sec1 (YDR164C)			79.7	2											
		Yfr018c (YFR018C)			79.5	1											
		Ctr3 (YLR411W)	76	1													
		Rax1 (YOR301W)			80	1											
		Rpl26a (YLR344W)			80	1											
		Rpc10 (YHR143W-A)			78	1											
		Ast2 (YER101C)			78	1											
		Sfk1 (YKL051W)			77	1											
		Rps19b (YNL302C)			79	2										*	
		Rpl7a (YGL076C)	85	1			X		X					*		*	
		Pus6 (YGR169C)			79	2								*			X
		Taf9 (YMR236W)	209.5	1	128.3	3								*		*	
		Srm1 (YGL097W)	196.7	5										*			
		Ole1 (YGL055W)	48	1	268	4			X				X	*		*	
		Ygl080w (YGL080W)	48	1	107.3	2				X		X		*		*	
		Tbf1 (YPL128C)	48	1													
		Ykl151c (YKL151C)	48	1													
		Ygr026w (YGR026W)	48	1									X			*	
		Sap30 (YMR263W)	47	1													
		Avl9 (YLR114C)			43	2											
		Nop1 (YDL014W)	47	1									X			*	
		Rps9b (YBR189W)	58	1	81	2									*	*	
		Ygr130c (YGR130C)	48	1	40	2			X							*	
		Moh1 (YBL049W)	47	1													
		Vps34 (YLR240W)			45	2										*	
		Rfc1 (YOR217W)	50	1	89	1											
		Rpp2b (YDR382W)			106	1							X				
		Pmc1 (YGL006W)	51	1	51	2											
		Yjr111c (YJR111C)	50	1												*	
		Far8 (YMR029C)	50	1												*	
		Yjl171c (YJL171C)	49	1					X	X		X		*			
		Rps3 (YNL178W)	154	1	236	3			X							*	
		Rpl2a (YFR031C-A)			48	1								*	*		
		Rps28b (YLR264W)	50	1	51	1								*	*	*	
		Ymr293c (YMR293C)			173.6	3				X		X					X
		Cdc48 (YDL126C)	50	1	44	1		X									
		Erg1 (YGR175C)	47	1													

		Alg1 (YBR110W)	44	1												*	
		Erj5 (YFR041C)	44	1	69.5	1										*	
		Hmo1 (YDR174W)	334.6	3	134.5	2			X								
		Pex31 (YGR004W)	44	1												*	
		Nup170 (YBL079W)	219.8	2	160.4	3			X					*			
		Dpl1 (YDR294C)	44	1									X			*	
		Sip4 (YJL089W)	43	1												*	
		Yhr198c (YHR198C)	43	1	379.2	6		X	X	X	X	X			*		
		Swi1 (YPL016W)	43	1	54	1											
		Trz1 (YKR079C)			199.3	3											
		Spt10 (YJL127C)	43	1													
		Dst1 (YGL043W)	97	1													
		Ste24 (YJR117W)	79	1							X		X	*			
		Sec18 (YBR080C)	45	1												*	
		Ubx2 (YML013W)	45	1							X						
		Chs1 (YNL192W)	47	1													
		Fit2 (YOR382W)	46	1												*	
		Snf12 (YNR023W)	46	1													
		Hxt5 (YHR096C)	260.9	4	187.8	4											
		Spt16 (YGL207W)	45	1	40	1											
		Ape3 (YBR286W)	44	1										*			
		Ydr020c (YDR020C)	45	1												*	
		Zta1 (YBR046C)	45	1										*			
		Rsp5 (YER125W)	45	1	197.8	4				X		X					
		Srp54 (YPR088C)	57	1													
		Mgs1 (YNL218W)	57	1										*			
		Ptr2 (YKR093W)	96	2	232	3											
		Yor390w (YOR390W)	59	1	129	1									*		
		Ypl279c (YPL279C)	59	1	129	1									*		
		Erg11 (YHR007C)			185.8	5			X				X			*	
		Mcm3 (YEL032W)			51	1											
		Erg25 (YGR060W)	47	1										*		*	
		Pab1 (YER165W)			206.6	5											
		Fcf2 (YLR051C)	41	1													
		Rpl27a (YHR010W)	57	1	68.5	2	X								* *		
		Yrr1 (YOR162C)	57	1	41	2										*	
		Cdc10 (YCR002C)	60	1	156.8	3								*			
		Vps13 (YLL040C)	60	1	56.8	6				X		X					
		Spt8 (YLR055C)	59	1													
		Pbi2 (YNL015W)	61	1	154.3	3											
		Hor2 (YER062C)	61	1	50	2											
		Plb1 (YMR008C)	60	1					X								
		Cta1 (YDR256C)	186.7	2	106	1											
		Ste18 (YJR086W)	127	1													

		Orm1 (YGR038W)	59	1	201.5	1								*			
		Brx1 (YOL077C)			45	1										*	
		Rps22b (YLR367W)	59	1												*	
		Dal81 (YIR023W)	59	1													
		Nup57 (YGR119C)	55	1													
		Scw4 (YGR279C)	52	1	125.3	2											
		Orc1 (YML065W)	52	1	44.5	1											
		Acc1 (YNR016C)	52	1	40	2				X		X					
		Rpl20a (YMR242C)	96.3	2	74	1	X						X		*	*	
		Rho1 (YPR165W)	114.7	2	385.1	6				X	X	X					
		Rpb8 (YOR224C)	52	1													
		Nug1 (YER006W)	51	1											*		
		Ymr194c-b (YMR194C-B)	51	1													
		Ybl095w (YBL095W)			114.5	2			X			X		*			
		Myo3 (YKL129C)	52	1	40	2											
		Act1 (YFL039C)	88.5	1	101.8	6		X					X				
		Rps10a (YOR293W)	51.5	1													
		Lhs1 (YKL073W)	54	1	171.7	2											
		Ssb1 (YDL229W)	344.5	8	457.1	9		X					X			*	
		Lag1 (YHL003C)	53	1													
		Pos5 (YPL188W)			61.5	2			X			X			* *		X
		Rsc9 (YML127W)	55	1													
		Rnq1 (YCL028W)	54	1													
		Msc7 (YHR039C)	53	1	57	2			X								
		Fpr3 (YML074C)	52	1													
		Glc7 (YER133W)	60	1												*	
		Mcm1 (YMR043W)	53	1													
		Mgr2 (YPL098C)	53	1	100.7	1								*			
		Hsf1 (YGL073W)	71.5	1	40	2				X		X					
		Bna4 (YBL098W)	101	3	155.2	4				X	X	X	X	*		*	
		Sfh5 (YJL145W)			137.5	2								*			
		Vac8 (YEL013W)			62	2							X				
		Ino80 (YGL150C)	136.3	1	112.3	3											
		Pho23 (YNL097C)	104.5	1													
		Htz1 (YOL012C)			117	1											
		Yor271c (YOR271C)	240.1	4	166.8	3			X			X				*	X
		Fpr1 (YNL135C)	140	2	84	1						X					
		Slm1 (YIL105C)	166.5	1						X		X					
		Pex19 (YDL065C)			71	1											
		Rhr2 (YIL053W)	61	1				X							* *		
		Rfc3 (YNL290W)	109	1										*		*	
		Rpl13a (YDL082W)	116	2	206.3	3							X	*	*		
		Van1 (YML115C)			88	2								*			
		Ada2 (YDR448W)			58	1											

		Pep4 (YPL154C)			148.3	2				X		X					
		Rrp14 (YKL082C)	41	1													
		Sec61 (YLR378C)	66	1									X			*	
		Ydr348c (YDR348C)			62	1								*			
		Ulp1 (YPL020C)	78.5	1	110	1											
		Yjl193w (YJL193W)	70	1											*		
		Rpp1b (YDL130W)			88	1							X				X
		Fat1 (YBR041W)			40	1								*		*	
		Yif1 (YNL263C)	41	1	116	1											
		Stl1 (YDR536W)			106.5	2			X						*		
		Rvb2 (YPL235W)	65.5	2	184.3	4											
		Ygr031w (YGR031W)	132	2	195.2	3						X		*	* *	*	
		Pmt2 (YAL023C)	82.5	1	341	4			X								
		Put1 (YLR142W)	181.1	5	263.7	5				X		X		*	* *	*	X
		Rli1 (YDR091C)			119	2											
		Ngl1 (YOL042W)			293.2	3						X			* *		
		Rsm28 (YDR494W)	291.1	7	444.5	5			X			X			*		X
		Irs4 (YKR019C)			40	1				X		X				*	
		Pmt4 (YJR143C)	75.5	1	91.3	4			X								
		Rps19a (YOL121C)			79	2										*	
		Tna1 (YGR260W)			46.5	1				X		X					
		Cdc12 (YHR107C)	111.8	3	60.7	3											
		Arc19 (YKL013C)			42	1								*			
		Yjl131c (YJL131C)			239.5	3						X			*	*	
		Rps8a (YBL072C)	79.5	2	63	1			X							*	
		Rpl17b (YJL177W)	94.3	2					X				X		*		
		Ndc1 (YML031W)	59	1	64	2											
		Sec17 (YBL050W)	213.5	2	246.5	3										*	
		Fet4 (YMR319C)			40	1											
		Rpl31a (YDL075W)			49	1										*	
		Rps22a (YJL190C)	59	1												*	
		Snl1 (YIL016W)	45	1						X		X				*	
		Rad5 (YLR032W)			53	1											
		Vps66 (YPR139C)			41	1								*		*	
		Yhr138c (YHR138C)			43	1											
		Arf1 (YDL192W)	90	1	68	1							X		*		
		Vtc2 (YFL004W)			77	1								*		*	
		Mid2 (YLR332W)	69.5	1												*	
		Rrf1 (YHR038W)	41	1	364.2	4	X		X	X		X		*	* *		X
		Erg9 (YHR190W)	41	1	247.2	4			X		X						
		Yet3 (YDL072C)	41	1	195.7	6								*			
		Bgl2 (YGR282C)			58	2											
		Ymr209c (YMR209C)			101.3	2										*	
		Ygr093w (YGR093W)			66	1											

		Var1 (Q0140)	127.6	2	88.5	1			X	X		X	X			*	X
		Sbh1 (YER087C-B)	42	1										*		*	
		Snz3 (YFL059W)	52	1													
		Not3 (YIL038C)	45	1													
		Car1 (YPL111W)			111	1								*			
		Rog1 (YGL144C)	42	1													
		Ecm4 (YKR076W)			248	2								*	*		
		Chs6 (YJL099W)	42	1													
		Sum1 (YDR310C)	42	1					X								
		Lsm4 (YER112W)	41	1													
		Rgr1 (YLR071C)	41	1													
		Pol2 (YNL262W)			56	1			X								
		Bbc1 (YJL020C)	42	1	40	1			X								
		Ydl177c (YDL177C)	121.5	1	43	1											
		Kre2 (YDR483W)	41	1										*			
		Alo1 (YML086C)	400.5	8	342.4	7		X	X	X	X	X			*		X
		Stt3 (YGL022W)	162	2	122.5	3										*	
		Ykl027w (YKL027W)	163.8	3	343	8		X	X	X	X	X		*		*	
		Vps1 (YKR001C)	63	1	331.1	9					X						
		Snz2 (YNL333W)	52	1													
		Mdh3 (YDL078C)	294.5	5	144	4								*		*	
		Alg2 (YGL065C)	51	1	164	2											
		Utr2 (YEL040W)	106	2												*	
		Ybl029c-a (YBL029C-A)	106.3	1													
		Ibd2 (YNL164C)			51	1											
		Dps1 (YLL018C)			57	1											X
		Mck1 (YNL307C)			58	2											
		Syp1 (YCR030C)			158.3	2											
		Put4 (YOR348C)			72	1											
		Ynr034w-a (YNR034W-			119	1											
		Rsc4 (YKR008W)	46	1													
		Ioc3 (YFR013W)	55	1													
		Smt3 (YDR510W)			81	1											
		Rps26b (YER131W)			66	1											
		Rap1 (YNL216W)	205.8	3	374.3	4											
		Hmg1 (YML075C)	52	1	73.5	2									* *		
		Ume6 (YDR207C)	261.2	2													
		Rho2 (YNL090W)			55.5	1											
		Taf5 (YBR198C)	543.2	5													
		Rpl25 (YOL127W)	198.5	2	321.5	4								*	*		
		Get1 (YGL020C)	122	1	171.3	2						X					
		Tcb1 (YOR086C)	146.8	4	569.3	11				X		X	X			*	
		Nif3 (YGL221C)	121	2	132.5	2						X					
		Hsp104 (YLL026W)			52	1								*			

		Oct1 (YKL134C)	126.4	2	139.3	3						X			* *		X
		Yet1 (YKL065C)	122.7	3	116	1											
		Yju3 (YKL094W)	116.3	3	136	1		X			X						
		Gea2 (YEL022W)			46	1											
		Rpl16a (YIL133C)			45	2	X										
		Ady2 (YCR010C)	129.7	2	305.4	4				X		X					
		Ydr061w (YDR061W)	146.4	4	124	3			X			X	X		*		
		Rfs1 (YBR052C)	116.3	1									X			*	
		Cpr5 (YDR304C)	136.3	1	90	2		X									
		Sin3 (YOL004W)	135	1													
		Cbf1 (YJR060W)	132	1						X		X					
		Sso2 (YMR183C)	138.3	2	143.3	3							X				
		Yil108w (YIL108W)	138	1	84	3											
		Ras1 (YOR101W)	137.7	2													
		Mgr1 (YCL044C)	120	2	133.6	4			X	X		X				*	X
		Bmh1 (YER177W)	128.3	2	68.5	2		X						*			
		Sar1 (YPL218W)	128	2	92	1	X						X				
		Ncp1 (YHR042W)	131.5	1	460.5	5				X	X	X		*			
		Rps20 (YHL015W)	130.7	2	71	1											
		Nsp1 (YJL041W)	130	1	191.3	2										*	
		Ste12 (YHR084W)	77	1													
		Mcm4 (YPR019W)	43	1	42	1										*	
		Rpl19b (YBL027W)	98	2	233	2			X				X		* *		
		Snq2 (YDR011W)			94.5	2			X	X		X					
		Scj1 (YMR214W)	104.5	1	60	1									*		
		Ydr381c-a (YDR381C-A)	149.8	2	40	2					X	X					
		Mdh2 (YOL126C)	44	1										*			
		Rpl27b (YDR471W)	57	1	68.5	2			X						* *		
		Rpl4b (YDR012W)	96.7	2	138.6	2			X				X	*		*	
		Rga2 (YDR379W)	96.5	1													
		Hyr1 (YIR037W)	98	3	113.5	1											
		Enb1 (YOL158C)	43	1													
		Gas3 (YMR215W)	97	1	89	2										*	
		Str3 (YGL184C)	113	2													
		Nhp6a (YPR052C)			52.8	3			X								
		Hht1 (YBR010W)	111	1					X						*		
		Ybr255c-a (YBR255C-A)			230	3								*		*	
		Smf3 (YLR034C)	53	1	63	1											
		Prd1 (YCL057W)	113.7	2	176.7	2	X		X	X		X		*		*	X
		Cho2 (YGR157W)	106.5	1	260	6			X								
		Yil087c (YIL087C)	157.3	1						X		X					
		Arf2 (YDL137W)	90	1	68	1							X		*	*	
		Hht2 (YNL031C)	111	1					X						*		
		Prp6 (YBR055C)			40	3								*			

		Crp1 (YHR146W)	109	1	53	1											
		Cpr1 (YDR155C)	179	4	532	4			X			X	X				
		Gnp1 (YDR508C)			49	1				X		X		*		*	
		Hom6 (YJR139C)			68	3		X									
		Rbg1 (YAL036C)			80	2								*			
		Tos1 (YBR162C)	151.7	2										*		*	
		Nup145 (YGL092W)	179.7	2					X					*		*	
		Ynr021w (YNR021W)	164	3	190.7	3							X	*		*	
		Ydr056c (YDR056C)			213	2											
		Yml050w (YML050W)	501.9	3											**	*	
		Rps27b (YHR021C)	62	1													
		Hho1 (YPL127C)	174.4	2	48	1											
		Ded1 (YOR204W)	80	1									X			*	
		Rps6a (YPL090C)	197.2	3	156.8	2			X				X			*	
		Cwh43 (YCR017C)	78	1	50	1									*		
		Stm1 (YLR150W)	142.3	2	102.7	3											
		Sec20 (YDR498C)			40	1											
		Faa4 (YMR246W)	201.8	3	118	2							X				
		Rps6b (YBR181C)	197.2	3	156.8	2			X				X			*	
		Mbf1 (YOR298C-A)	59	1						X		X					
		Ypt1 (YFL038C)	184	2	160	3				X		X	X				
		Ygr235c (YGR235C)	183.3	5	365.6	9			X	X		X				*	
		Nca2 (YPR155C)	195.8	3	536.3	8				X	X	X	X			*	
		Gsf2 (YML048W)	193.8	4	130	4					X					*	
		Fun14 (YAL008W)	188.7	1	193	2				X	X	X	X	*	*		
		Erp2 (YAL007C)	161.3	2	116.3	2											
		She9 (YDR393W)	145.3	2	466.1	11			X					*	*	*	X
		Hta1 (YDR225W)	493.7	6	128.3	2			X				X				
		Fmp46 (YKR049C)	143.3	2	369.1	7			X	X		X			*		
		Erp4 (YOR016C)			104	1								*			
		Snz1 (YMR096W)	52	1													
		Mls1 (YNL117W)	118.7	3	40	1											
		Eft2 (YDR385W)	139	3	229.8	9							X				
		Yro2 (YBR054W)	138.7	2	40	1			X	X		X					
		Hsp82 (YPL240C)			171.3	2		X									
		Top1 (YOL006C)	196.5	3										*			
		Hsp26 (YBR072W)	140.3	2	40	1											
		Eft1 (YOR133W)	139	3	229.8	9		X					X				
		Isw1 (YBR245C)	155.3	3	132.5	3											
		Arp4 (YJL081C)	154	2													
		Taf6 (YGL112C)	49	1	129.7	2											
		Asg1 (YIL130W)	159	3										*			
		Hfd1 (YMR110C)	158.3	5	237	4	X		X	X	X	X		*			X
		Rpl8b (YLL045C)	93.7	1	69	1							X				

		Yer004w (YER004W)	151.4	3	138.8	4	X	X	X	X	X	X				*	
		Ykr070w (YKR070W)	103.5	2	329.4	6			X			X		*			X
		Ypl107w (YPL107W)	148.5	1	239.5	1									* *		
		Mcm6 (YGL201C)	154	2	108	2											
		Wbp1 (YEL002C)	153.4	3					X				X				
		Assembly4 (YDL088C)	181	2													
		Nup53 (YMR153W)	214.5	1													
		Rpl40b (YKR094C)	70	1	144	1				X		X					
		Ubi4 (YLL039C)	70	1	144	1											
		Rfc4 (YOL094C)			73	1										*	
		Rpl18a (YOL120C)	71	1	41	1	X							*			
		Rpl18b (YNL301C)	71	1	41	1								*			
		Dig1 (YPL049C)	70	1													
		Faa2 (YER015W)	69	1						X		X				*	
		Rps21a (YKR057W)	68	1												*	
		Hch1 (YNL281W)	68	1													
		Rps31 (YLR167W)	70	1	144	1							X				
		Ycp4 (YCR004C)	69.5	1	462	5				X		X	X			*	
		Ent4 (YLL038C)			120.5	1								*			
		Rpl3 (YOR063W)	74.5	1	96	2			X				X	*			
		Rpl15b (YMR121C)	73.5	1													
		Ssh1 (YBR283C)			60	1							X				
		Cox19 (YLL018C-A)	76	1													X
		Gcn1 (YGL195W)			66.7	3				X		X					
		Ygl231c (YGL231C)	75	1													
		Rrp5 (YMR229C)	72.5	1	51	2											
		Aro10 (YDR380W)	72	2										*			
		Gpm1 (YKL152C)	71	1	171.4	5		X	X			X					
		Rpl15a (YLR029C)	73.5	1	40	1										*	
		Rpl30 (YGL030W)	73	1										*		*	
		Rpt6 (YGL048C)	73	1												*	
		Rho5 (YNL180C)			87	1											
		Yor020w-a (YOR020W-	278.9	2	144	1						X					
		Pex30 (YLR324W)	63	1	273.6	4										*	
		Ynr040w (YNR040W)	63	1	109.3	2				X		X				*	
		Vhs3 (YOR054C)	64	1												*	
		Nsg2 (YNL156C)	64	1													
		Rps7a (YOR096W)	64	1	61.5	2			X				X			*	
		Ygl118c (YGL118C)	62	2													
		Epl1 (YFL024C)	62	2													
		Arp2 (YDL029W)			60	1										*	
		Cue1 (YMR264W)	63	1	75.5	3				X		X					
		Ybl059c-a (YBL059C-A)	176	2	209.1	3								*			
		Pom34 (YLR018C)			53	1										*	

		Ycl033c (YCL033C)			57	1								*	* *		
		Rpl12a (YEL054C)			102.7	3							X			*	
		Tyw1 (YPL207W)	66	1	66	2								*			
		Rps21b (YJL136C)	68	1													
		Yhr199c (YHR199C)	68	2	95	2			X	X		X		*	*		
		Pat1 (YCR077C)	67	1													
		Irr1 (YIL026C)	64.5	1													
		Ydr476c (YDR476C)	64.5	1													
		Ycr051w (YCR051W)			54	1											
		Ykl133c (YKL133C)	66	1	40	2									*	*	
		Hoc1 (YJR075W)			40	1								*		*	
		Pob3 (YML069W)	65	1													
		Rrp12 (YPL012W)			48	1											
		Ypl099c (YPL099C)			132	1			X	X		X		*	* *	*	
		Rtn1 (YDR233C)	258.2	2	158	6				X		X	X	*			
		Ylr225c (YLR225C)			61.5	1											
		Erv29 (YGR284C)	44	1	68	1							X				
		Rpl16b (YNL069C)	89.5	2													
		Lcb2 (YDR062W)	83.5	2	59	1											
		Ssm4 (YIL030C)	83	1													
		Grx1 (YCL035C)			104.5	1											
		Ngg1 (YDR176W)	85	1										*			
		Stu2 (YLR045C)	59	1													
		Coa1 (YIL157C)	83.5	2	152.6	8	X	X	X	X		X	X	*	* *	*	X
		Pox1 (YGL205W)	94.5	2				X						*		*	
		Ylr356w (YLR356W)	152.6	1	80	1											
		Rpl17a (YKL180W)	94.3	2									X		*		
		Ymc1 (YPR058W)	146.7	1	49.5	2	X		X			X	X			*	X
		Ast1 (YBL069W)			63	1											
		Isd11 (YER048W-A)	95.8	3	102.7	2	X		X			X			*	*	
		Fps1 (YLL043W)	93	1													
		Gal11 (YOL051W)	92.5	1													
		Gis2 (YNL255C)	91.3	2													
		Hpc2 (YBR215W)	94	1												*	
		Rpl8a (YHL033C)	93.7	1	69	1							X		*		
		Sec31 (YDL195W)			91.7	2										*	
		Alg9 (YNL219C)	82	1													
		Fre1 (YLR214W)	78.5	1	49	1								*			
		Gpt2 (YKR067W)	78	2	310.9	6										*	
		Rps18b (YML026C)	78	1	88	2			X			X				*	
		Sbh2 (YER019C-A)	79	1											*	*	
		Rpl23a (YBL087C)	79	1	129	1			X				X			*	
		Sec9 (YGR009C)	110	1													
		Zrc1 (YMR243C)	77	1													

		Htb2 (YBL002W)	115.8	2	93	3			X				X				
		Mpd2 (YOL088C)	77	1												*	
		Taf2 (YCR042C)	48	1										*			
		Pus9 (YDL036C)			129.2	3								*			
		Fre7 (YOL152W)	77.5	2													
		Ypr098c (YPR098C)	81	2	46.7	1					X	X		*		*	
		Reb1 (YBR049C)	80.5	2												*	
		Afg1 (YEL052W)	80.5	2	366.8	7			X	X	X	X		*	*		
		Adh2 (YMR303C)	81.5	2	155.5	4		X					X				
		Icl1 (YER065C)	81	1													
		Mic17 (YMR002W)	369.2	8										*	*	*	
		Rps8b (YER102W)	79.5	2	63	1			X								
		Bud14 (YAR014C)	45	1													
		Dfm1 (YDR411C)	79	1										*		*	
		Yef3 (YLR249W)	165	1	270.6	3							X				
		Sok2 (YMR016C)	80	1													
		Rsc58 (YLR033W)	48	1	55	1											

nazwy na podstawie bazy SGD z 12/12/2007

Supporting Table S2

Click here to download Supplementary Material (for online publication): Supporting TableS2.xls

ORF name	Common Protein Name
YLL018C	Asprs Dps1
YKL055C	Oar1
YDL164C	Mms8 Cdc9
YCL004W	Pel1 Pgs1 Ycl003w
YKL114C	Apn1
YPR163C	Rbl3 Tif3 Stm1
YNL066W	Scw3 Sun4
YGR046W	Ygr046w
YHL038C	Cbp2
YPR181C	Sec23
YBR029C	Cdg1 Cds1
YKR087C	Oma1
YOR147W	Mdm32
YMR166C	Ymr166c
YHR086W	Mre2 Nam8 Mud15
YHR011W	Dia4
YNR020C	Ynr020c
YNL081C	Sws2
YDL107W	Mss2
YHR116W	Cox23
YPL060W	Lpe10
YGR257C	Mtm1
YGR169C	Pus6
YNL292W	Pus4
YPL005W	Aep3
YNL328C	Mdj2
YDL045W-A	Mrp10
YGL236C	Ips1 Mto1
YHR168W	Mtg2
YEL059C-A	Som1
YLL018C-A	Cox19
YPR159W	Cwh48 Kre6
YOR226C	Nua2 Isu2
YLR289W	Guf1

Supporting Table S3

Click here to download Supplementary Material (for online publication): Supporting TableS3.xls

Modules according to Perocchi at al. [36]		number of proteins predicted	this study FTICR	Oth
No.	description			Pflieger et al. [22]
79	Components of the large subunit of mitochondrial ribosomes-MRPL	48	44	14
99	Components of the small subunit of mitochondrial ribosomes-MRPS	38	33	3
155	Respiratory Chain Complex-V	18	16	12
16	Tim23/Tim22 complex	16	16	2
58	Vacuolar acidification	16	3	0
62	Translation regulator activity	15	11	2
1	Respiratory Chain Complex-IV	14	11	10
20	Iron-sulfur cluster assembly	13	11	2
37	Pyruvate/α-ketoglutarate dehydrogenase	13	11	8
95	NAD metabolism/TCA cycle	13	13	9
132	Cytoplasmic ribosome	13	8	1
61	RNA splicing	12	8	0
7	Ubiquinone metabolism	11	8	0
49	TOM complex	11	11	3
98	tRNA/rRNA processing	11	1	0
8	Branched chain amino acid biosynthesis	10	9	6
15	Matrix protein import	10	9	6
46	Folate and glycine metabolism	10	6	2
103	Alcohol/aldehyde dehydrogenase	10	7	3
156	Respiratory Chain Complex-III	10	9	6
6	Mitochondrial organisation and morphology	9	7	1
147	Respiratory Chain Complex-II	9	7	7
22	Secretory pathway	8	4	0
41	DNA replication	8	3	0
45	cytoplasmic lipid metabolism	8	3	1
48	Glycerol metabolism	8	6	1
66	Amino acid metabolism	8	4	0
35	Response to DNA damage	7	3	1
80	tRNA aminoacylation	7	5	0
9	Respiratory Chain Complex assembly 1	6	5	0
27	Unknown module 1	6	4	0
31	Glutamate biosynthesis	6	3	2
64	Fusion/fission	6	5	1

149	Isocitrate metabolism	6	5	4
4	Cell growth regulation	5	3	0
10	Mitochondrial protein targeting	5	5	0
12	Fatty acid biosynthesis	5	2	0
17	Unknown module 2	5	2	0
24	Glutamine family metabolism	5	1	0
28	Respiratory Chain Complex assembly 2	5	5	1
30	Mitochondrial/cytoplasmic lipid metabolism	5	5	2
51	Arginine biosynthesis	5	3	0
54	Cell wall organisation and biogenesis	5	4	0
69	Respiratory Chain Complex-IV assembly	5	3	0
105	Mismatch repair	5	0	0
115	Transport	5	5	0

er MS based proteomic studies

Ohlmeier et al. [23]	Prokisch et al. [24]	Sickmann at al. [25]	Zahedi et al. [26]	Reinders et al. [27]	Prokisch at al.N. crassa
6	24	39	1	42	7
6	22	27	2	32	4
9	16	17	4	18	14
4	7	13	3	16	5
2	1	0	0	0	0
1	2	14	0	14	1
6	13	14	0	13	10
5	8	9	0	10	0
11	10	12	3	12	8
7	13	13	5	13	8
0	10	2	0	2	4
2	2	8	0	8	2
5	5	7	0	8	1
4	8	10	10	11	6
0	1	1	0	1	0
7	9	8	2	8	5
7	9	9	3	9	2
3	6	8	0	8	1
6	5	7	1	7	3
5	8	10	2	10	8
3	3	5	3	6	2
5	7	8	2	8	9
1	2	1	0	1	0
2	1	3	0	4	1
1	2	4	1	4	0
1	1	4	1	4	1
3	2	4	0	5	0
1	3	4	0	4	0
1	2	4	0	4	2
1	2	3	0	4	1
0	0	1	0	2	0
3	3	6	0	6	0
1	3	5	5	6	5

5	6	6	0	6	5
0	1	2	0	2	0
1	2	4	1	4	4
0	0	3	0	4	0
0	0	2	0	2	0
1	2	2	0	2	2
0	2	4	0	4	0
2	5	5	1	5	2
3	3	3	0	3	1
0	3	3	0	3	0
1	2	5	0	5	2
0	0	2	0	2	0
0	1	3	0	4	2

Supporting Table S4

Click here to download Supplementary Material (for online publication): Supporting TableS4.xls

Modules according to Perocchi at al. [36]		*protein name (ORF)*	*FTICR*		*WPES*		
module No.	*predicted mitochondrial complex*		*PSI+/psi-*	*P*	*PSI+/psi-*	*P*	*mean PSI+/psi-*
1	Respiratory Chain Complex-IV	Cox4 (YGL187C)	**0.68**	0.02	N/A	N/A	**0.68**
		Cox5a (YNL052W)	**1.67**	0.05	N/A	N/A	**1.67**
		Cox2 (Q0250)	**0.28**	0.00	**0.37**	0.00	**0.32**
		Cox6 (YHR051W)	**0.36**	0.01	N/A	N/A	**0.36**
		Cox13 (YGL191W)	**1.66**	0.12	**1.43**	0.02	**1.54**
5		Odc2 (YOR222W)	**0.20**	0.03	N/A	N/A	**0.20**
6	Mitochondrial organisation and morphology	Phb2 (YGR231C)	**0.75**	0.11	**0.67**	0.00	**0.71**
		Phb1 (YGR132C)	**0.53**	0.06	**0.61**	0.00	**0.57**
8	Branched chain amino acid biosynthesis	Ilv2 (YMR108W)	N/A	N/A	**1.28**	0.00	**1.28**
		Ilv6 (YCL009C)	N/A	N/A	**1.35**	0.00	**1.35**
		Ilv3 (YJR016C)	N/A	N/A	**1.22**	0.01	**1.22**
		Ilv5 (YLR355C)	**0.67**	0.00	**0.74**	0.00	**0.70**
		Leu4 (YNL104C)	**1.31**	0.04	**1.32**	0.00	**1.31**
		Bat1 (YHR208W)	**1.43**	0.11	**1.43**	0.00	**1.43**
9	Respiratory Chain Complex assembly 1	Atp11 (YNL315C)	**0.41**	0.09	N/A	N/A	**0.41**
13		Abf2 (YMR072W)	N/A	N/A	**1.35**	0.00	**1.35**
		Mmf1 (YIL051C)	N/A	N/A	**1.51**	0.00	**1.51**
15	Matrix protein import	Ssc1 (YJR045C)	**0.75**	0.00	**0.74**	0.00	**0.74**
		Hsp10 (YOR020C)	N/A	N/A	**1.33**	0.00	**1.33**
		Hsp78 (YDR258C)	**2.16**	0.00	**1.92**	0.00	**2.04**
		Hsp60 (YLR259C)	N/A	N/A	**1.13**	0.00	**1.13**
		Ecm10 (YEL030W)	N/A	N/A	**0.71**	0.00	**0.71**
16	Tim23/Tim22 complex	Tim44 (YIL022W)	**1.29**	0.15	N/A	N/A	**1.29**
19		Lys12 (YIL094C)	N/A	N/A	**1.52**	0.00	**1.52**
21		Tdh3 (YGR192C)	**0.67**	0.05	**2.00**	0.00	**1.16**
22	Secretory pathway	Kar2 (YJL034W)	**1.42**	0.07	**2.13**	0.00	**1.74**
25		Cbp3 (YPL215W)	**2.52**	0.09	N/A	N/A	**2.52**
		Cbp4 (YGR174C)	**1.77**	0.14	N/A	N/A	**1.77**
29		Lsp1 (YPL004C)	**2.56**	0.01	**3.70**	0.00	**3.08**
30	Mitochondrial/cytoplasmic lipid metabolism	Psd1 (YNL169C)	**0.17**	0.01	N/A	N/A	**0.17**
		Yhm2 (YMR241W)	N/A	N/A	**0.67**	0.01	**0.67**
31	Glutamate biosynthesis	Put2 (YHR037W)	N/A	N/A	**1.61**	0.00	**1.61**
35	Response to DNA damage	Mgm101 (YJR144W)	**1.39**	0.15	N/A	N/A	**1.39**
		Pdb1 (YBR221C)	**1.39**	0.11	N/A	N/A	**1.39**
		Pdx1 (YGR193C)	**1.94**	0.06	N/A	N/A	**1.94**

1

37	Pyruvate/α-ketoglutarate dehydrogenase	Lat1 (YNL071W)	N/A	N/A	**1.29**	0.00	**1.29**
		Prx1 (YBL064C)	**3.34**	0.00	**1.64**	0.00	**2.34**
		Kgd2 (YDR148C)	**1.27**	0.14	N/A	N/A	**1.27**
		Kgd1 (YIL125W)	**0.76**	0.02	**0.90**	0.00	**0.83**
		Pda1 (YER178W)	N/A	N/A	**1.34**	0.00	**1.34**
41	DNA replication	Adk2 (YER170W)	**0.48**	0.05	N/A	N/A	**0.48**
		Mam33 (YIL070C)	**0.25**	0.00	**0.76**	0.00	**0.44**
43		Cpr3 (YML078W)	**0.73**	0.14	**0.65**	0.00	**0.69**
45	Cytoplasmic lipid metabolism	Pil1 (YGR086C)	**2.40**	0.02	**4.00**	0.00	**3.10**
46	Folate and glycine metabolism	Gcv3 (YAL044C)	N/A	N/A	**1.54**	0.02	**1.54**
		Gcv1 (YDR019C)	**1.29**	0.11	**1.96**	0.00	**1.59**
49	TOM complex	Tom22 (YNL131W)	N/A	N/A	**1.75**	0.00	**1.75**
		Tom20 (YGR082W)	**0.53**	0.08	N/A	N/A	**0.53**
		Tom40 (YMR203W)	**0.71**	0.11	**0.75**	0.00	**0.73**
54	Cell wall organisation and biogenesis	Gas1 (YMR307W)	N/A	N/A	**2.17**	0.00	**2.17**
58	Vacuolar acidification	Tfp1 (YDL185W)	**3.97**	0.01	**10.00**	0.00	**6.30**
62	Translation regulator activity	Pet54 (YGR222W)	**4.46**	0.11	N/A	N/A	**4.46**
63		Odc1 (YPL134C)	**0.29**	0.01	**0.60**	0.00	**0.42**
66	Amino acid metabolism	Ilv1 (YER086W)	**1.42**	0.11	**1.72**	0.01	**1.56**
		Cha1 (YCL064C)	**1.84**	0.12	**1.61**	0.01	**1.72**
67		Tuf1 (YOR187W)	**0.73**	0.09	N/A	N/A	**0.73**
70		Mir1 (YJR077C)	**0.74**	0.02	N/A	N/A	**0.74**
71		Ccp1 (YKR066C)	**1.80**	0.11	N/A	N/A	**1.80**
72		Nuc1 (YJL208C)	**0.27**	0.07	N/A	N/A	**0.27**
75		Erg6 (YML008C)	N/A	N/A	**1.49**	0.01	**1.49**
		Eht1 (YBR177C)	**10.67**	0.10	N/A	N/A	**10.67**
79	Components of the large subunit of mitochondrial ribosomes-MRPL	Mrpl6 (YHR147C)	**2.87**	0.11	N/A	N/A	**2.87**
		Rml2 (YEL050C)	**0.40**	0.14	N/A	N/A	**0.40**
		Mrpl10 (YNL284C)	**0.31**	0.10	N/A	N/A	**0.31**
81		Sod1 (YJR104C)	N/A	N/A	**0.57**	0.01	**0.57**
		Sod2 (YHR008C)	N/A	N/A	**1.20**	0.00	**1.20**
85		Ecm33 (YBR078W)	N/A	N/A	**2.28**	0.00	**2.28**
93		Por1 (YNL055C)	**0.73**	0.01	**0.94**	0.00	**0.83**
95	NAD metabolism/TCA cycle	Dld1 (YDL174C)	**0.64**	0.04	N/A	N/A	**0.64**
		Ypr004c (YPR004C)	**0.50**	0.05	N/A	N/A	**0.50**
		Nde2 (YDL085W)	**1.46**	0.11	N/A	N/A	**1.46**
		Cit1 (YNR001C)	N/A	N/A	**0.92**	0.00	**0.92**
		Ndi1 (YML120C)	**0.79**	0.10	**0.83**	0.00	**0.81**
		Mdh1 (YKL085W)	**0.71**	0.02	N/A	N/A	**0.71**

		Nde1 (YMR145C)	**1.64**	0.00	**1.52**	0.00	**1.58**
		Yor356w (YOR356W)	**2.51**	0.06	N/A	N/A	**2.51**
		Cit3 (YPR001W)	**6.35**	0.03	N/A	N/A	**6.35**
96		Mdl2 (YPL270W)	**1.59**	0.11	N/A	N/A	**1.59**
99	Components of the small subunit of mitochondrial ribosomes-MRPS	Mrp13 (YGR084C)	**0.30**	0.12	N/A	N/A	**0.30**
102		Leu9 (YOR108W)	**1.81**	0.01	**1.69**	0.00	**1.75**
103	Alcohol/aldehyde dehydrogenase	Ald4 (YOR374W)	**0.66**	0.00	**0.85**	0.00	**0.75**
		Adh3 (YMR083W)	N/A	N/A	**0.79**	0.00	**0.79**
		Ach1 (YBL015W)	**0.66**	0.00	**0.70**	0.00	**0.68**
		Ald5 (YER073W)	N/A	N/A	**0.74**	0.01	**0.74**
104		Sfc1 (YJR095W)	**0.57**	0.02	N/A	N/A	**0.57**
109		Pdh1 (YPR002W)	**0.69**	0.07	N/A	N/A	**0.69**
		Om45 (YIL136W)	**1.43**	0.01	**1.41**	0.00	**1.42**
123		Cat2 (YML042W)	N/A	N/A	**0.71**	0.01	**0.71**
128		Grx2 (YDR513W)	**1.80**	0.09	N/A	N/A	**1.80**
129		Msw1 (YDR268W)	**0.35**	0.11	N/A	N/A	**0.35**
134		Pet9 (YBL030C)	**0.64**	0.05	**0.83**	0.00	**0.73**
		Aac1 (YMR056C)	N/A	N/A	**0.54**	0.00	**0.54**
		Aac3 (YBR085W)	N/A	N/A	**0.60**	0.00	**0.60**
144		Cyt2 (YKL087C)	**0.20**	0.03	N/A	N/A	**0.20**
147	Respiratory Chain Complex-II	Lsc2 (YGR244C)	**1.53**	0.01	**1.16**	0.00	**1.33**
		Sdh2 (YLL041C)	N/A	N/A	**0.63**	0.00	**0.63**
		Yjl045w (YJL045W)	N/A	N/A	**0.76**	0.00	**0.76**
		Lsc1 (YOR142W)	N/A	N/A	**1.27**	0.00	**1.27**
		Sdh1 (YKL148C)	**0.61**	0.00	**0.63**	0.00	**0.62**
		Sdh3 (YKL141W)	N/A	N/A	**0.59**	0.00	**0.59**
148		Cbr1 (YIL043C)	**1.81**	0.11	N/A	N/A	**1.81**
		Mcr1 (YKL150W)	**0.36**	0.00	**0.38**	0.00	**0.37**
149	Isocitrate metabolism	Idh1 (YNL037C)	**0.54**	0.02	**0.82**	0.00	**0.67**
		Aco1 (YLR304C)	**0.66**	0.00	**0.78**	0.00	**0.72**
		Idp3 (YNL009W)	N/A	N/A	**1.39**	0.00	**1.39**
		Idp1 (YDL066W)	N/A	N/A	**1.47**	0.00	**1.47**
		Idh2 (YOR136W)	**0.47**	0.00	N/A	N/A	**0.47**
155	Respiratory Chain Complex-V	Atp4 (YPL078C)	N/A	N/A	**1.11**	0.01	**1.11**
		Atp15 (YPL271W)	N/A	N/A	**0.77**	0.00	**0.77**
		Atp1 (YBL099W)	**0.62**	0.00	**0.89**	0.00	**0.74**
		Atp16 (YDL004W)	**0.61**	0.04	N/A	N/A	**0.61**
		Atp3 (YBR039W)	**0.52**	0.00	**0.87**	0.00	**0.67**
		Atp2 (YJR121W)	**0.61**	0.00	**0.83**	0.00	**0.71**
		Cyt1 (YOR065W)	**0.40**	0.01	N/A	N/A	**0.40**

156	Respiratory Chain Complex-III	Qcr2 (YPR191W)	N/A	N/A	**1.19**	0.00	**1.19**	
		Qcr10 (YHR001W-A)	**0.08**	0.01	N/A	N/A	**0.08**	
		Qcr6 (YFR033C)	**0.49**	0.09	N/A	N/A	**0.49**	
		Rip1 (YEL024W)	N/A	N/A	**1.32**	0.00	**1.32**	
158		Pma2 (YPL036W)	N/A	N/A	**3.28**	0.00	**3.28**	
		Pma1 (YGL008C)	**1.29**	0.06	**2.94**	0.00	**1.95**	
160		Hxt7 (YDR342C)	N/A	N/A	**1.43**	0.00	**1.43**	
		Hxt6 (YDR343C)	**0.52**	0.03	**1.72**	0.00	**0.95**	1
		Alo1 (YML086C)	**1.48**	0.11	N/A	N/A	**1.48**	
		Tdh1 (YJL052W)	**1.40**	0.10	**2.70**	0.00	**1.94**	
		Sec61 (YLR378C)	N/A	N/A	**1.96**	0.01	**1.96**	
		Tef2 (YBR118W)	N/A	N/A	**3.70**	0.00	**3.70**	
		Rsm28 (YDR494W)	**1.72**	0.12	N/A	N/A	**1.72**	
		Ynl208w (YNL208W)	**15.49**	0.05	N/A	N/A	**15.49**	
		Sar1 (YPL218W)	**4.44**	0.12	N/A	N/A	**4.44**	
		Hht1 (YBR010W)	N/A	N/A	**5.56**	0.00	**5.56**	
		Tef1 (YPR080W)	N/A	N/A	**3.85**	0.00	**3.85**	
		Ycp4 (YCR004C)	**5.24**	0.03	**4.17**	0.00	**4.67**	
		Hht2 (YNL031C)	N/A	N/A	**5.56**	0.00	**5.56**	
		Ssa2 (YLL024C)	**0.51**	0.11	**2.70**	0.01	**1.17**	1
		Tdh2 (YJR009C)	N/A	N/A	**2.32**	0.00	**2.32**	
		Htb1 (YDR224C)	N/A	N/A	**4.08**	0.00	**4.08**	
		Hta1 (YDR225W)	N/A	N/A	**4.17**	0.00	**4.17**	
		Hhf2 (YNL030W)	N/A	N/A	**4.78**	0.00	**4.78**	
		Hho1 (YPL127C)	N/A	N/A	**3.33**	0.00	**3.33**	
		Htb2 (YBL002W)	N/A	N/A	**4.08**	0.00	**4.08**	
		Yor084w (YOR084W)	N/A	N/A	**2.97**	0.00	**2.97**	
		Faa4 (YMR246W)	**4.75**	0.07	N/A	N/A	**4.75**	
		Hmo1 (YDR174W)	N/A	N/A	**2.94**	0.00	**2.94**	
		Hta2 (YBL003C)	N/A	N/A	**4.76**	0.00	**4.76**	
		Ssb1 (YDL229W)	N/A	N/A	**3.33**	0.00	**3.33**	
		Hhf1 (YBR009C)	N/A	N/A	**4.57**	0.00	**4.57**	
		Pdi1 (YCL043C)	N/A	N/A	**1.72**	0.01	**1.72**	
		Idp2 (YLR174W)	N/A	N/A	**1.33**	0.00	**1.33**	
		Nce102 (YPR149W)	**3.60**	0.06	N/A	N/A	**3.60**	
		Ynr018w (YNR018W)	**0.53**	0.11	N/A	N/A	**0.53**	
		Bna4 (YBL098W)	**2.98**	0.12	N/A	N/A	**2.98**	
		Put1 (YLR142W)	**3.07**	0.12	N/A	N/A	**3.07**	
		Ras2 (YNL098C)	**6.30**	0.10	N/A	N/A	**6.30**	
		Pos5 (YPL188W)	**3.13**	0.07	N/A	N/A	**3.13**	
		Pck1 (YKR097W)	**0.30**	0.02	N/A	N/A	**0.30**	
		Pgk1 (YCR012W)	**0.14**	0.02	N/A	N/A	**0.14**	

Supporting Figure S1
Click here to download high resolution image

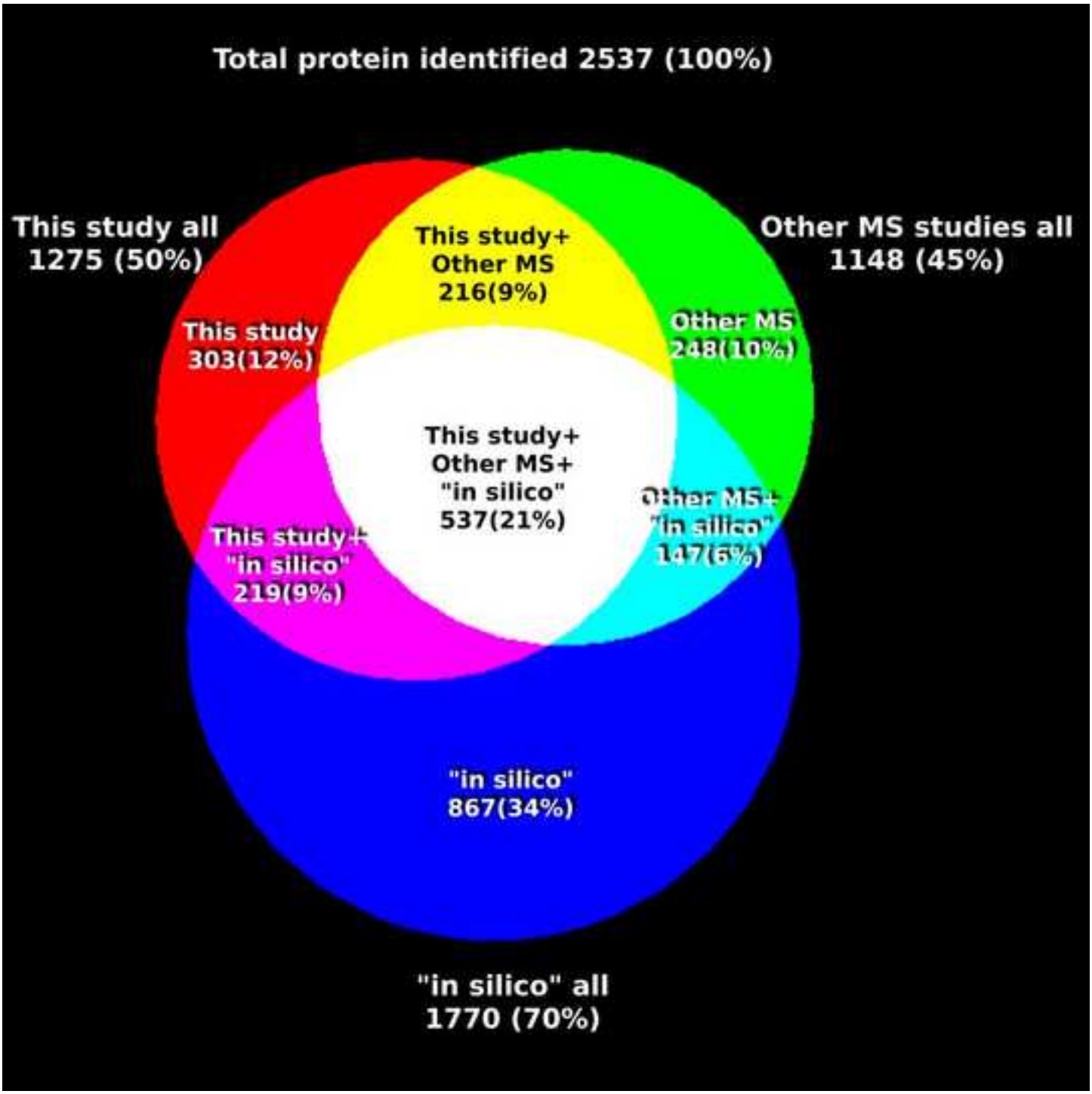

Supporting Figure S2

Click here to download high resolution image

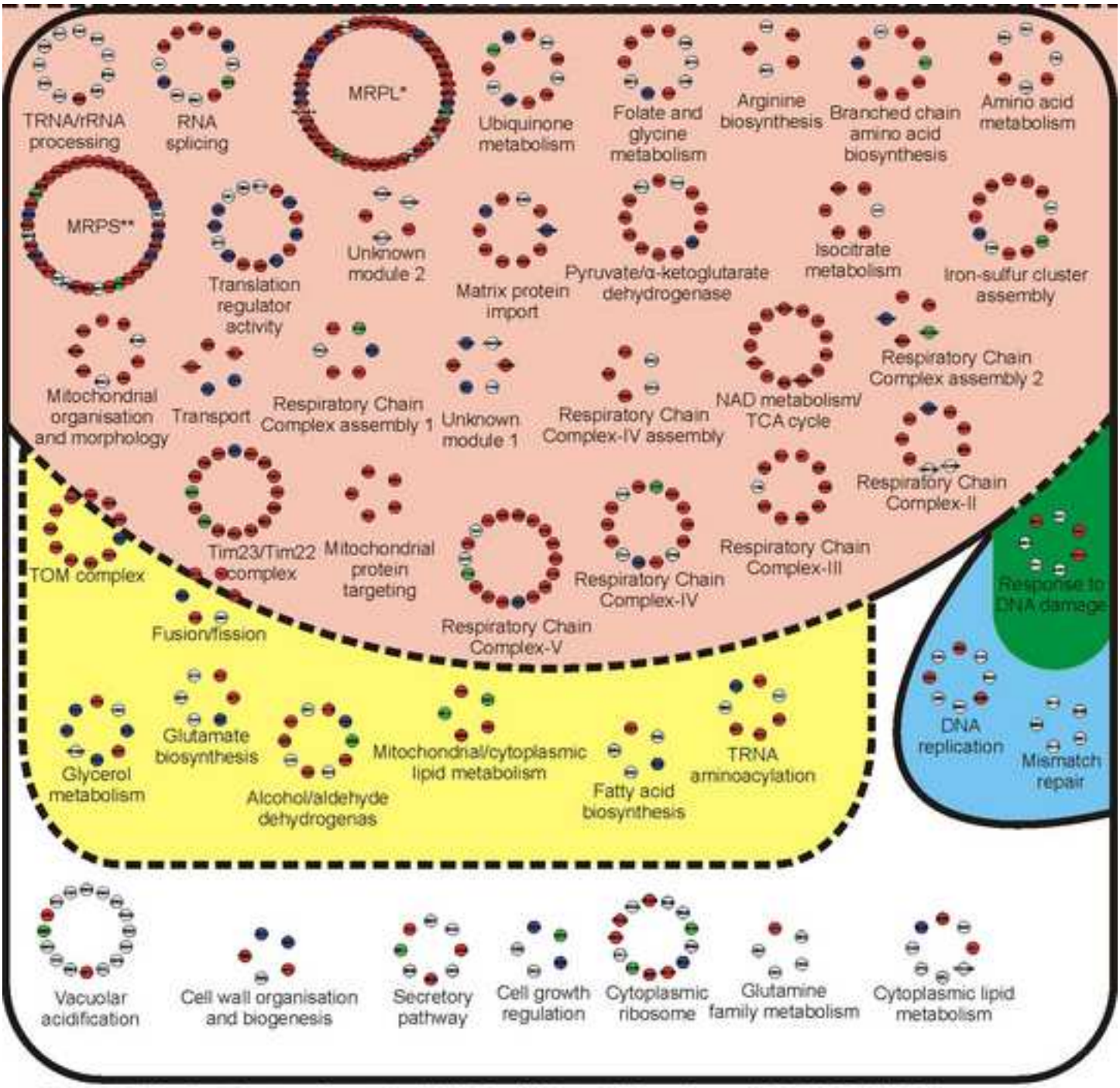

Supporting Figure S3

Click here to download high resolution image

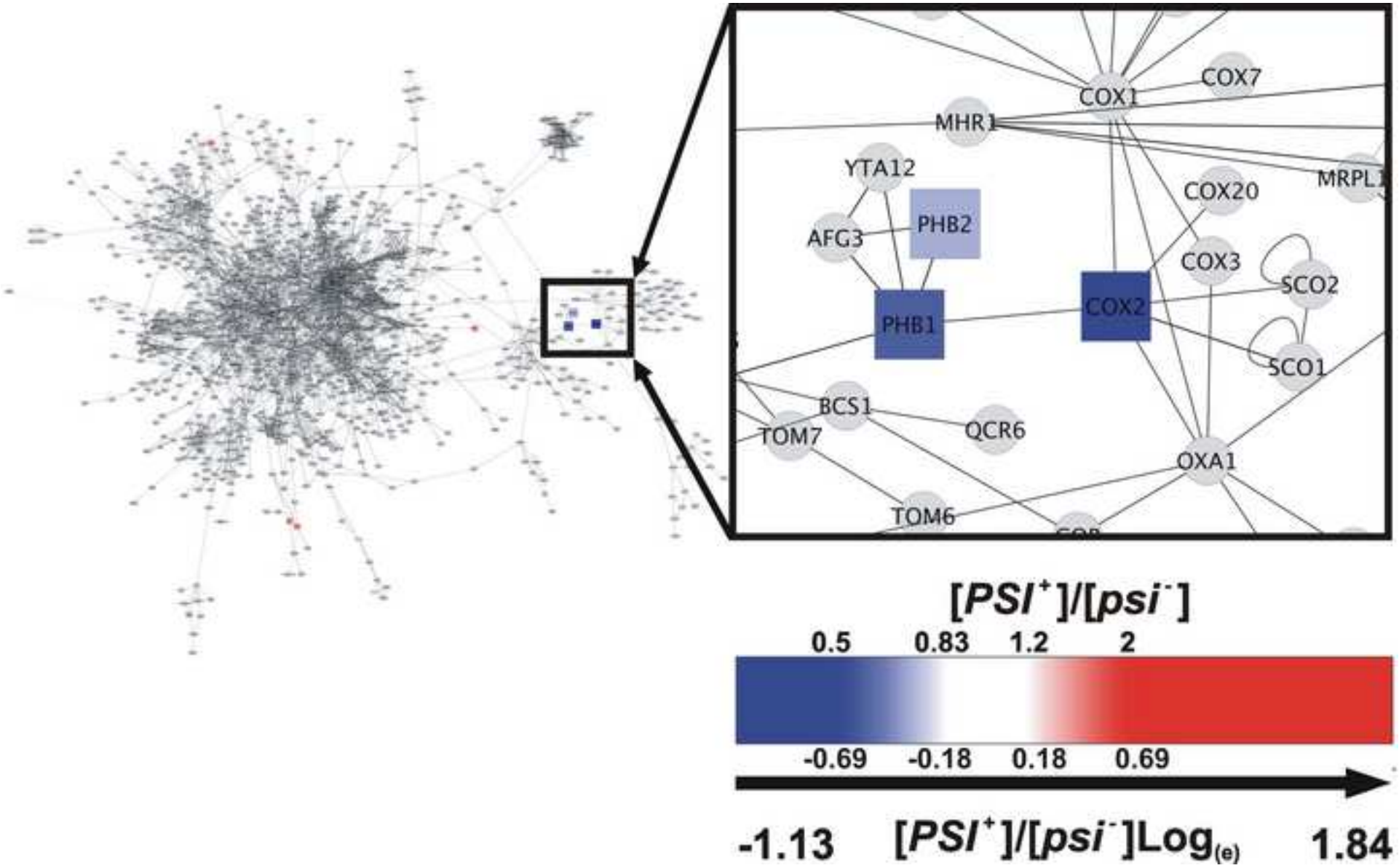

Supporting Figure S4 AB

Click here to download high resolution image

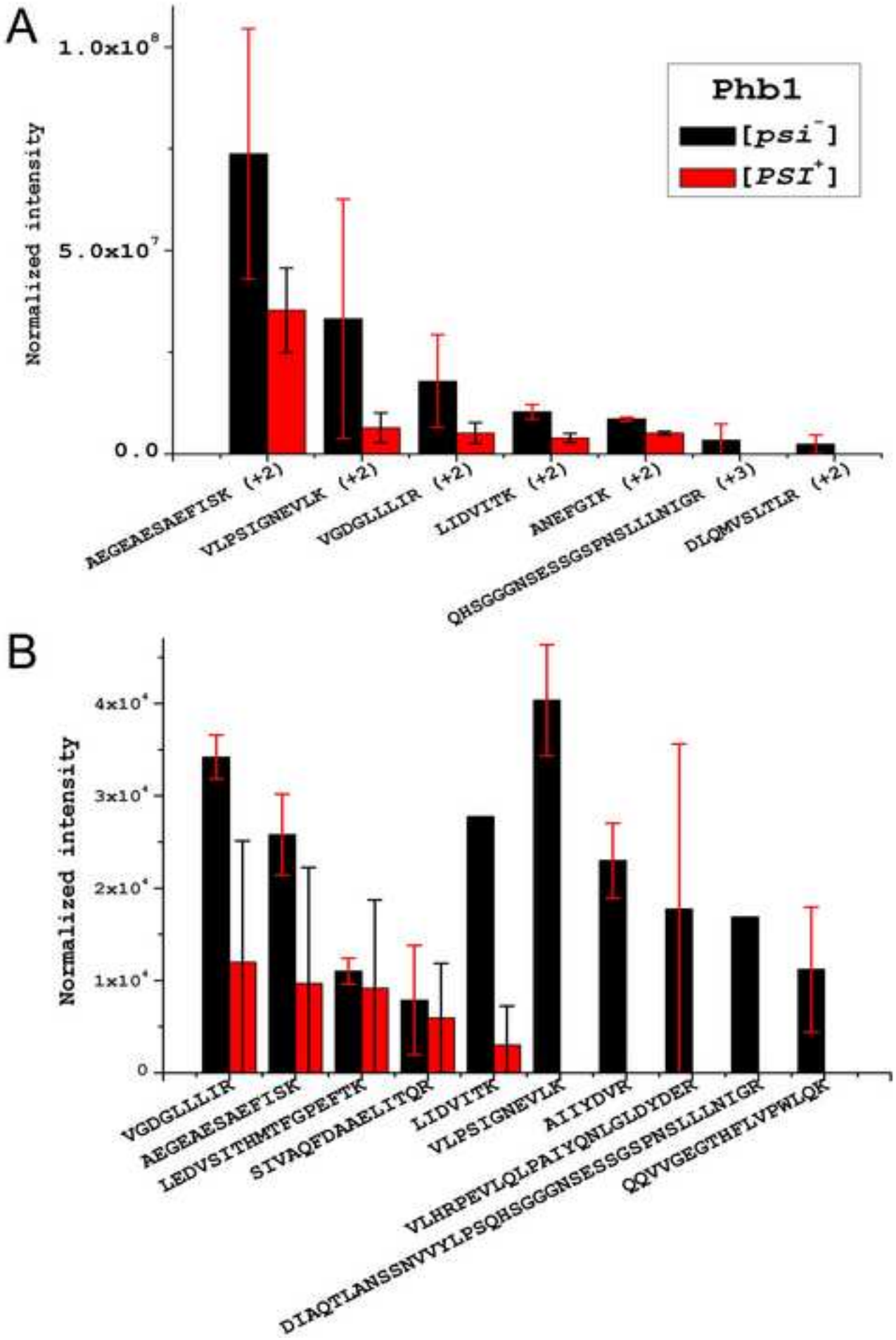

Supporting Figure S4 CD

Click here to download high resolution image

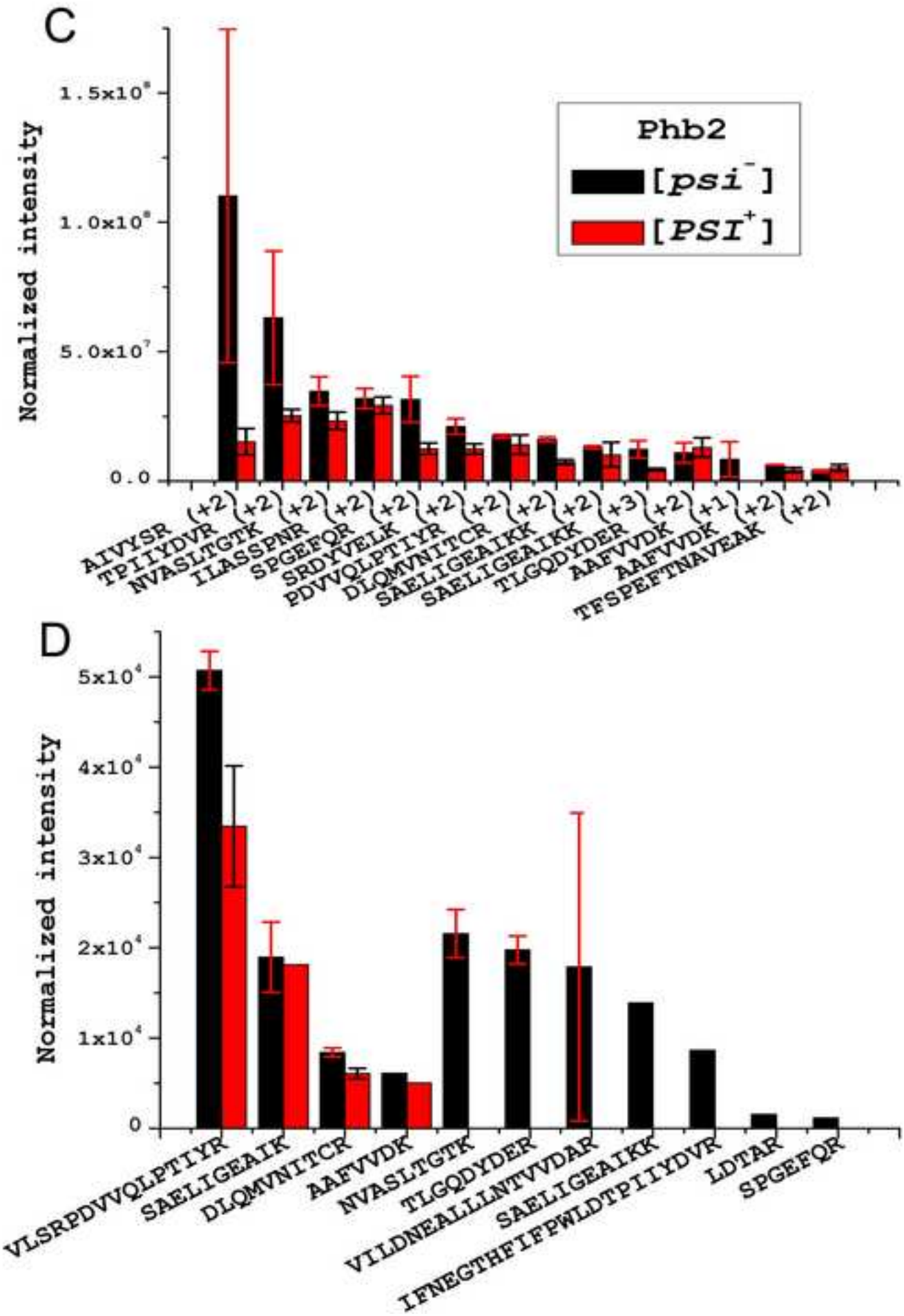

Supporting Figure S4 EF

Click here to download high resolution image

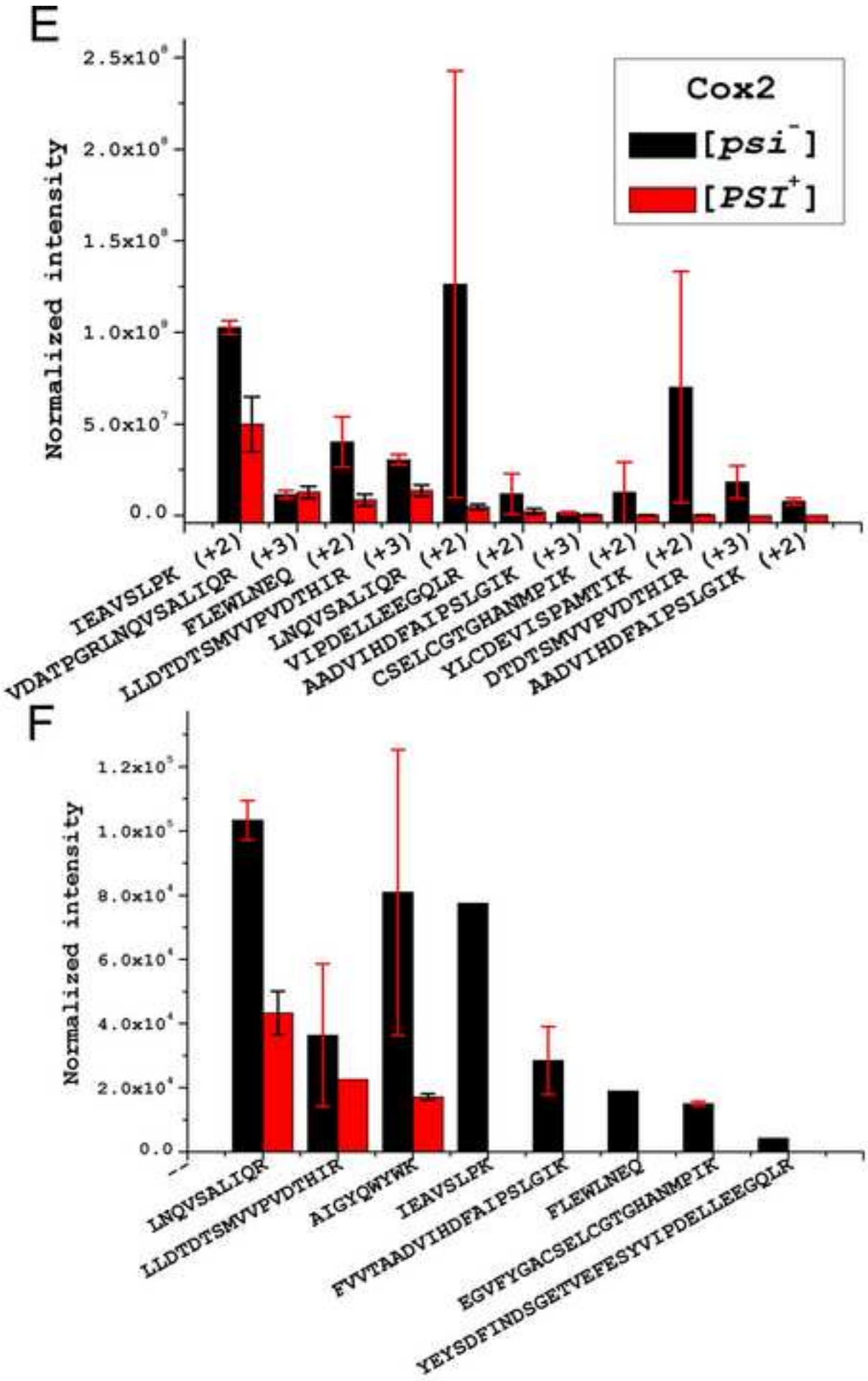

Supporting Figure S5

Click here to download high resolution image

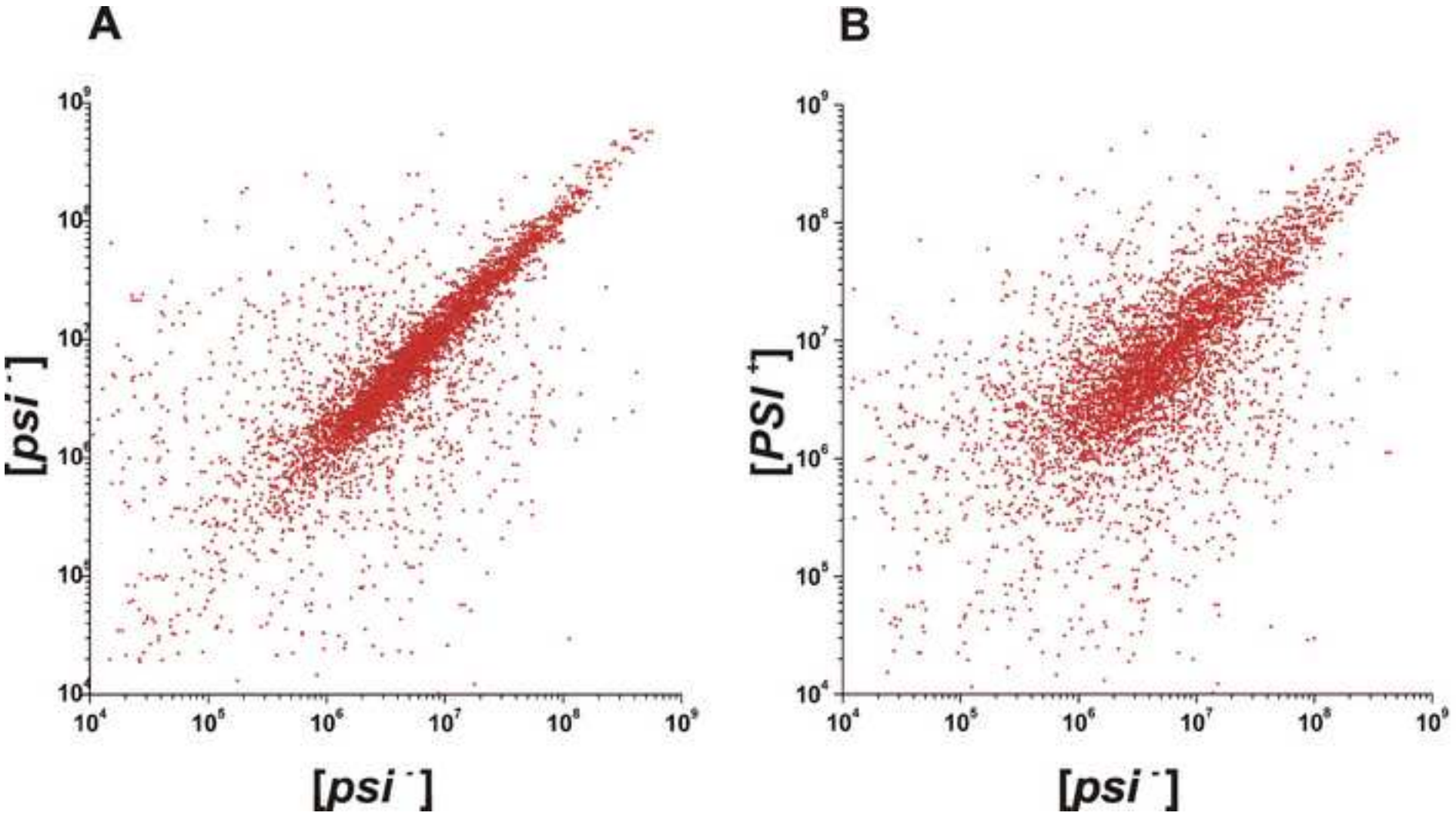

Supporting Figure S6

Click here to download high resolution image